



DIRECT METHANOL SYNTHESIS FROM GLYCEROL OVER MODIFIED BASIC METAL OXIDE
CATALYSTS



By

MISS Mukrawee MANEEWUTHIWORASAKUL

A Thesis Submitted in Partial Fulfillment of the Requirements
for Master of Engineering (CHEMICAL ENGINEERING)

Department of CHEMICAL ENGINEERING

Graduate School, Silpakorn University

Academic Year 2018

Copyright of Graduate School, Silpakorn University

การสังเคราะห์เมทานอลแบบทางตรงจากกลีเซอรอลด้วยตัวเร่งปฏิกิริยาที่ปรับปรุงบน
พื้นฐานของโลหะออกไซด์



โดย
นางสาวมุกะวี มณีวุฒิวรสกุล

วิทยานิพนธ์นี้เป็นส่วนหนึ่งของการศึกษาตามหลักสูตรวิศวกรรมศาสตรมหาบัณฑิต

สาขาวิชาวิศวกรรมเคมี แผน ก แบบ ก 2 ระดับปริญญามหาบัณฑิต

ภาควิชาวิศวกรรมเคมี

บัณฑิตวิทยาลัย มหาวิทยาลัยศิลปากร

ปีการศึกษา 2561

ลิขสิทธิ์ของบัณฑิตวิทยาลัย มหาวิทยาลัยศิลปากร

DIRECT METHANOL SYNTHESIS FROM GLYCEROL OVER MODIFIED BASIC
METAL OXIDE CATALYSTS



A Thesis Submitted in Partial Fulfillment of the Requirements
for Master of Engineering (CHEMICAL ENGINEERING)
Department of CHEMICAL ENGINEERING
Graduate School, Silpakorn University
Academic Year 2018
Copyright of Graduate School, Silpakorn University

Title	Direct methanol synthesis from glycerol over modified basic metal oxide catalysts
By	Mukrawee MANEEWUTHIWORASAKUL
Field of Study	(CHEMICAL ENGINEERING)
Advisor	Weerawat Patthaveekongka

Graduate School Silpakorn University in Partial Fulfillment of the Requirements
for the Master of Engineering

..... Dean of graduate school
(Associate Professor Jurairat Nunthanid, Ph.D.)

Approved by

..... Chair person
(Assistant Professor Tarawipa Puangpetch , Ph.D.)

..... Advisor
(Assistant Professor Weerawat Patthaveekongka , D.Eng.)

..... Co Advisor
(Rujira Jitrwung , Ph.D.)

..... Examiner
(Mutsee Termtanan , Ph.D.)

..... External Examiner
(Sophon Sirisattha , Ph.D.)

59404205 : Major (CHEMICAL ENGINEERING)

Keyword : Glycerol, Methanol, Modified MgO catalyst, Direct synthesis

MISS MUKRAWEE MANEEWUTHIWORASAKUL : DIRECT METHANOL SYNTHESIS FROM GLYCEROL OVER MODIFIED BASIC METAL OXIDE CATALYSTS THESIS ADVISOR : ASSISTANT PROFESSOR WEERAWAT PATTHAVEEKONGKA, D.Eng.

Crude glycerol is obtained as a by-product from biodiesel production via transesterification. However, it is hard to utilize directly due to its impurity. Therefore, the transformation of glycerol to valuable chemicals is interesting and has been developing continuously. One of the promising products is methanol because it is an important raw material for biodiesel and chemical industries. In this research, the direct methanol synthesis from glycerol was investigated using modified MgO catalysts prepared by wet impregnation method with the various metal oxides loading (CaO, CoO and CuO). It was found that the amount of metal loading equal to 3 wt.% enhanced the surface area, pore size and basicity of all modified MgO catalysts. The response surface methodology (RSM) based on central composite design (CCD) with Minitab program was used as a tool in order to study the optimum conditions and significant factors, for sample, glycerol concentration (5-15 wt.%), feed flow rate (0.1-0.3 ml/min), reaction temperature (240-390°C) to the catalytic activity of methanol synthesis in one step. The results showed that the optimum condition was 10 wt.% glycerol concentration and 0.1 ml/min feed flow rate at 330°C. The 3%Ca/MgO catalyst provided glycerol conversion and the highest methanol yield of 75.60% and 16.23%, respectively, and generated by-products including ethanal, ethanol, propanol, 2,3-butanedione, acetol, ethylene glycol, CO, CO₂ and H₂. Moreover, The 3%Ca/MgO catalyst had high stability over 30 hours using pure glycerol as raw material for methanol synthesis. Meanwhile, the performance of the catalyst was almost unchanged by using crude glycerol at the same condition, which presented glycerol conversion and methanol yield of 87.40% and 16.81%, respectively. It was indicated that the impurities of crude glycerol did not affect to catalytic activity of 3%Ca/MgO catalyst for the direct methanol synthesis. Additionally, the effect of catalyst preparation was also studied by comparing between co-precipitation and wet impregnation method. The results displayed that the 3%Ca/MgO catalyst prepared by

co-precipitation had platelet-like structure and its particle size was uniform and higher order than the catalyst prepared by wet impregnation method. The catalyst prepared by co-precipitation showed that the catalytic activity proceeded rapidly to stable and increased the performance in term of glycerol conversion to 95.48%, whereas methanol yield was decreased to 10.85%. The result indicated that the 3%Ca/MgO catalyst prepared by co-precipitation can promote the generation of by-products such as ethanal, ethanol, CO and CO₂, leading to decreasing methanol production.



ACKNOWLEDGEMENTS

This research has been done successfully with the cooperation of Department of Chemical Engineering, Faculty of Engineering and Industrial Technology, Silpakorn University and Expert Centre of Innovative Clean Energy and Environment, Thailand Institute of Scientific and Technological Research, which has provided funding for this research. The author would like to express our sincere gratitude and appreciation to my advisor, Assistant Professor Dr. Weerawat Patthaveekongka, lecturer of the Department of Chemical Engineering, Silpakorn University and my co advisor, Dr. Rujira Jitwung, senior researcher of Expert Centre of Innovative Clean Energy and Environment, TISTR, for their valuable suggestions, simulation and useful discussions throughout this research and devotion to revise this thesis.

The author would like to appreciate Dr. Sasikarn Nuchdang and Dr. Dussadee Rattanaphra from Research and Development Division, Thailand Institute of Nuclear Technology and office of Atoms for Peace, for suggestions and support about analytical instrument of catalyst.

In particular, the author also appreciated for kind comments and suggestions from Assistant Professor Dr. Tarawipa Puangpetch, Dr. Mutsee Termtanun from the Department of Chemical Engineering, Silpakorn University, and Dr. Sophon Sirisattha from Biodiversity Research Centre, TISTR who have been the chair and members of the thesis committee, respectively.

Finally, the author would like to thank everyone who has contributed to help for collecting samples and encouraged research (members of INNOEN TISTR) and would like to acknowledge my family (parents and sister) for encouragement and love. This research would not have been possible without them.

Mukrawee MANEEWUTHIWORASAKUL

TABLE OF CONTENTS

	Page
ABSTRACT	D
ACKNOWLEDGEMENTS	F
TABLE OF CONTENTS	G
LIST OF TABLES	I
LIST OF FIGURES	J
CHAPTER 1 INTRODUCTION	14
1.1 Motivation	14
1.2 Objective of Research	16
1.3 Scope of Research	16
1.4 Contribution of Research	17
CHAPTER 2 LITERATURE REVIEWS	18
CHAPTER 3 THEORY	32
CHAPTER 4 METHODOLOGY	41
4.1 Chemicals	41
4.2 Equipment	42
4.3 Catalyst preparation	44
4.4 Catalytic activity evaluation	46
4.5 Design of experiments for direct methanol synthesis from glycerol	46
4.6 Product analyses and Catalyst characterization	50
CHAPTER 5 RESULTS AND DISCUSSIONS	53
CHAPTER 6 CONCLUSIONS AND RECOMMENDATIONS	90

REFERENCES 92

APPENDICES 97

VITA 123



LIST OF TABLES

	Page
Table 1 Chemical and physical properties of glycerol.....	19
Table 2 Types of solid base catalysts[30].	36
Table 3 Chemicals list.	41
Table 4 Crude glycerol component from GI Green Power Company limited.	42
Table 5 Experimental range and levels for central composite design.	47
Table 6 Experimental design and code levels for central composite design.	48
Table 7 Experimental design and Independent variables for central composite design.	49
Table 8 The performance of methanol synthesis from glycerol over MgO catalyst. ..	53
Table 9 Modified MgO catalyst properties by using BET technique.	54
Table 10 The elemental composition of the modified MgO catalyst by using XRF technique.	58
Table 11 CaO loading on MgO catalyst properties by using BET technique.....	73
Table 12 The elemental composition of CaO loading on MgO catalyst by using XRF technique.	74
Table 13 The 3%Ca/MgO catalyst properties with difference method by using BET technique	82
Table 14 Comparison studies of methanol synthesis from glycerol	88

LIST OF FIGURES

	Page
Figure 1 The production of biodiesel and glycerol from transesterification reaction..	14
Figure 2 Production of methanol from glycerol in biodiesel production[1].	15
Figure 3 Molecular structure of glycerol.....	18
Figure 4 Reaction pathways of steam reforming of glycerol over modified Ni-based with different acidity.....	22
Figure 5 Reaction pathways for the glycerol steam reforming reaction.	23
Figure 6 Block flow diagram of the synthesis of methanol from syngas obtained from reforming of glycerol.....	25
Figure 7 The reaction pathways for the formation of methanol from glycerol.....	26
Figure 8 The reaction pathway model from methanol production from glycerol under supercritical water.	27
Figure 9 Brønsted acidity from inductive effect of Lewis acid centre coordinated to a silica support.	34
Figure 10 A face centered central composite design.	38
Figure 11 The steps in the application of response surface methodology (RSM)[11]..	39
Figure 12 Equipment of reactor.....	43
Figure 13 Gas Chromatography for gas and liquid products.	43
Figure 14 Karl Fischer titration	43
Figure 15 The image of 3%Ca/MgO catalyst obtained from wet impregnation method.	44
Figure 16 The image of 3%Co/MgO catalyst obtained from wet impregnation method.	44

Figure 17 The image of 3%Cu/MgO catalyst obtained from wet impregnation method.	45
Figure 18 The image of 3%Ca/MgO catalyst obtained from co-precipitation method.	45
Figure 19 Block flow diagram of direct methanol synthesis from glycerol.....	46
Figure 20 N ₂ adsorption/desorption isotherm of MgO, 3%Ca/MgO, 3%Cu/MgO and 3%Co/MgO catalyst.....	55
Figure 21 XRD pattern of MgO, 3%Ca/MgO, 3%Co/MgO and 3%Cu/MgO catalyst.....	56
Figure 22 SEM images of (A) MgO, (B) 3%Ca/MgO, (C) 3%Cu/MgO and (D) 3%Co/MgO catalyst.....	57
Figure 23 EDX elemental mapping of MgO, 3%Ca/MgO, 3%Co/MgO and 3%Cu/MgO catalyst.....	58
Figure 24 CO ₂ -TPD of MgO, 3%Ca/MgO, 3%Co/MgO and 3%Cu/MgO catalyst.....	59
Figure 25 Glycerol conversion and methanol yield over MgO and modified MgO catalysts.....	61
Figure 26 Product distribution over MgO and modified MgO catalysts.....	61
Figure 27 Proposed mechanism for the formation of methanol from direct methanol synthesis from glycerol.....	62
Figure 28 Glycerol conversion over 3%Ca/MgO and 3%Co/MgO catalyst.....	63
Figure 29 Methanol yield over 3%Ca/MgO and 3%Co/MgO catalyst.	64
Figure 30 Fresh and used catalyst of 3%Ca/MgO and 3%Co/MgO catalyst.....	64
Figure 31 XRD pattern of fresh and used catalysts of 3%Ca/MgO and 3%Co/MgO catalyst.....	65
Figure 32 Product distribution over 3%Ca/MgO and 3%Co/MgO catalyst.....	66
Figure 33 3D Surface plot: Glycerol conversion versus concentration, temperature and feed flow rate.....	69

Figure 34 Contour plot: Glycerol conversion versus glycerol concentration and temperature.....	70
Figure 35 3D Surface plot: Methanol yield versus concentration, temperature and feed flow rate.....	72
Figure 36 Contour plot: Methanol yield versus feed flow rate and temperature.	72
Figure 37 Glycerol conversion and methanol yield over 3%Ca/MgO catalyst at optimum condition.	73
Figure 38 XRD pattern of 3%Ca/MgO, 5%Ca/MgO and 10%Ca/MgO catalyst.....	75
Figure 39 CO ₂ -TPD of 3%Ca/MgO, 5%Ca/MgO and 10%Ca/MgO catalyst.....	75
Figure 40 Glycerol conversion and methanol yield over 3%Ca/MgO, 5%Ca/MgO and 10%Ca/MgO catalyst.....	76
Figure 41 Products distribution over 3%Ca/MgO, 5%Ca/MgO and 10%Ca/MgO catalyst.....	77
Figure 42 Glycerol conversion for pure and crude glycerol as function of reaction time.	78
Figure 43 Methanol yield for pure and crude glycerol as function of reaction time... ..	78
Figure 44 Products distribution for pure and crude glycerol as function of reaction time.	79
Figure 45 The experimental and RSM predicted responses for direct methanol synthesis from crude glycerol over 3%Ca/MgO catalyst.....	80
Figure 46 XRD pattern of 3%Ca/MgO with difference method.....	81
Figure 47 N ₂ adsorption/desorption isotherm of 3%Ca/MgO catalyst properties with difference method.	83
Figure 48 The SEM images of the 3%Ca/MgO prepared with different methods of (A) wet impregnation and (B) co-precipitation.....	84
Figure 49 Glycerol conversion over 3%Ca/MgO catalyst with difference method.	85

Figure 50 Methanol yield over 3%Ca/MgO catalyst with difference method.....	86
Figure 51 Products distribution over 3%Ca/MgO catalyst with difference method.	87
Figure 52 Differential method to determine reaction order.....	120
Figure 53 First-order reaction	121
Figure 54 Second-order reaction	121
Figure 55 Third-order reaction	122



CHAPTER 1 INTRODUCTION

1.1 Motivation

Biodiesel is an alternative diesel fuel derived from vegetable oils (castor, palm, soya, coconut and jatropha curcas L.) or animal fats via transesterification reaction with methanol by using strong base catalyst, e.g. sodium hydroxide (NaOH) or potassium hydroxide (KOH). In the biodiesel process, glycerol is a by-product, which it is generated. It is known that 3 mole of biodiesel can produce 1 mole of glycerol as showed in Figure 1.

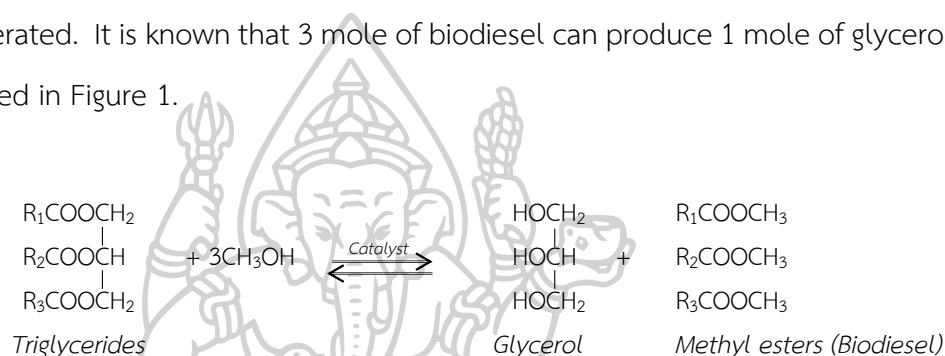


Figure 1 The production of biodiesel and glycerol from transesterification reaction.

Department of Alternative Energy Development and Efficiency (DEDE) in Ministry of Energy reported that biodiesel consumption of Thailand was 2.89 million liters per day in 2014 and forecasted that it is increasing in every year. Moreover, DEDE issued Alternative Energy Development Plan (AEDP 2015-2036) to increase the proportion of renewable energy to 30% of the total energy consumption in the country by 2036 and set target of biodiesel consumption around 14 million liters per day. This means that crude glycerol will raise hugely as trend of increasing biodiesel production. Therefore, the biodiesel industry has been attempted to manage surplus crude glycerol with many methods, such as glycerol purification and glycerol transformation to value-added products (e.g. acrolein, 1,2-propanediol, n-butanol, 2,3-butanediol, propylene glycol and lactic acid). However, the converting glycerol to methanol is very interesting because methanol is used as raw material for biodiesel production or used in other applications such as solvent in plastic, plywood, paint and fuel industries.

Commercial methanol is usually acquired from petroleum sources such as coal and nature gas. Biomethanol is produced from biomass sources: biogas. Glycerol obtained from biodiesel process is classified as a biochemical source and it can also be a raw material for methanol synthesis. The glycerol to methanol process consists of two steps: reforming of glycerol and CO/CO₂ hydrogenation. In the first step, the reforming of glycerol can generate syngas (H₂, CO₂, CO) along with the small amount of CH₄ gas. The obtained syngas is transferred to the second step for methanol synthesis via CO/CO₂ hydrogenation. The process of methanol production from glycerol can be linked with the biodiesel industry as showed in Figure 2. It seems that the process is complex and carried out at high temperature and pressure, resulting to over power consumption. Therefore, methanol synthesis from glycerol in a one-step has been investigating to reduce multiple steps and carry out under mild condition, resulting in minimizing cost of equipment, energy and process.

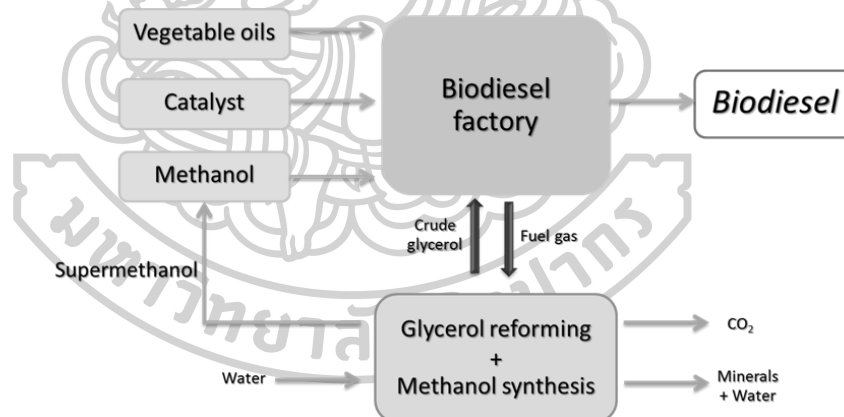


Figure 2 Production of methanol from glycerol in biodiesel production[1].

In this research, it was focused on an improvement of MgO catalysts for the conversion of glycerol to methanol in a single step called direct methanol synthesis. The modified MgO catalysts were prepared by impregnation method using metal oxide such as CaO, CoO and CuO. The performances of the modified MgO catalyst in terms of glycerol conversion and methanol yield were investigated by comparing with the activity of MgO catalyst in order to describe the behavior of the catalyst. Moreover,

the optimum condition obtained from modified MgO catalyst was tested with pure and crude glycerol. Finally, the comparison of catalyst preparation between impregnation and co-precipitation method for the best modified MgO catalyst was tested with crude glycerol. Furthermore, these catalysts were analyzed structural and chemical and properties such as surface area, pore volume, pore size, crystal structure and basicity, etc.

1.2 Objective of Research

To study and improve the appropriate catalysts for direct methanol synthesis from glycerol.

1.3 Scope of Research

1.3.1 To test conditions of direct methanol synthesis from glycerol by using 4 g of commercial MgO catalysts at atmospheric pressure and vary parameters as following by

- Feed concentration (glycerol/water): 10, 30, 50 wt.%
- Feed flow rate: 0.1, 0.3, 0.5 ml/min
- Temperature: 240 to 390°C

1.3.2 To synthesize modified catalysts by loading metal oxide such as CaO, CuO, CoO in ranging of 3, 5, 10 wt.%. For testing catalytic activity of direct methanol synthesis from pure glycerol.

1.3.3 The optimum condition obtained from direct methanol synthesis from pure glycerol is tested with crude glycerol.

1.3.4 Comparison of catalyst preparation between wet impregnation and co-precipitation method for the best catalyst obtained from the optimum condition and test with crude glycerol.

1.4 Contribution of Research

1.4.1. Obtain effective catalyst for high purity methanol via direct methanol synthesis from glycerol and a catalyst preparation method.

1.4.2. Obtain the appropriate condition for direct methanol synthesis from glycerol.



CHAPTER 2 LITERATURE REVIEWS

This chapter reviewed about the properties of glycerol and the utilization of glycerol to produce value-added products, which it was focused on the operating process and mechanism pathways. Moreover, the preparation and characterization of catalyst were also reviewed in the chapter 2.

2.1 Glycerol

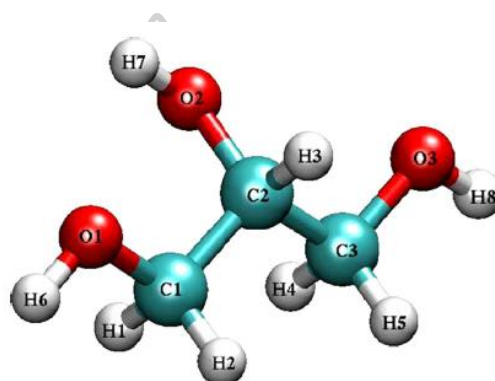


Figure 3 Molecular structure of glycerol.

Glycerin or Glycerol is a compound of sugar and alcohol, and core of the molecule of the main component of triglycerides found in animal fat and vegetable oil. The molecular structure of glycerol is showed in Figure 3. Glycerol has physical properties as clear liquid, colorless, odorless, sweet, non-toxic, solubility in water and chemical properties showed in Table 1. Glycerol is used as a substrate in a variety of chemical industries such as pharmaceutical, food, industrial, and cosmetic products. Glycerol is a substance obtained from petrochemical source and biochemical source. However, the biobased glycerol is a major by-product derived from biodiesel production through transesterification with methanol and alkaline catalyst. It is known that 9 kg of biodiesel can produce 1 kg of crude glycerol. Characteristics of crude glycerol are different from pure glycerol, including smell, color and traces of impurities. The composition of the crude glycerol depends on the substrate such as vegetable oils and animal fats, which is composed of glycerol 50-90, 1-20% methanol, 5-15%

salts, 11-5% water, 1-5% fatty acids, and 1-5% matter organic non-glycerol (MONG) by weight[2].

Crude glycerol can be converted to pure glycerol by purification processes which includes neutralization, ion-exchange resin adsorption, acidification, filtration, solvent extraction and vacuum distillation[3]. However, refining crude glycerol to a high degree is very expensive and the purification processes is complex. Thus, the development of transforming glycerol into value-added products to reducing process and more cost effective to manufacture. This is explained in the next section.

Table 1 Chemical and physical properties of glycerol.

Properties		Unit
Molecular formula	$C_3H_8O_3$	
Molar mass	92	g/mol
Relative density	1260	kg/m ³
Viscosity	1.41	Pa s
Melting point	18	°C
Boiling point (101.3 kPa)	290	°C
Flash point	160	°C
Specific heat	2435 (25°C)	kJ/kg
Heat of vaporization	82.12	kJ/k-mol
Thermal conductivity	0.28	W/(m K)
Heat of formation	667.8	kJ/mol
Surface tension	63.4	mN/m
pH (solution)	7	
Auto flammability	393	°C

2.2 Conversion of glycerol to value-added products.

In addition to the pathway of crude glycerol into pure glycerol. Another interesting approach, glycerol can be introduced into biological processes and chemical process

for value-added products such as 1,2-propanediol, n-butanol, 2,3-butanediol, docosahexaenoic acid (DHA), eicosapentaenoic acid (EPA), citric acid, lipids, acrolein H_2 and CO_2 [4, 5]. This research focuses on the use of glycerol into chemical processes to reduce the complexity of the processes and to obtain the highest yield. The reaction of glycerol into value-added products was studied as based on the previous knowledge including: Hydrogen production from glycerol steam reforming, syngas production from glycerol and methanol synthesis from glycerol.

2.2.1 Hydrogen production from glycerol steam reforming

For glycerol steam reforming, the main products are hydrogen (H_2), carbon dioxide (CO_2) and carbon monoxide (CO). The reaction conditions were investigated in the range of temperature 400-800°C under atmospheric pressure using catalysts. Glycerol is reformed under using steam by passing multiple reaction as following;

- (1) Glycerol steam reforming: $C_3H_8O_3 + 3H_2O \leftrightarrow 3CO_2 + 7H_2$ ($\Delta H^\circ = 123$ kJ/mole)
- (2) Glycerol decomposition: $C_3H_8O_3 \leftrightarrow 3CO + 4H_2$ ($\Delta H^\circ = 245$ kJ/mole)
- (3) Water-gas shift: $CO + H_2O \leftrightarrow CO_2 + H_2$ ($\Delta H^\circ = -41$ kJ/mole)
- (4) Methanation: $CO_2 + 4H_2 \leftrightarrow CH_4 + 2H_2O$ ($\Delta H^\circ = -165$ kJ/mole)
- (5) Methane dry reforming: $CH_4 + CO_2 \leftrightarrow 2H_2 + 2CO$ ($\Delta H^\circ = 247$ kJ/mole)
- (6) Methane steam reforming: $CH_4 + H_2O \leftrightarrow 3H_2 + CO$ ($\Delta H^\circ = -206$ kJ/mole)

Hydrogen production from this reaction has been studied by many researchers focusing on the development of catalysts.

Cheng, Foo et al. studied on the mechanism of glycerol steam reforming over 5wt% Co-10wt% Ni/ Al_2O_3 catalysts prepared by wet coimpregnation. Typically, the reforming reaction is carried out at high temperature, but this system was operated in range of temperature 500-550°C under atmospheric pressure. The glycerol and water ratio was determined as function of partial pressure. It was found that products consist of H_2 , CO_2 , CO, and CH_4 . Although H_2 selectivity is a maximum value of 65%, but low H_2 yield is obtained of 5.19% at 500°C with glycerol concentration of 30 wt.%. In

addition, it was showed that increasing in glycerol partial pressure affected to decreasing slightly $H_2:CO$ ratio, whereas $H_2:CO$ ratio was increased with increasing steam partial pressure. The results indicated that both glycerol and steam affected to the formation of H_2 , whereas CO production dropped with increasing steam via water gas shift reaction[6].

Pompeo, Santori et al. studied glycerol steam reforming at temperatures lower than $450^\circ C$ and glycerol concentration of 10 wt.% using Pt catalysts supported on SiO_2 , ZrO_2 , $\gamma-Al_2O_3$ modified with Ce and Zr. 1%Pt loaded on supports were prepared by two methods: ion exchange and impregnation. It was found that SiO_2 support can promote the activity of Pt catalyst by C-C decomposition and dehydrogenation. At $350^\circ C$, Pt/ SiO_2 catalyst provided high conversion to gas of 100% and H_2 selectivity of 69% because it has high surface area. The obtained syngas comprised of H_2/CO ratio equal to 2.1 at $350^\circ C$ and space time of 1.5 minutes. Therefore, the Pt/ SiO_2 catalyst is suitable for synthetic gas production used as further reactant for methanol synthesis[7].

Sanchez and Comelli investigated deactivation process and catalyst regeneration during glycerol steam reforming reaction at temperatures $700^\circ C$ under atmospheric pressure. The process consists of four cycles (12 hours each one), which Ni/ Al_2O_3 catalyst in each cycle was generated by 50/50 helium/air at temperature between 30 and $700^\circ C$. The results showed that H_2 was the main product obtained from this process, while CO and CH_4 were formed in low amount. The H_2 production generated from steam reforming of glycerol in all of cycles was the same trend. Moreover, the results displayed that decreasing in H_2 production but increasing CO and CH_4 along with reaction time. This phenomenon can be explained that the catalyst occurs deactivation due to coke formation[8].

Kousi, Chourdakis et al. studied the effect of B_2O_3 and La_2O_3 loading on Ni/ Al_2O_3 catalysts for synthetic gas production or hydrogen via glycerol steam reforming. The result showed that Ni/ $B_2O_3-Al_2O_3$ catalyst had the highest surface area, whereas Ni/ $La_2O_3-Al_2O_3$ catalyst had the highest average pore diameter, and both catalysts are

acidic. The performance of catalysts was carried out by using a fixed bed plug-flow reactor with glycerol/water ratio of 20 wt.% and varying temperatures 400-600°C under atmospheric pressure. It was found that temperature between 400 and 600°C, the main products were acetol, acrolein, acetaldehyde, acetone and acetic acid. Above temperature 700°C, the result indicated that glycerol occurred cleavage severely to produce gaseous product composed of methane, ethylene, propane, CO, CO₂ and H₂, while glycerol conversion was completely of 100% by increasing temperature. These products are explained by reaction pathways as showed in Figure 4. Moreover, Kousi, Chourdakis et al. reported that the addition of La₂O₃ on the catalyst enhanced glycerol conversion and hydrogen yield. On the other hand, the B₂O₃ loading on the catalyst favored dehydration of glycerol pathway to acrolein[9].

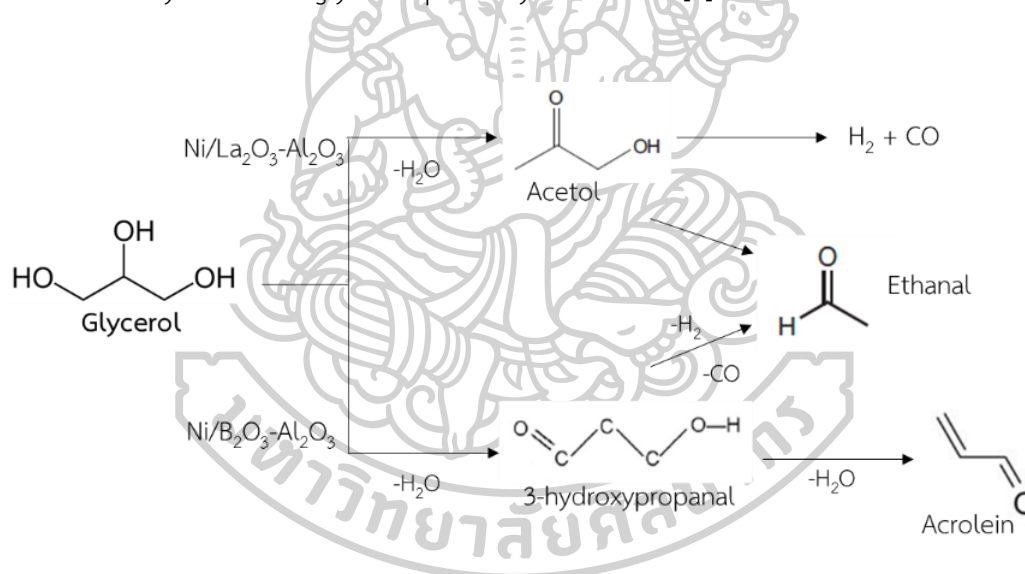


Figure 4 Reaction pathways of steam reforming of glycerol over modified Ni-based with different acidity.

Papageridis, Siakavelas et al. studied hydrogen production via the glycerol steam reforming reaction over Ni, Co, Cu supported on γ -alumina catalysts. Reaction was carried in a continuous flow, fixed-bed, single pass, tubular stainless steel reactor with glycerol concentration of 20 wt.% at temperature ranging from 400 to 750°C, atmospheric pressure. Prior to catalytic testing, 200 mg of undiluted catalyst was reduced in situ under a flow of 100 v/v % hydrogen at 800 °C for 1 hour. The result

was showed that selectivity of H_2 was 63%, 42% and 40% for Ni/Al, Co/Al and Cu/Al catalysts, respectively at 750°C and selectivity of CO was 79, 74 and 69% for Ni/Al, Co/Al and Cu/Al catalysts, respectively at 600°C . H_2 Yield was maximum using 4 mol/mol glycerol for Ni/Al catalyst at 650-750°C. To explain more detail about gas and liquid product distribution, the reaction pathways were drawn in the reaction scheme[10] showed in Figure 5.

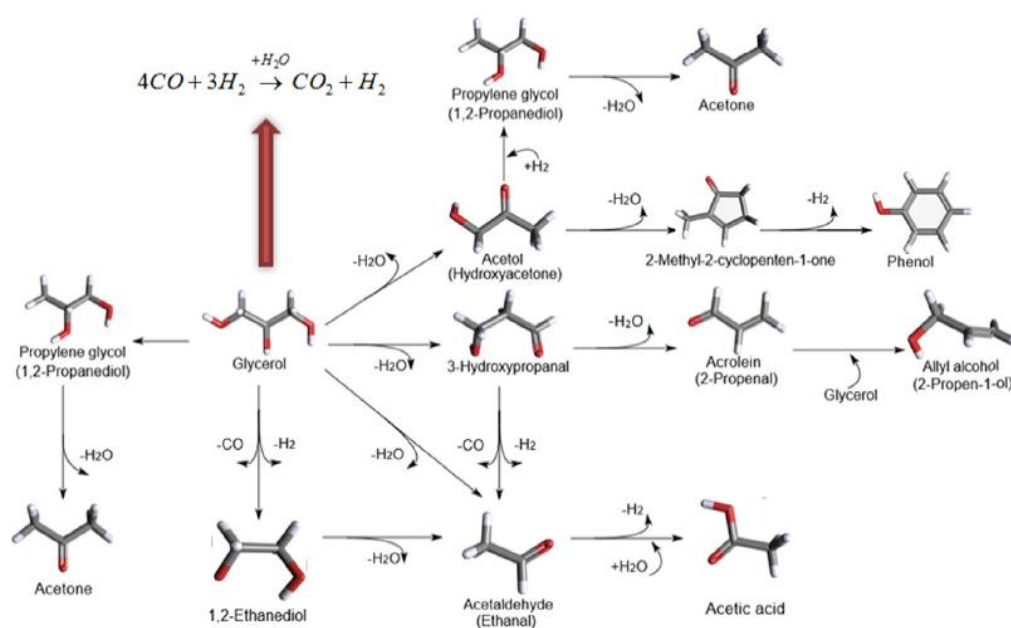


Figure 5 Reaction pathways for the glycerol steam reforming reaction.

Zarei Senseni, Seyed Fattahi et al. synthesized of 15wt.% Ni/Al₂O₃ catalyst by impregnation and design of experiments for glycerol steam reforming by a Box-Behnken design of response surface methodology. All 17 experimental runs were performed at the temperature 600-750°C and the ratio of glycerol to water with N₂/Ar (50/50%) carrier of 15 ml/min. The data were analyzed by analysis of variance (ANOVA) for response of glycerol conversion and production yield. The result showed that the predicted factors for the optimized condition of glycerol steam reforming reaction was GHSV 36,787 mL g⁻¹ h⁻¹, temperature 671.8°C and glycerol to water feed ratio at 9

resulted to glycerol conversion, H₂, CH₄, CO and CO production were found to be were 97.53%, 74.41%, 0.16%, 23.87% and 1.55% respectively[11].

2.2.2 Syngas production from glycerol

Synthesis gas (Syngas) is a mixture gas of hydrogen, carbon monoxide and carbon dioxide. Syngas can be produced by thermochemical from many sources such as natural gas, coal and biomass. Syngas is used in electricity generation and chemical industries such as synthetic hydrocarbon fuel, hydrogen, ammonium and methanol. Thus, the production of syngas from glycerol was interesting and approaching to many researchers.

Van Bennekom, Venderbosch et al. experimented by converting glycerol to syngas by glycerol reforming in supercritical water at pressure of 24-27 MPa and temperature of 675-725°C using Ni/CaO-6Al₂O₃ catalyst. Finally, the methanol synthesis from syngas was operated at the same pressure and reducing temperature to 195-245°C under Cu/ZnO/Al₂O₃ catalyst. The experiment was relatively complex, which carried on of five reforming reactors and three methanol synthesis reactors. In addition, the system had the recycling of effluent water to the reforming reactor and external H₂ was added to the methanol synthesis reactor. The results of glycerol reforming were showed high glycerol conversion of 95.0-99.9% and yielded syngas composition range of H₂/CO/CO₂/C_xH_y = 44-67/1-21/16-34/2-18 vol.%. In addition, hydrogen added to the system increased the CO, CO₂ and CH₄ ratios. The result was that the maximum yield of methanol was 0.62 kg methanol/kg glycerol for an experiment with a time on stream of 16 hours, which it corresponded to a carbon conversion of 60%. By-products including ethanol, 1-propanol and 2-butanol[12].

Gutiérrez Ortiz, Serrera et al. investigated the process design for the synthesis of methanol from syngas obtained from reforming of glycerol using super-critical water at high temperature (700-1000°C) and high pressure (240 bar). The whole process was simulated by AspenPlus™, NRTL and STEAMNBS methods as showed in Figure 6. The

results showed that the suitable condition of reforming process was water/glycerol mass ratio of 1.68 at 1000°C and purge ratio of 0.2, while the optimum condition of methanol synthesis was at 250°C and 85 bar. The methanol production under the optimum condition was 0.270 kg methanol/kg glycerol and overall energy efficiency was 38.0%[13].

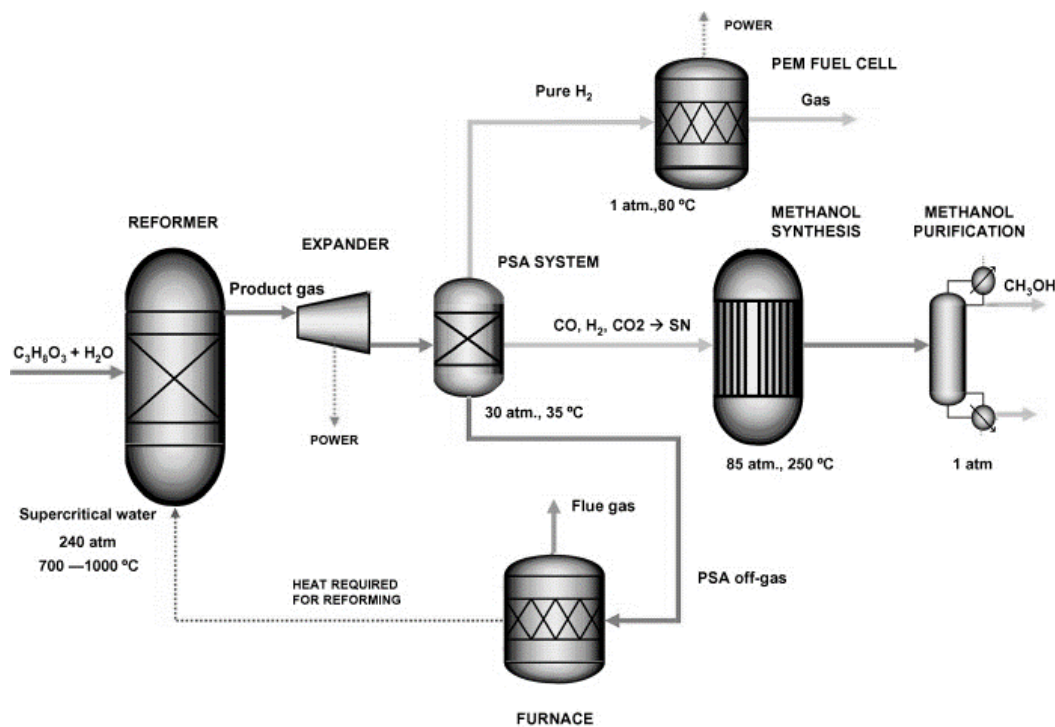


Figure 6 Block flow diagram of the synthesis of methanol from syngas obtained from reforming of glycerol.

Nor Shahirah, Abdullah et al. studied the kinetics of syngas production from glycerol via pyrolysis reaction over samarium (Sm) loaded on Ni/Al_2O_3 catalyst prepared by impregnation method. The results demonstrated that 3wt.%Sm on Ni/Al_2O_3 catalyst had more surface area than Ni/Al_2O_3 catalyst and its structural particle was very fine and porous. After catalytic testing, it was seen that adding of samarium (Sm) can improve the efficiency of Ni/Al_2O_3 catalyst, which it provided high glycerol conversion and syngas yield (H_2/CO ratio = 1.3–1.6). In addition, the results showed

the activation energy of Ni/Al₂O₃ catalyst was higher power consumption than 3wt.%Sm on Ni/Al₂O₃ catalyst[14].

2.2.3 Methanol synthesis from glycerol

According to the study of the formation of methanol from glycerol, it consist of two pathways. First, C–C bond cleavage in glycerol leads to ethylene glycol and methanol. Finally, the first dehydration of glycerol to acetol, further two-steps hydrogenation into ethanol and methanol with propylene glycol as an intermediate, and dehydration-hydrogenation to 1-propanol and 2-propanol[15-17] as showed in Figure 7. Generally, the nature of the obtained products depended on several parameters like the catalysts and the supports, the reaction conditions (temperature and pressure) which presented in the previous research as following.

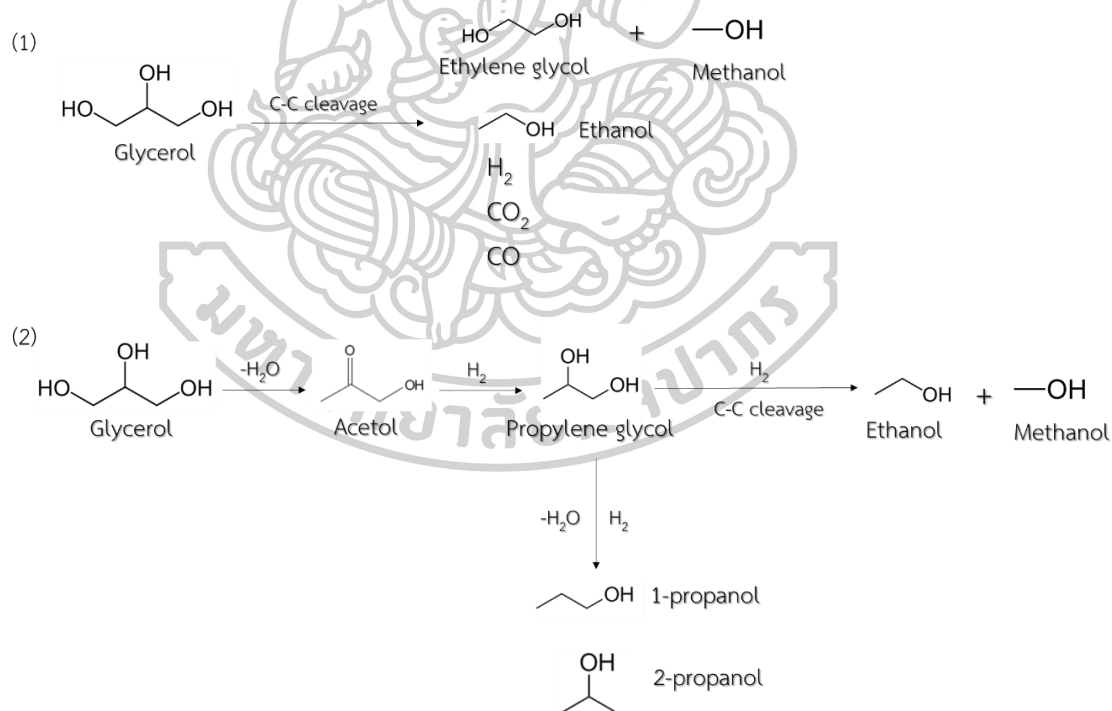


Figure 7 The reaction pathways for the formation of methanol from glycerol.

Mohamed, Ting et al. experimented to convert glycerol to methanol by HZSM-5 catalyst impregnated with different loading of Cu and Ni metal. The

performance of catalyst was carried out using a packed bed reactor at 500°C under atmospheric pressure for 4 hours. On the other hand, Cu/HZSM-5 catalyst showed methanol yield of 6.70%. Ni/HZSM-5 catalyst reduced the methanol yield because Ni based catalysts are promptly deactivated by the deposition of carbon on the active centres[18].

Carr, Shi et al. studied on methanol production from glycerol under supercritical water condition and the effect of ethylsulfide was spiked into the reactor. The result showed the highest yield of methanol at 450°C, 300 bar after 30 min residence time. Interestingly, they have proposed the direct methanol production pathway from glycerol occurs via reaction mechanism generator (RMG) modeling method in as showed in Figure 8. It was found that methanol was produced via the hydroxymethyl radical[19].

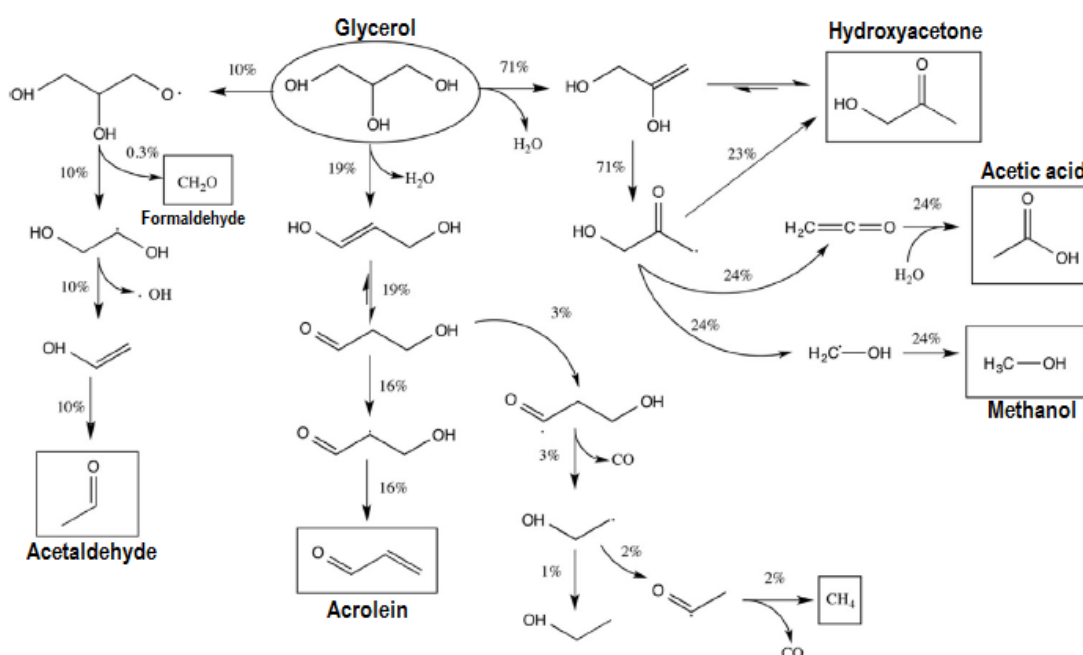


Figure 8 The reaction pathway model from methanol production from glycerol under supercritical water.

Haider, Dummer et al. studied synthesis of methanol from glycerol with various catalysts such as CaO, CeO₂, MgO and SrO. The reaction condition was operated at temperature of 175–400°C under atmospheric pressure with glycerol/H₂O ratio of 10–30 wt.% and catalyst content of 0.5-2 g. The obtained products were analyzed by gas chromatograph. The results displayed that conversion of glycerol increased with increasing temperature for all of catalysts. It was found that MgO, SrO and CaO catalysts provided the methanol space time yield of 7.1, 5.8 and 7.5 g_{methanol}kg_{cat}⁻¹h⁻¹ at 300°C, respectively, Moreover, it showed that CeO₂ catalyst had the highest activity of 19.0 g_{methanol}kg_{cat}⁻¹h⁻¹ for methanol synthesis from glycerol at high temperature compared with the other catalysts. In the addition, the methanol production from crude glycerol was investigated as well. The result displayed that the CeO₂ catalyst had glycerol conversion of 70% and methanol selectivity of 55% at 340°C by using weight of CeO₂ catalyst of 1.0 g with feed ratio of 15 wt.% glycerol/H₂O[16].

Samad, Goto et al. synthesized fluorine-doped tin oxide (FTO) catalyst for methanol synthesis from glycerol in sub-critical water. The experiments were carried in a stainless steel tube reactor using feed glycerol concentration 20wt.% and 0.01 g FTO catalyst at temperature 300°C and reaction time of 30-180 min. Then, the catalyst was separated from liquid product and washed using centrifugation with distilled water in order to remove any reactant after each reaction. The result showed that effect of temperature resulted to conversion of glycerol increased with increasing in the temperature from 150 to 300°C. Both conversion of glycerol and methanol selectivity increased from zero to nearly 80% and 100%, respectively. The recyclability result to the reaction time of 30 minutes was the best time, a conversion rate of 85% and then decreased to 77% at last cycle. Methanol selectivity of 100%, explained that under the sub-critical point of water, C-C and C-O bond cleavage occurred at an optimal rate[20].

2.3 Preparation of modified MgO catalysts

MgO catalyst is used to convert glycerol into methanol and other products as previously studied. As a result of that MgO contained surface sites of strong (low coordination O^{2-} anions), medium (oxygen in $Mg^{2+}-O^{2-}$ pairs) and weak (OH^- groups) basicity[21] affect to the reaction of glycerol. Therefore, this research investigated the modified MgO catalysts by loading metals Ca, Co and Cu for improvement of catalyst activity. The modified MgO catalyst was prepared as following.

2.3.1 Ca/MgO catalyst

Calcium oxide (CaO) is commonly used as a catalyst in chemical reactions, as cheap, easily available, non-corrosive, environmentally friendly, easy to handle material with low solubility and high basicity that can be regenerated and reused. In addition, CaO also serves as co-catalysts and promoter, which can be prepared by co-precipitation and impregnation method.

For the impregnation method, Ca precursor is dissolved in water, then the solution is added and finally, the catalyst is calcined at the temperature between $500^{\circ}C$ and $900^{\circ}C$ in order to transform the precursor to the active form to obtain CaO catalyst[22].

Daud and Vignesh et al. synthesized CaO/MgO catalysts by co-precipitation of $Ca(NO_3)_2 \cdot 4H_2O$ and $Mg(NO_3)_2 \cdot 6H_2O$. The precursors were mixed with ethanol and DI water as solvent and heat at $35^{\circ}C$. Then, 0.1 M NaOH was added dropwise into the mixture under stirring and washed several times using ethanol and DI water. The precipitates were then dried at $60^{\circ}C$ in air overnight and calcined at $650^{\circ}C$ and $800^{\circ}C$ for 2 hours using a muffle furnace with a heating rate of $10^{\circ}C/min$. The result showed that CaO/MgO catalyst has high surface and pore volume[23].

2.3.2 Co/MgO catalyst

Cobalt is used in chemical transformation of glycerol into valuable products such as hydrogen production, methane and 1, 2-propanediol. Therefore, interested in combination with MgO catalyst, and studied of the preparation as following.

Guo and Li et al. synthesized Co–MgO mixed oxide catalysts by co-precipitation method of $\text{Mg}(\text{NO}_3)_2 \cdot 6\text{H}_2\text{O}$ and $\text{Co}(\text{NO}_3)_2 \cdot 6\text{H}_2\text{O}$ in distilled water. After that, an aqueous solution of potassium carbonate was added with nitrate solution until achieving pH 10. Next, the formed precipitate was filtered and washed by distilled water for removing excess ions. Then, the precipitate was dried overnight at 110°C and calcined at 500°C with a heating rate of $3^\circ\text{C}/\text{min}$ for 6 hours. It was found that MgO, Co_3O_4 and minor MgCo_2O_4 phase were detected and the catalyst had high specific surface area[24].

2.3.3 Cu/MgO catalyst

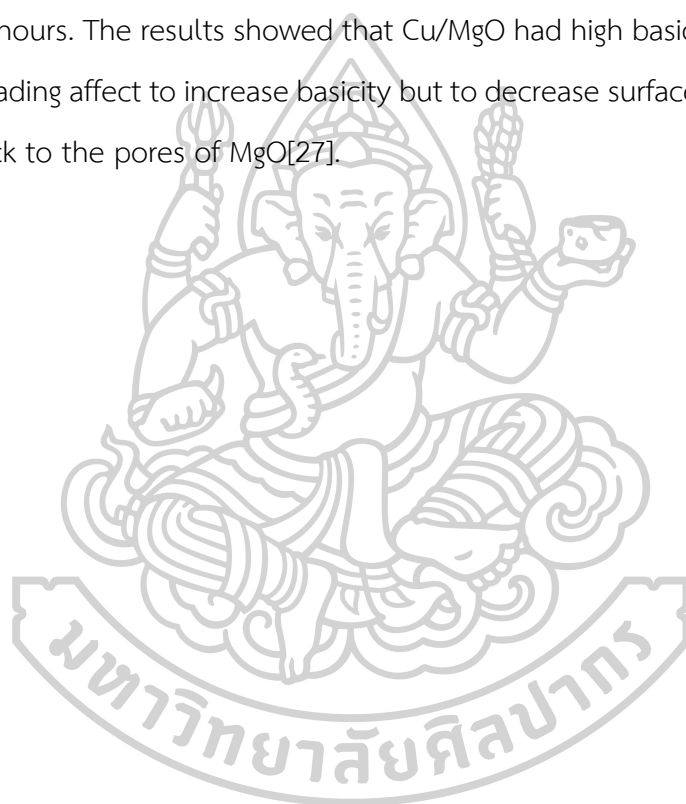
Copper is usually used in methanol synthesis and glycerol process. The Cu metal form is used in terms of metal oxide (CuO and Cu_2O) catalysts depending on the reaction. In this research, CuO/MgO catalyst and preparation methods were studied as following.

El-Molla synthesized CuO/MgO by wet impregnation of finely powdered $\text{Mg}(\text{OH})_2$ solid and aqueous solution of $\text{Cu}(\text{NO}_3)_2 \cdot 3\text{H}_2\text{O}$. Next, the precursor was dried in air at 100°C followed by calcination at 400°C and 500°C for 4 hours. It was found that increasing of the calcination temperature resulting in increasing the crystallite size of MgO and CuO while the surface area was slightly decreased [25].

Yuan and Wang et al. synthesized CuO/MgO by two preparation methods. Firstly, Cu/MgO catalyst was prepared by co-precipitation of $\text{CuCl}_2 \cdot 2\text{H}_2\text{O}$ and $\text{MgCl}_2 \cdot 6\text{H}_2\text{O}$ in distilled water. The aqueous Na_2CO_3 of 1 mol/L was added into the solution under stirring. After that, the precipitate was aged at room temperature for 12 hours followed by filtration. This precipitate was dried in ambient air at 110°C overnight and calcined at 550°C for 4 hours. In case of the CuO/MgO was prepared by wet impregnation, MgO was pretreated at 550°C for 4 hours before it was impregnated in aqueous solution of $\text{Cu}(\text{NO}_3)_2 \cdot 3\text{H}_2\text{O}$. Next, the catalyst was dried in ambient air at 110°C overnight, then followed by calcination at 550°C for 4 hours. The results showed

that CaO/MgO prepared by co-precipitation had high catalytic more than the catalyst prepared by wet impregnation for glycerol hydrogenolysis[26].

Zhou and Deng et al. synthesized Cu/MgO catalysts by co-precipitation of $\text{Cu}(\text{NO}_3)_2 \cdot 3\text{H}_2\text{O}$ and $\text{Mg}(\text{NO}_3)_2 \cdot 6\text{H}_2\text{O}$ in distilled water. The aqueous K_2CO_3 was added into solution under stirring for 30 min and then aged for 4 hours. Subsequently, the solid was separated by centrifugation and washed three times by using distilled water each time. Finally, the catalyst was dried in air at 110°C overnight and calcined at 400°C for 3 hours. The results showed that Cu/MgO had high basicity and surface area. When Cu loading affect to increase basicity but to decrease surface area, because Cu_xO and Cu block to the pores of MgO[27].



CHAPTER 3 THEORY

3.1 Catalyst

A catalyst is a substance that increases the reaction rate without itself being consumed. In addition, catalyst is a substance that convert substrates into products. Catalyst is divided into three types, based on the phase of the catalyst and substrate including solid, liquid and gas.

3.1.1 Homogeneous catalyst

The catalyst is in the same phase as the reactants. Typically, all the reactants and catalysts are either in one single liquid phase or gas phase. Most industrial homogeneous catalytic processes are carried out in liquid phase. Examples of such systems or catalysts are:

- General acid and base catalysis (ester hydrolysis),
- Lewis acids as catalysts (Diels-Alder reactions),
- Organic catalysts (thiazolium ions in Cannizzarro reactions),
- Porphyrin complexes (epoxidations, hydroxylations),
- Enzymatic processes,
- Co-ordination complexes (polyester condensations).

3.1.2 Heterogeneous catalyst[28]

The catalyst is in different phases as the reactants. For example, the reactions of liquid or gases in the presence of solid catalysts.

3.1.2.1 Steps in a Heterogeneous Catalytic Reaction

During an overall catalytic reaction, the reactants and products undergo a series of steps over the catalyst, including:

1. Diffusion of the reactants through a boundary layer surrounding the catalyst particle.

2. Intraparticle diffusion of the reactants into the catalyst pores to the active sites.
3. Adsorption of the reactants onto active sites.
4. Surface reactions involving formation or conversion of various adsorbed intermediates, possibly including surface diffusion steps.
5. Desorption of products from catalyst sites.
6. Intraparticle diffusion of the products through the catalyst pores.
7. Diffusion of the products across the boundary layer surrounding the catalyst particle.

Accordingly, different regimes of catalytic rate control can exist, including: (i) film diffusion control (Steps 1 and 7); (ii) pore diffusion control (Steps 2 and 6); and (iii) intrinsic reaction kinetics control (Steps 3 to 5) of catalyst performance. In addition to mass transfer effects, heat transfer effects can also occur in heterogeneous catalysis for highly exothermic or endothermic reactions.

3.1.2.2 Desired characteristics of a catalyst

1. The catalyst should exhibit good selectivity for production of the desired products and minimal production of undesirable byproducts.
2. The catalyst should achieve adequate rates of reaction at the desired reaction conditions of the process (remembering that achieving good selectivity is usually more important than achieving high catalytic activity).
3. The catalyst should show stable performance at reaction conditions for long periods of time, or it should be possible to regenerate good catalyst performance by appropriate treatment of the deactivated catalyst after short periods.
4. The catalyst should have good accessibility of reactants and products to the active sites such that high rates can be achieved per reactor volume.

3.1.3 Acid-base catalyst

3.1.3.1 Solid acid catalysts[29]

Solid acid catalysts are applicable to a plethora of acid-promoted processes in organic synthesis. They have served as important materials due to their various advantages such as:

- Separation of the products from the reaction medium is easy.
- Catalyst can be separated easily and re-used several times without loss of activity.
- Reactions are generally clean and products are obtained in high purity.
- Reactions are generally selective.

Solid acids can be described in terms of their Brønsted/Lewis acidity, the strength and number of these sites, and the morphology of the support (typically in terms of surface area and porosity). High product selectivity can depend on the fine-tuning of these properties. For example, acetal formation and hydrolysis reactions generally require medium acid strength sites, while electrophilic additions of alcohols or water to olefins, skeletal rearrangements, esterification, and alkylation reactions require strong acid sites. Likewise, the importance of the nature of the acid site is demonstrated in Friedel–Crafts alkylation reactions, where Lewis acid sites are required for alkylation of toluene using benzyl chloride, while Brønsted sites are preferred for reactions using benzyl alcohol. The synthesis of pure Brønsted and pure Lewis acid catalysts attracts a great degree of academic interest, although the latter is harder to achieve because Brønsted acidity often arises from Lewis acid-base complexation as showed in Figure 9.

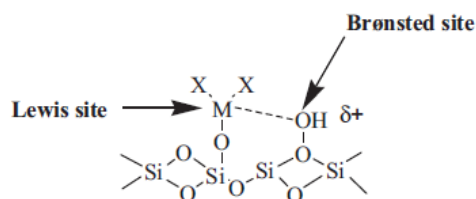


Figure 9 Brønsted acidity from inductive effect of Lewis acid centre coordinated to a silica support.

It has been showed that the type of support material used is acritical factor in the performance of the resulting supported catalyst or reagent in an organic reaction system. The main factors that should be considered when employing a material as a support are:

- thermal and chemical stability during the reaction process and for batch reactions during the separation stage;
- accessibility and good dispersion of the active sites.

There are numerous inorganic supports which can be used for supporting reagents such as zeolites, silicas, polymers, hydroxyapatite, zirconia, carbons etc. All of these materials have high surface area (100–1000 m²/g) and are normally porous with average pore diameters ranging from the microporous zeolites to some macroporous silicas. The particle size of these materials can range from coarse to very fine. However, the choice of support material for the preparation of supported reagents can be the more difficult step.

3.1.3.2 Solid base catalysts [30]

In the definition by Brønsted–Lowley, a base B⁻ accepts a proton from a reactant. In the definition by Lewis, a base B donates an electron pair to a reactant. Basic sites (B) abstract a proton from the reactant molecules (AH) to form anions (A⁻).



Here, the basic site B⁻ on the surface acts as a Brønsted base.

Examples of this type of the formation of anionic intermediates are 1-butene isomerization where an H⁺ is abstracted from C³ position to form allylic anion, and aldol condensation and Knoevenagel condensation where an H⁺ is abstracted from ketone with α -H to form anions.

Basic sites (B) donate an electron pair to form anionic intermediates. For example, ketones can be activated without proton transfer.



An example of this type of acid–base interaction is



Here, the basic site acts as a Lewis base.

Table 2 Types of solid base catalysts[30].

Type	Catalysts
1. Single component metal oxides	
- alkaline earth metal oxides	MgO, CaO, SrO, BaO
- rare earth oxide	La ₂ O ₃ , Sm ₂ O ₃
- other oxide	Al ₂ O ₃ , ZrO ₂ , Y ₂ O ₃ , ZnO, TiO ₂ , MoO ₃ , ThO ₂
2. Double components metal oxide	ZnO–Al ₂ O ₃ , MgO–TiO ₂
3. Zeolites	
- alkali ion-exchanged zeolites	Na–X, Cs–X
- alkali ion-added zeolites	Cs ₂ O/Cs–X
4. Supported alkali metal compounds	
- alkali metal compounds on alumina	Na ⁰ /Al ₂ O ₃ , Na ₂ O/Al ₂ O ₃
- alkali metal compound on silica	Na ⁰ /SiO ₂ , Na ₂ O/SiO ₂
- alkali metal ions on alkaline earth oxides	Na ₂ O/MgO
5. Clay minerals	
- hydrotalcite	Mg ₆ Al ₂ (OH) ₁₆ CO ₃ ·4H ₂ O
- chrysilite	Mg ₃ (Si ₂ O ₅)O ₃ (OH) ₄
- sepiolite	Mg ₄ Si ₆ O ₁₅ (OH) ₂
6. Non-oxide	
- KF supported on alumina	KF/Al ₂ O ₃
- lanthanide imide and nitride on zeolite	
- metal oxynitrides	ALPON, VALPON

An example of this type for base-catalyzed reaction is Tishchenko reaction where basic site donates an electron pair to the carbonyl C atom to form anionic intermediate. It should be noted that the same surface site can serve as either Brønsted base (proton acceptor) or Lewis base (electron pair donor) depending on the nature of the reactant. The naming of base should be based on its function (H^+ abstraction or electron pair donation).

Types of solid base catalysts are listed in Table 3.1. The reasons for which these catalysts are recognized as solid base catalysts are as following.

1. Characterization of the surfaces indicates the existence of basic sites. Color change of the acid–base indicators, adsorption of acidic molecules and spectroscopies indicate that basic site exist on the surfaces.
2. Catalytic activities correlated with the amount or strength of basic sites. In addition, the active sites are poisoned by acidic molecules such as CO_2 , H_2O , and HCl.
3. The reactions proceeding over the materials are similar to the “base-catalyzed reactions” which are well-known in homogeneous systems. These reactions include alkylation, isomerization, Michael addition, aldol addition, Tishchenko reaction, etc.
4. Mechanistic studies of the reactions and spectroscopic observations of the surface species indicate that anionic intermediates are involved in the reactions.

3.2 Design of experiment (DOE)

The design of experiment (DOE) is a statistical tool used in product research and development. Experimental design allows for the proper configuration of components or proportions of product components. The effects of factors and interactions can be studied in a single experiment. It helps to save on experiment costs and simplify calculations.

In this work, attention to experimental design techniques by response surface methodology (RSM). This is a popular way of expressing the ideal relationship equations, either by the curve equation or the quadratic equation.

3.2.1 Response surface methodology (RSM)

In statistics, response surface methodology (RSM) explores the relationships between several explanatory variables and one or more response variables. The method was introduced by George E. P. Box and K. B. Wilson in 1951. The main idea of RSM is to use a sequence of designed experiments to obtain an optimal response. Box and Wilson suggested that using a second-degree polynomial model to do this. They acknowledged that this model is only an approximation, but they used it because such a model is easy to estimate and apply. The steps in the application of RSM as showed in Figure 11. By design, this experiment uses central composite design, CCD by the Minitab program.

3.2.2 Central composite design, CCD

The central composite test is a highly efficient method for analyzing where the required curve equation is required. Generally, CCD has been widely used statistical method based on the multivariate nonlinear model for the optimization of process variables and also used to determine the regression model equations and operating conditions from the appropriate experiments. It is also useful in studying the interactions of the various parameters affecting the process[31]. Two factorial studies were performed by adding axial point experiments to analyze the quadratic equations. For the Minitab program, there are 3 types of axes.

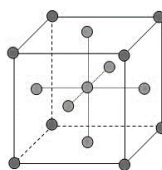


Figure 10 A face centered central composite design.

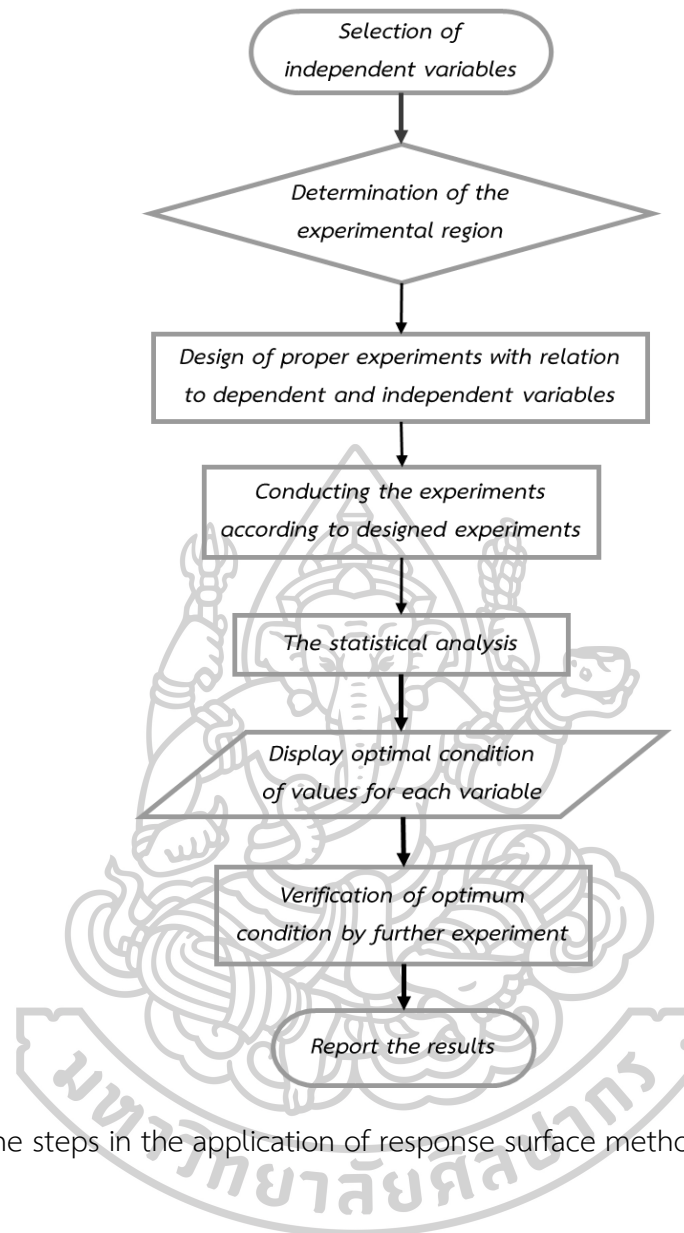


Figure 11 The steps in the application of response surface methodology (RSM)[11].

1. Default is to set the vertical axis to $n^{1/4}$ (n is the number of experiments that do not include the central position and repetition).
2. Face center is to change the vertical axis to -1 or +1, making it easy to experiment.
3. Custom is a customized point-to-point design for customization.

The CCD consists of $2n$ factorial runs (coded to the usual \pm notation) with $2n$ axial runs $(\pm\alpha, 0, 0, \dots, 0)$, $(0, \pm\alpha, 0, 0, \dots, 0)$, ..., $(0, 0, \dots, \pm\alpha)$ and center runs (six

replicates, 0, 0, 0,..., 0). The number of factors n increases the number of runs for a complete replicate of the design which is given in Eq. (3-4).

$$N = 2^n + 2n + n_c \quad (3-4)$$

Basically the optimization process involves three major steps: (1) performing the statistically designed experiments, (2) estimating the coefficients in a mathematical model and (3) predicting the response and checking the adequacy of the model[31].

The relationship between the variables and the response was calculated by the second order polynomial equation. The form of the full quadratic model is showed in Eq. (3-5) [32] as follows:

$$y = \beta_0 + \sum \beta_i x_i + \sum \beta_{ii} x_i^2 + \sum \beta_{ij} x_i x_j \quad (3-5)$$

R-Square is the most reliable factor for investigation of variability in independent variables. The R-square was calculated by Eq. (3-6) [11].

$$R^2 = \frac{SS_{\text{model}}}{SS_{\text{model}} + SS_{\text{Residual}}} \quad (3-6)$$

R^2 is the most important factor to show the variability of independent variables. Adj- R^2 which is a measure of the amount of variation around the mean determined by experiments and fitted for various terms in the model by Eq. (3-7) [11].

$$\text{Adj-}R^2 = \frac{SS_{\text{Residual}}/DF_{\text{Residual}}}{SS_{\text{model}} + \left(\frac{SS_{\text{Residual}}}{DF_{\text{Residual}}} + DF_{\text{model}} \right)} \quad (3-7)$$

CHAPTER 4 METHODOLOGY

4.1 Chemicals

This research studied direct methanol synthesis from pure and crude glycerol using modified MgO catalyst. Therefore, the chemicals were used as showed in Table 3-4.

Table 3 Chemicals list.

Name	Chemical formula	Company
Glycerol or glycerin	$C_3H_8O_3$	DAEJUNG
Magnesium oxide	MgO	TC Chemicals
Calcium nitrate tetrahydrate	$Ca(NO_3)_2 \cdot 4H_2O$	Ajax Finechem
Copper(II) nitrate trihydrate	$Cu(NO_3)_2 \cdot 3H_2O$	Sigma-Aldrich
Cobalt(II) nitrate hexahydrate	$Co(NO_3)_2 \cdot 6H_2O$	Ajax Finechem
Magnesium nitrate hexahydrate	$Mg(NO_3)_2 \cdot 6H_2O$	Alfa Aesar
Sodium hydroxide	NaOH	MERCK
Sodium carbonate anhydrous	Na_2CO_3	DAEJUNG
HYDRANAL™-Methanol dry	-	S.M. Chemical
HYDRANAL™-Composite 5	-	S.M. Chemical
Acetone	C_3H_6O	Ajax Finechem
DI water	-	
Nitrogen	N_2	TSG
Hydrogen	H_2	TSG
Air zero	-	TSG
Helium	He	TSG

Table 4 Crude glycerol component from GI Green Power Company limited.

Glycerol	65.69 wt.%
Ash	1.65 wt.%
water	0.05 wt.%
Methanol	4.21 wt.%

4.2 Equipment

The experiment was performed in a continuous reactor, which consists of 3 parts including input, reaction and output part. Equipment are listed as following.

- 4.2.1 Chemical bottle for entering, 500-1000 ml
- 4.2.2 Weighing, 3000 g
- 4.2.3 HPLC pump, flow rate 0.10-10.00 ml/min
- 4.2.4 Valve
- 4.2.5 Mass flow meter/controller, flow rate 0-300 ml/min
- 4.2.6 Pre-heater and Heater
- 4.2.7 Stainless steel fixed bed reactor of 1.50 cm diameter
- 4.2.8 Condenser
- 4.2.9 Chiller by AMPLECOOL
- 4.2.10 Gas counter, 17 times/min

The compositions of liquid products were analyzed by Agilent 7890B gas chromatography equipped with flame ionization detector (FID) and DB-1701 column. Meanwhile, gaseous products were determined on-line by means of Agilent 7890B gas chromatography equipped with thermal conductivity detectors (TCD) and MolSieve 13X column. Finally, the water content in liquid products was analyzed by Karl Fischer titration.



Figure 12 Equipment of reactor.

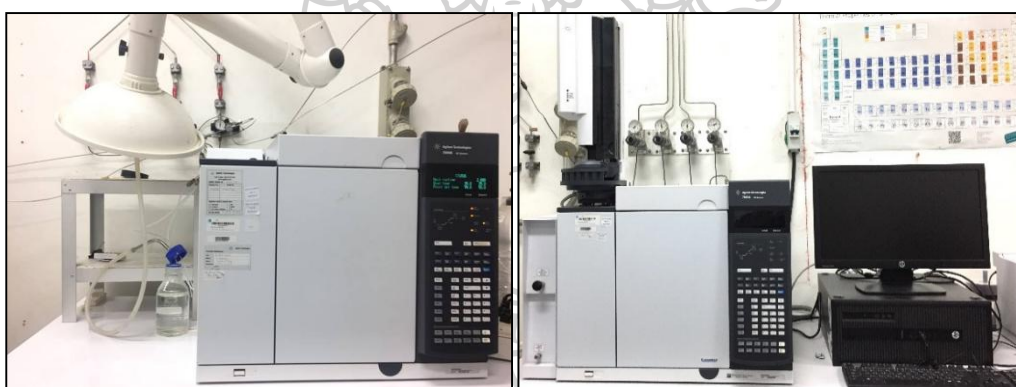


Figure 13 Gas Chromatography for gas and liquid products.



Figure 14 Karl Fischer titration

4.3 Catalyst preparation

4.3.1 Wet impregnation method

4.3.1.1 3%Ca/MgO catalyst

First, MgO catalyst was calcined at 650°C for 6 hours. Second, Calcium nitrate tetrahydrate ($\text{Ca}(\text{NO}_3)_2 \cdot 4\text{H}_2\text{O}$) as a precursor was dissolved in deionized water and then the solution was dropped into MgO catalyst. After that, the obtained 3wt.%Ca/MgO catalyst was dried at 120°C overnight and calcined at 600°C for 6 hour in air.

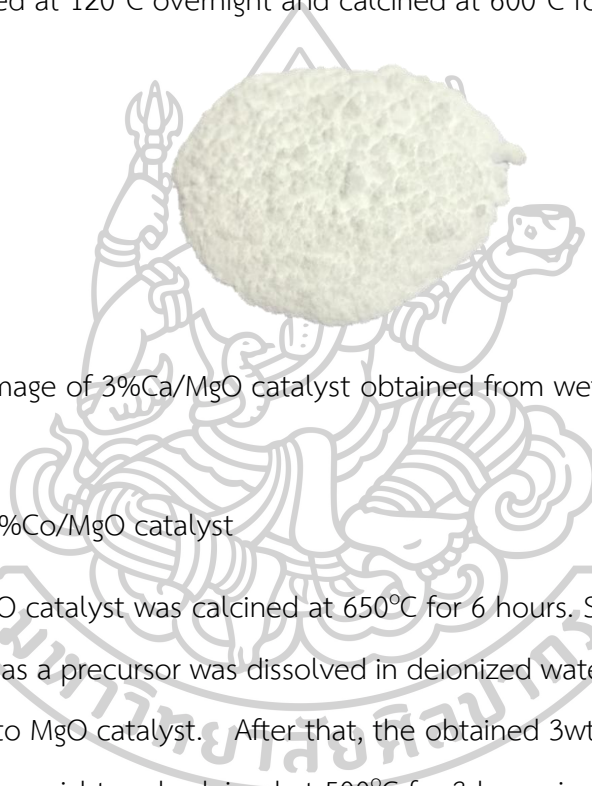


Figure 15 The image of 3%Ca/MgO catalyst obtained from wet impregnation method.

4.3.1.2 3%Co/MgO catalyst

First, MgO catalyst was calcined at 650°C for 6 hours. Second, Cobalt(II) nitrate ($\text{Co}(\text{NO}_3)_2 \cdot 6\text{H}_2\text{O}$) as a precursor was dissolved in deionized water and then the solution was dropped into MgO catalyst. After that, the obtained 3wt.%Co/MgO catalyst was dried at 105°C overnight and calcined at 500°C for 3 hours in air.



Figure 16 The image of 3%Co/MgO catalyst obtained from wet impregnation method.

4.3.1.3 3%Cu/MgO catalyst

First, MgO catalyst was calcined at 650°C for 6 hours. Second, Copper (II) nitrate trihydrate ($\text{Cu}(\text{NO}_3)_2 \cdot 3\text{H}_2\text{O}$) as a precursor was dissolved in deionized water and then the solution was dropped into MgO catalyst. After that, the obtained 3wt.%Cu/MgO catalysts was dried at 110°C overnight and calcined at 550°C for 4 hours in air.



Figure 17 The image of 3%Cu/MgO catalyst obtained from wet impregnation method.

4.3.2 Co-precipitation method

3%Ca/MgO catalyst was prepared by co-precipitation. The solution of mixed Magnesium nitrate hexahydrate, ($\text{Mg}(\text{NO}_3)_2 \cdot 6\text{H}_2\text{O}$) and Calcium nitrate tetrahydrate ($\text{Ca}(\text{NO}_3)_2 \cdot 4\text{H}_2\text{O}$) was prepared in DI water. For a typical catalyst preparation, an aqueous solution of Na_2CO_3 and NaOH with molar ratio of 3:1 was prepared and was added to the mixture, pH value of 10-11. The mixture was vigorously stirred in water bath at 70°C for 1 hour and then aged for an additional 1 hour. After vacuum filtration, the solid was washed with DI water, pH value was 7. Finally, solid was dried at 60°C overnight and calcination was carried out in air at 600°C for 6 hours.



Figure 18 The image of 3%Ca/MgO catalyst obtained from co-precipitation method.

4.4 Catalytic activity evaluation

Direct methanol synthesis from glycerol is performed in a stainless steel fixed bed reactor (Diameter 1.50 cm). The aqueous glycerol (glycerol in water 10-15 wt.%) feed is introduced using an HPLC pump with a precisely controlled flow rate of 0.1-0.3 ml/min into a preheater at 230°C. The fluid is flowed by combining with nitrogen carrier at 70 ml/min. The reaction is continuously operated ranging of temperature 240-390°C under atmospheric pressure and using 4 g of catalysts. The product are condensed by cooling water, and stored in a product trap. The liquid product is sampled every hour and gas product is passed to gas chromatography analyzer.

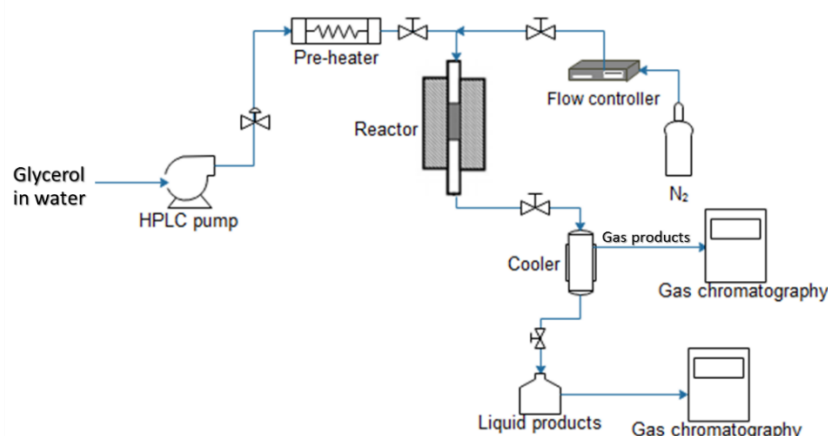


Figure 19 Block flow diagram of direct methanol synthesis from glycerol.

4.5 Design of experiments for direct methanol synthesis from glycerol

Design experiments to find the optimal conditions for direct methanol synthesis from glycerol using response surface methodology (RSM) is set using central composite design, CCD. Experimental design and data analysis were performed by using Minitab 17 program.

4.5.1. The variables were studied of glycerol concentration of 5-15 wt.%, temperature of 270-390°C and feed flow rate of 0.1-0.3 ml/min. The required factors

were run at only five levels that are represented by [-1.6818, 1, 0, 1, 1.6818] and experimental ranges of each independent variable are given in Table 5. The output responses were glycerol conversion and methanol yield.

Table 5 Experimental range and levels for central composite design.

Independent variables	Range and level				
	-1.68	-1	0	1	1.68
Glycerol concentration (wt.%)	1.59	5	10	15	18.41
Temperature (°C)	229.09	270	330	390	430.91
Feed flow rate (ml/min)	0.03	0.1	0.2	0.3	0.37

4.5.2. The central composite design was divided into 20 runs. Defined code and response in each experiment design are showed in Table 6. Codes are transformed into real valued of each parameters are showed in Table 7. Experiments were run in sequence.

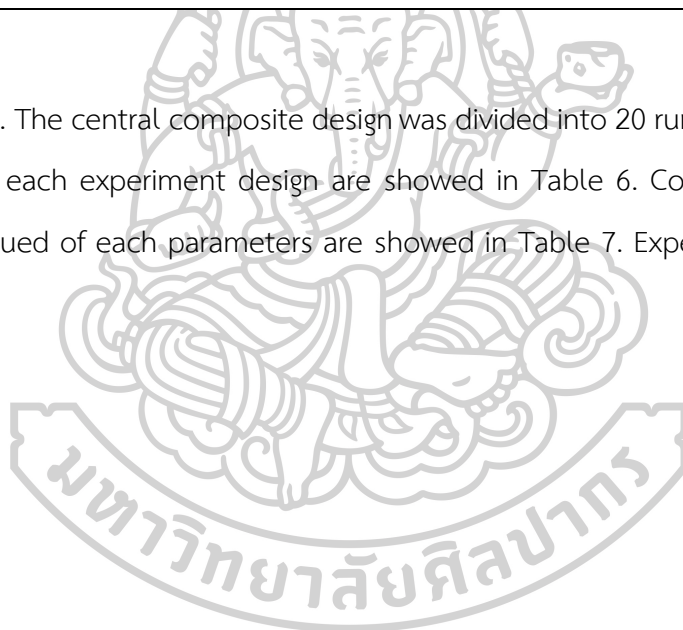


Table 6 Experimental design and code levels for central composite design.

Run Order	Code level			Response	
	Glycerol concentration	Temperature	Feed flow rate	Glycerol conversion	Methanol yield
1	-1	-1	-1		
2	1	-1	-1		
3	-1	1	-1		
4	1	1	-1		
5	-1	-1	1		
6	1	-1	1		
7	-1	1	1		
8	1	1	1		
9	-1.68179	0	0		
10	1.68179	0	0		
11	0	-1.68179	0		
12	0	1.68179	0		
13	0	0	-1.68179		
14	0	0	1.68179		
15	0	0	0		
16	0	0	0		
17	0	0	0		
18	0	0	0		
19	0	0	0		
20	0	0	0		

Table 7 Experimental design and Independent variables for central composite design.

Run Order	Independent variables			Response	
	Glycerol concentration (wt.%)	Temperature (°C)	Feed flow rate (ml/min)	Glycerol conversion (%)	Methanol yield (%)
1	5	270	0.1		
2	15	270	0.1		
3	5	390	0.1		
4	15	390	0.1		
5	5	270	0.3		
6	15	270	0.3		
7	5	390	0.3		
8	15	390	0.3		
9	1.591	330	0.2		
10	18.409	330	0.2		
11	10	229.093	0.2		
12	10	430.908	0.2		
13	10	330	0.0318		
14	10	330	0.368		
15	10	330	0.2		
16	10	330	0.2		
17	10	330	0.2		
18	10	330	0.2		
19	10	330	0.2		
20	10	330	0.2		

4.6 Product analyses and Catalyst characterization

4.6.1. Gas Chromatography

Gas Chromatography is used in analytical chemistry for separating and analyzing compounds that can be vaporized without decomposition. Typical uses of gas chromatography are to test the purity of a particular substance, or separating the different components of a mixture. The gas composition of the off gas from the process was analyzed using an online PoraPLOT Q-HT column as chromatograph equipped with flame ionization detector, online MolSieve 13X column and Porapak Q column gas chromatograph equipped with thermal conductivity detectors. The liquid composition from the process was analyzed using DB-1701 column gas chromatograph equipped with flame ionization detector.

4.6.2. Karl Fischer titration

Karl Fischer titration is a classic titration method in analytical chemistry that uses coulometric or volumetric titration to determine trace amounts of water in a sample. The liquid product from the process is used to analyze the amount of water prior to analysis by gas chromatograph.

4.6.3. X-Ray diffraction (XRD)

X-ray diffraction (XRD) is a rapid analytical technique primarily used for phase identification of a crystalline material and can provide information of catalyst on unit cell dimensions. The analyzed material is finely ground, homogenized and determined the average bulk composition. XRD is a technique for the study of crystal structures and atomic spacing of catalyst. XRD is based on constructive interference of monochromatic X-rays and a crystalline sample.

X-ray diffraction (XRD) patterns for phase identification of catalysts were obtained in a 2θ range of $2-80^\circ$ on Rigaku diffractometer using $\text{Cu K}\alpha$ radiation, 40kV, 40mA ($\lambda=1.541862 \text{ \AA}$).

4.6.4. Scanning electron microscopy (SEM) with Energy Dispersive X-ray Spectroscopy (EDX/EDS)

The scanning electron microscope (SEM) produces images of a sample by scanning the sample with a focused beam of electron. The electrons interact with atoms in the sample, producing various signals that can be detected and that contain information about the sample's surface including external morphology (texture), chemical composition, crystalline structure and orientation of materials making up the sample. The electron beam is generally scanned in a raster scan pattern, and the beam's position is combined with the detected signal to produce an image. An Energy Dispersive X-Ray Analyser (EDX or EDA) is also used to provide elemental identification and quantitative compositional information.

The morphologies of samples were investigated by using scanning electron microscope (SEM: TESCAN VEGA3) operating at 20 kV. The elemental compositions of the modified catalysts were determined by using energy dispersive x-ray analyser (EDX: OXFORD instrument X-MaxN).

4.6.5. N₂ physisorption equipment

N₂ physisorption equipment is used to characterise porous materials allowing for the determination of specific surface area, pore size distribution and pore volume. N₂ physisorption equipment is used in surface area measurements of powder samples and pore size distribution. The equipment determines needed gas quantity to cover the sample surface with a molecular layer and calculates surface area using Brunauer, Emmett and Teller (BET) theory. The equipment analyses active surface area in m²/g unit with chemical absorption technique.

Specific surface area, pore size distribution and pore volume were determined by N₂ physisorption at -196°C, using BEL JAPAN, INC. Prior to the measurement, the samples were degassed at 200°C for 2 hours.

4.6.6. X-Ray fluorescence spectroscopy (XRF)

XRF can be used to identify the type and amount of metal contained in an alloy compounds or mixed oxide. The principle of this technique is firing X-rays down to the sample, then detect the x-rays emitted from the sample by relaxation process. The amount of X-ray measurement is showed as a function versus energy.

4.6.7. Temperature Programmed Desorption of carbon dioxide

CO₂-TPD has been widely used to study the adsorption of gas on a catalyst and characterize the basicity of alkali and alkaline earth-modified metal oxide catalyst. This technique is performed by the surface area of the sample that adsorbs the gas until it is saturated, then increasing the temperature and measuring the concentration of gas desorbed. The result shows the temperature as peaks appear and indicates the amount of basic site then calculated from the area under graph.

The basicity of catalysts were studied by CO₂-TPD. The catalysts were preheated under helium stream at 150°C for 1 hour. Next, the temperature was decreased to 100°C and then CO₂ (30 ml/min) was subsequently introduced into reactor for 1 hour. The CO₂-TPD was carried out between 100 and 800°C (10°C/min) under a helium flow (30 ml/min).

CHAPTER 5 RESULTS AND DISCUSSIONS

According to the academic report in title of “Reforming of Methanol from Glycerol for reuse in Biodiesel Production” by Thailand Institute of Scientific and Technological Research (TISTR), it was demonstrated that methanol can be produced as major product from glycerol over MgO catalyst in a one step. Moreover, by-products comprised of ethanal, ethanol, propanol, 2,3-butanedione, acetol, ethylene glycol, CO and CO₂ were also detected as showed in Table 8. The experiments were carried out using a stainless steel fixed bed reactor in laboratory scale at reaction temperature between 270 and 390°C under atmospheric pressure with glycerol concentration in range of 10–30 wt.% and feed flow rate of 0.1- 0.5 ml/min. The results showed that the MgO catalyst provided glycerol conversion and the highest methanol yield of 67.71% and 18.38%, respectively, at 330°C with 10 wt.% glycerol/H₂O and 0.1 ml/min feed flow.

In this study, first, the activity improvement of MgO catalyst with metal oxide loading such as CaO, CoO and CuO were prepared by wet impregnation method. Second, the design of experimental (DOE) for direct methanol synthesis from glycerol using response surface methodology (RSM). Then, the optimum condition was investigated with crude glycerol by using the best modified catalyst. Finally, the comparison of catalyst preparation between wet impregnation and co-precipitation method for activity of the catalyst with crude glycerol. These catalysts were analyzed structural and chemical properties such as surface area, pore volume, pore size, crystal structure and basicity, etc.

Table 8 The performance of methanol synthesis from glycerol over MgO catalyst.

Glycerol Conversion (%)	Product distribution (%)									Methanol Yield (%)
	CO ₂	CO	Ethanal	Methanol	Ethanol	Propanol	2,3-Butanedione	Acetol	Ethylene glycol	
67.71	9.78	2.80	16.90	38.92	6.41	5.16	2.55	13.51	3.99	18.38

5.1 The effect of metal oxide loaded on MgO catalyst on performance of direct methanol synthesis from glycerol

5.1.1 Characterization of modified MgO catalysts

In this research, the metal oxide such as CaO, CoO and CuO were used as promoter to improve the catalytic activity of MgO catalyst. The modified MgO catalysts were prepared by wet impregnation at constant metal oxide amount of 3wt.%, which were denoted as 3%Ca/MgO, 3%Co/MgO and 3%Cu/MgO catalyst. The physical properties including BET surface area, pore volume and mean pore diameter of MgO and modified MgO catalyst were summarized in Table 9. The MgO catalyst had BET surface area, pore volume and mean pore diameter of 29.60 m²/g, 0.085 cm³/g and 11.503 nm, respectively. After metal loading on MgO catalyst, it was found that 3%Co/MgO catalyst had highest surface area (67.7 m²/g) than 3%Cu/MgO (53.60 m²/g) and 3%Ca/MgO (39.95 m²/g) catalyst. The report of Mirzaei, F., et al. explained that the specific surface area of the catalyst enhances contact between the reactant molecules and the catalytic active sites[24], which occurred to solid catalyst. On the other hand, 3%Ca/MgO catalyst had highest pore diameter (50.94 nm) than 3%Cu/MgO (40.14 nm) and 3%Co/MgO (13.14 nm) catalyst due to CaO has large pore diameter[33]. This indicated that the metal oxide loading enhanced the physical properties of modified MgO catalyst.

Table 9 Modified MgO catalyst properties by using BET technique.

Catalyst	Surface area (m ² /g)	Pore volume (cm ³ /g)	Mean pore diameter (nm)
MgO	29.60	0.09	11.50
3%Ca/MgO	39.95	0.51	50.94
3%Cu/MgO	53.60	0.54	40.14
3%Co/MgO	67.70	0.22	13.14

In addition, the nitrogen adsorption/desorption isotherm of MgO and modified MgO catalyst were presented in Figure 20. The MgO catalyst displayed a type IV isotherm (following the IUPAC 1985 classification of adsorption isotherms), which was associated with capillary condensation taking place in mesopores. The hysteresis loop according to the type H₃, suggesting that aggregates of plate-like particles giving rise to slit-shaped pores [34, 35]. For 3%Ca/MgO and 3%Cu/MgO catalyst, it was showed that a type II isotherm based on IUPAC's classification which exhibited multilayer adsorption[36]. Whereas, 3%Co/MgO catalyst showed a type IV isotherm with hysteresis loop, type H₃, similar to MgO catalyst.

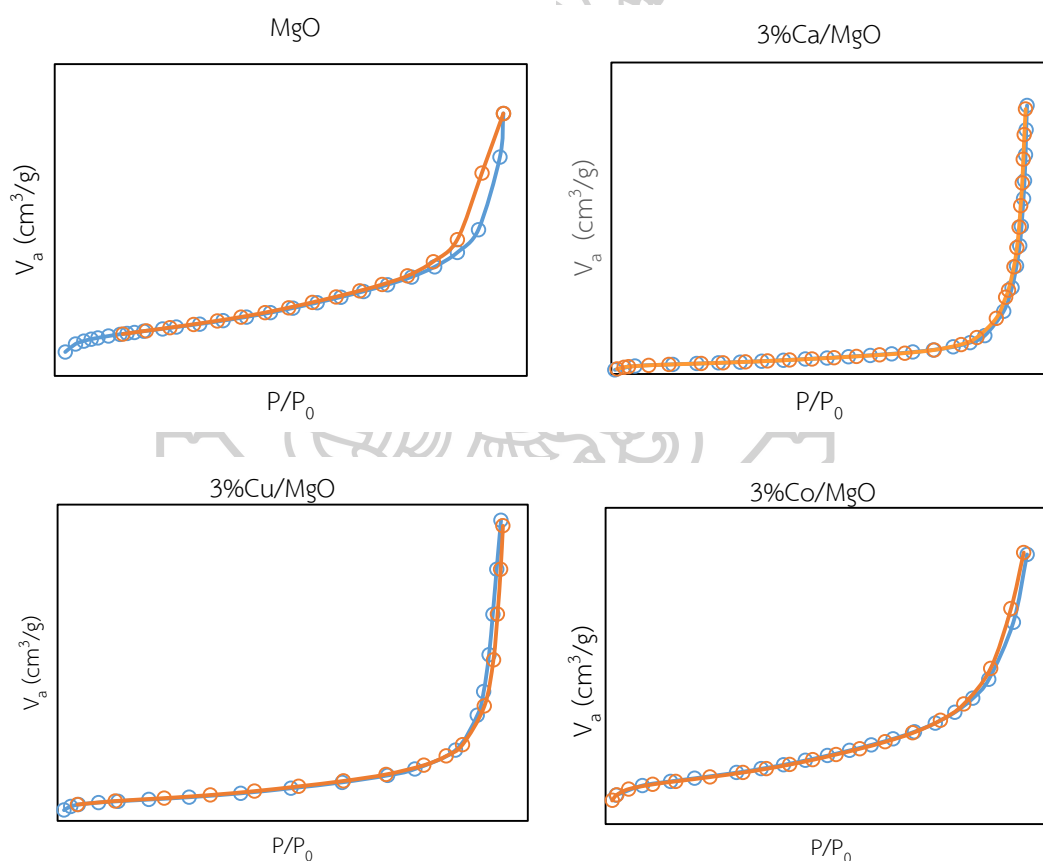


Figure 20 N₂ adsorption/desorption isotherm of MgO, 3%Ca/MgO, 3%Cu/MgO and 3%Co/MgO catalyst.

The XRD patterns of fresh catalysts are showed in Figure 21. After calcination at 650°C, the XRD pattern of the MgO catalyst appeared diffraction peaks at 2θ of

37.0°, 43.0°, 62.5°, 74.6° and 78.4°, corresponding to MgO phase (JCPDS: 78-0430) [37, 38]. Impregnation metal oxide including CaO, CoO and CuO on MgO catalyst did not affect the phase of MgO. However, the XRD pattern of 3%Ca/MgO catalyst showed additional diffraction peak at 2θ of 32.2°, 37.36° and 53.8°, consistent with characteristic of CaO phase (JCPDS: 77-2376) [38]. For 3%Co/MgO catalyst showed only the diffraction peaks of MgO phase. Typically, the XRD patterns of CoO was overlapped with peaks of MgO (JCPDS: 87-0653), Co_3O_4 (JCPDS: 74-1656) and Co_2MgO_4 (JCPDS: 02-1073) [24, 39]. It also appeared that intensity of MgO crystalline peaks decreased and no other diffraction peaks corresponding to other species are found. Therefore, the cobalt oxide was highly dispersed in low cobalt content catalysts and nanocrystalline structure [24, 39]. Meanwhile, the XRD pattern of 3%Cu/MgO catalyst was not observed the diffraction peak of CuO, suggesting that the CuO was either amorphous or highly dispersed[40].

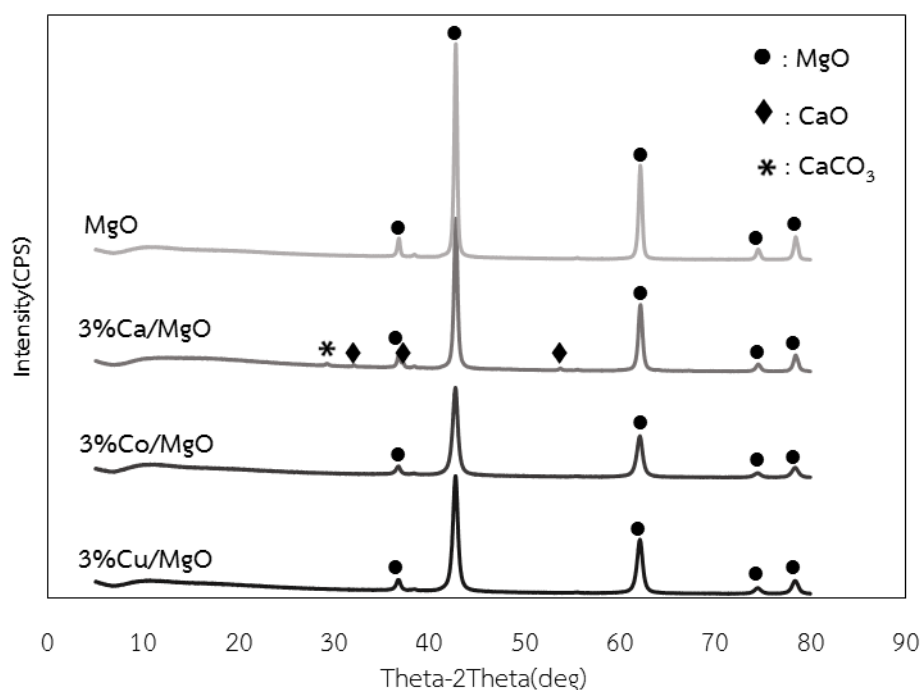


Figure 21 XRD pattern of MgO, 3%Ca/MgO, 3%Co/MgO and 3%Cu/MgO catalyst.

The morphology of catalysts were investigated by means of scanning electron micrograph (SEM) as showed in Figure 22. The result demonstrated that MgO catalyst

was uncertain shape and small particles. The addition of metals improved aggregation and particle size as a result of porosity. The 3%Ca/MgO catalyst showed that the size of particles was large and exposing rough surface. Meanwhile, 3%Co/MgO and 3%Cu/MgO catalysts had many porous agglomerates with irregular shaped small particles [41, 42]. Then, the distribution of metal elements on MgO catalyst represented by EDX elemental mapping were showed in Figure 23. It was found that the good distribution of Ca, Co and Cu element on MgO catalyst. Moreover, the analysis resulted in the XRF technique proved that the metal loading into the MgO catalyst at 3 wt.% as resulted in Table 10. It was confirmed that the metal oxide loading (CaO, CoO and CuO) was found into modified MgO catalyst prepared by impregnation method.

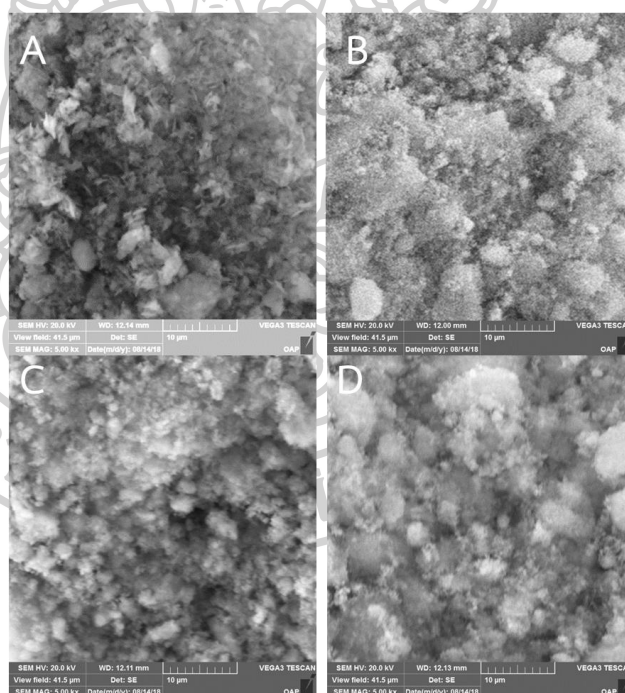


Figure 22 SEM images of (A) MgO, (B) 3%Ca/MgO, (C) 3%Cu/MgO and (D) 3%Co/MgO catalyst.

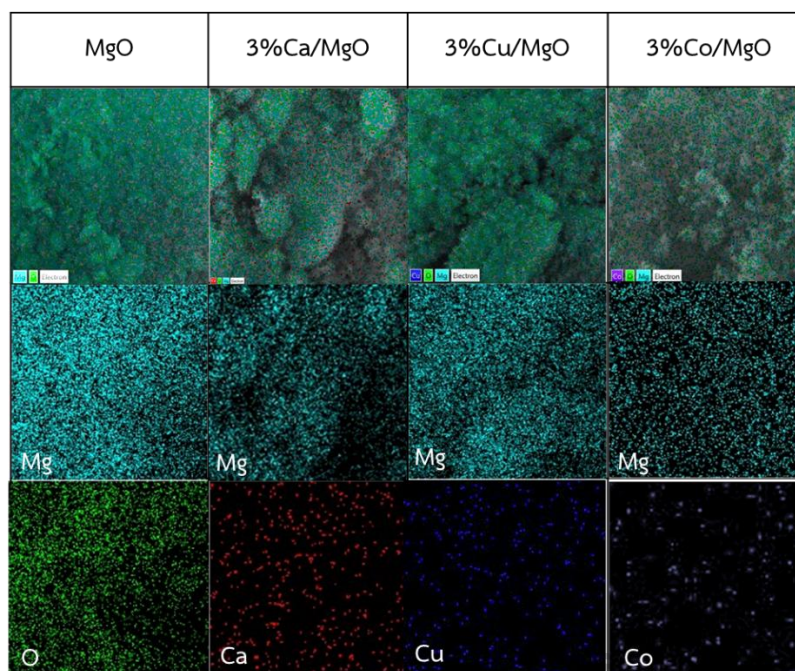


Figure 23 EDX elemental mapping of MgO, 3%Ca/MgO, 3%Co/MgO and 3%Cu/MgO catalyst.

Table 10 The elemental composition of the modified MgO catalyst by using XRF technique.

3%Ca/MgO			3%Cu/MgO			3%Co/MgO		
Mg	Ca	unknown	Mg	Cu	unknown	Mg	Cu	unknown
60.0	3.3	36.7	60.0	3.3	36.7	60.0	3.5	36.5

CO₂-TPD profiles of the MgO and modified MgO catalysts are displayed in Figure 24. Typically, MgO catalyst had three desorption band at below 200°C, 200-300°C and 300-850°C, which assigned to the interaction of CO₂ with basic sites of weak, medium and strong strengths, respectively[21, 43]. Therefore, MgO catalyst presented certain medium base sites which chemical adsorption peak appeared at 280°C. After metals oxide (Ca, Co and Cu) loaded on MgO catalyst, the very broad desorption band extending from 100-400°C related to the interaction of CO₂ with basic sites of weak

and medium mainly associated with $\text{Mg}^{2+}\text{-O}^{2-}$ pair. It was found that 3%Ca/MgO catalyst showed a CO_2 desorption band around 500-700°C, which associated with $\text{Ca}^{2+}\text{-O}^{2-}$ pairs[33]. Thus, 3%Ca/MgO catalyst had high basicity. For 3%Co/MgO and 3%Cu/MgO catalyst, the chemical adsorption peak appeared 200-300°C, which defined as medium-strong basicity[39]. Therefore, the 3%Co/MgO catalyst possessed more and stronger basic sites than the 3%Cu/MgO because there was more desorption peak area.

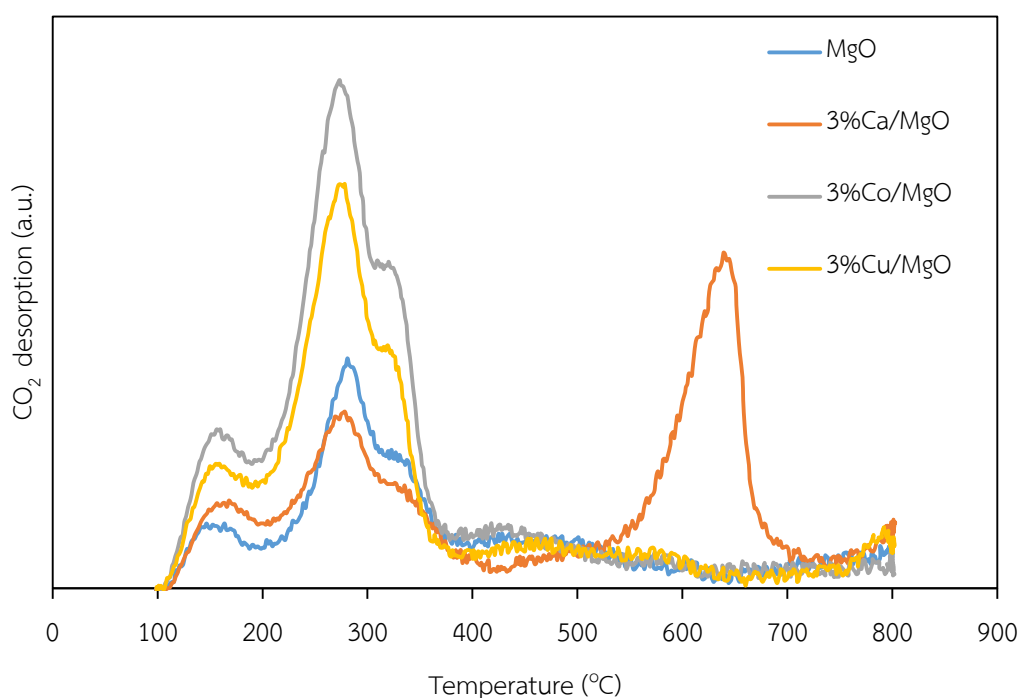


Figure 24 CO_2 -TPD of MgO, 3%Ca/MgO, 3%Co/MgO and 3%Cu/MgO catalyst.

5.1.2 Catalyst activity in direct methanol synthesis from glycerol

The reaction results of direct methanol synthesis from glycerol over MgO catalyst and modified MgO catalysts at 10wt.% glycerol concentration, 0.1 mL/min feed flow rate, 330°C under atmospheric pressure for 10 hours are showed in Figure 25. The glycerol conversion increased from 67.71% to 97.48% when loaded of metal oxide on MgO catalyst, it was indicated that all metal oxide was promoter. Therefore, the glycerol conversion appeared in an order of 3%Ca/MgO (97.48%) > 3%Co/MgO

(95.79%) > 3%Cu/MgO (95.62%) > MgO (67.71%), respectively. It can be seen that high methanol yield was 20.17% and 18.65% for 3%Ca/MgO and 3%Co/MgO catalyst, respectively. On the other hand, 3%Cu/MgO catalyst caused the decrease of methanol yield to 11.56%. It was indicated that the surface area, pore size and basicity of modified MgO catalyst, which improved interaction between metal oxides and generation of more metallic sites, the activity increases[24].

Figure 26 shows the products distribution, methanol is a main product for all catalysts. It was found that CO₂ and ethanol were increased significantly, whereas acetol was decreased obviously for all modified MgO catalysts. In addition, propanol, 2,3-butanedione and ethylene glycol decreased slightly. It can be proposed reaction mechanism of glycerol from the literature reviews, as showed in Figure 27. Methanol was produced from glycerol into two pathways. First, glycerol dehydration to form acetol and then double hydrogenolysis to propylene glycol, ethanol and methanol. By the same mechanism, propylene glycol lead to the by-products such as ethanal (acetaldehyde) [44], 1-propanol, 2-Propanol[15, 17] and 2,3-butanedione[16]. Second, methanol was produced directly from glycerol via a C-C bond cleavage reaction by ethylene glycol as a by-product. Furthermore, CO, CO₂ and H₂ were formed through over decomposition and reforming reaction [15-17, 44]. It was concluded that 3%Ca/MgO and 3%Co/MgO catalyst enhanced methanol yield, which was expected as a result of increasing basicity of these catalysts. However, Cu loading improving side reaction to CO₂ and H₂ due to partial alcohol reforming[45].

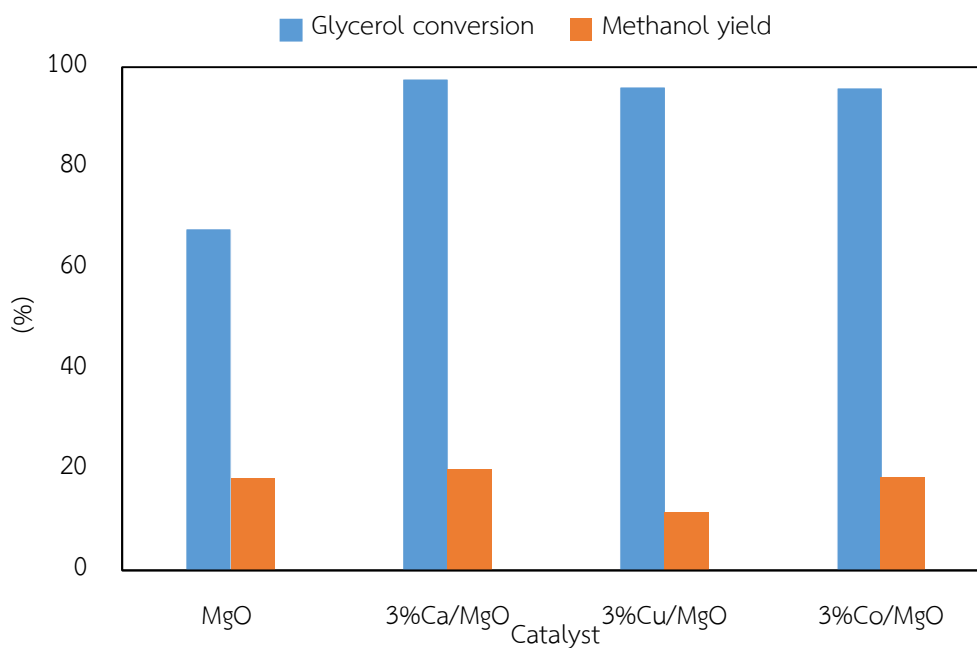


Figure 25 Glycerol conversion and methanol yield over MgO and modified MgO catalysts.

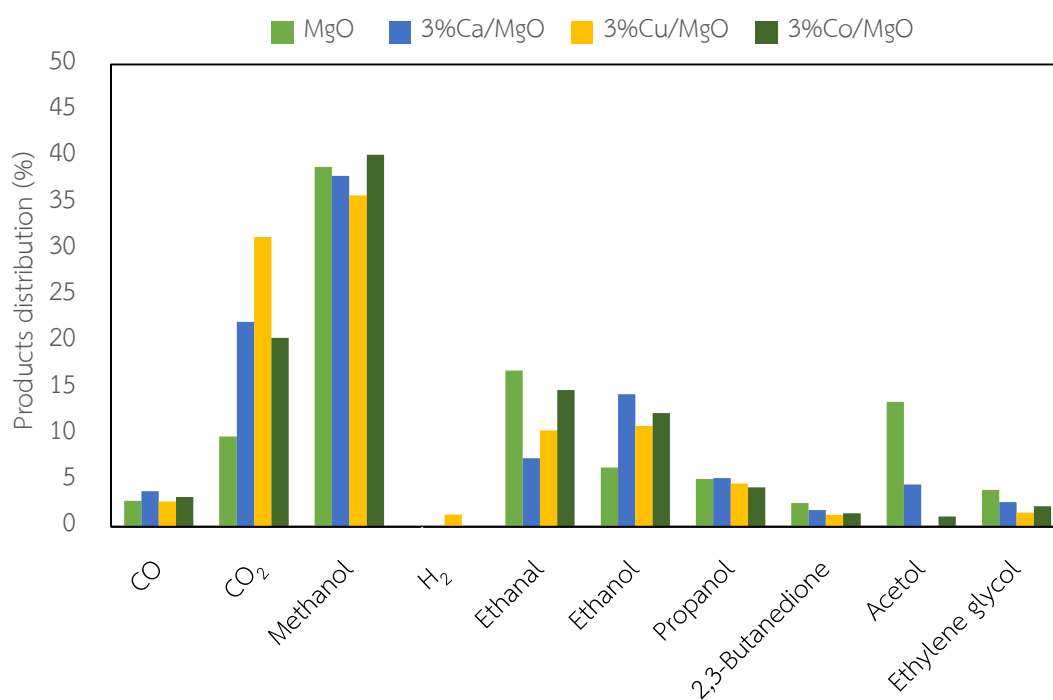


Figure 26 Product distribution over MgO and modified MgO catalysts.

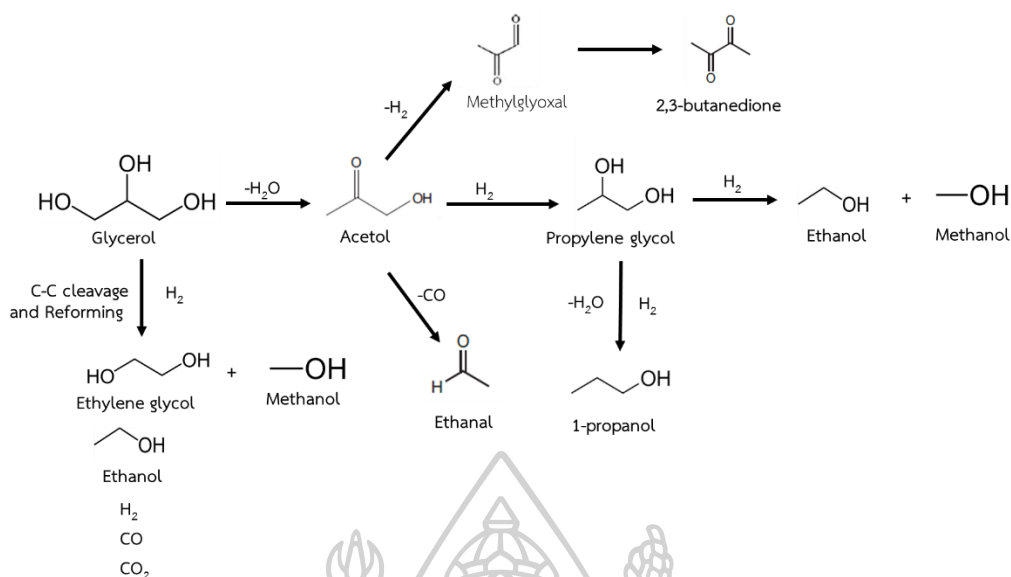


Figure 27 Proposed mechanism for the formation of methanol from direct methanol synthesis from glycerol.

5.2 Analysis of data and development of response surface methodology (RSM)

The results of the screening of catalysts, 3%Ca/MgO and 3%Co/MgO catalyst showed a high methanol yield and glycerol conversion. Thus, the experimental design has been performed to evaluate the effect of parameters on direct methanol synthesis from glycerol by using 3%Ca/MgO and 3%Co/MgO catalyst. First, the experiment was carried at the code level [0,0,0] that operated at 10wt.% glycerol concentration, 0.2 ml/min feed flow rate and 330°C under atmospheric pressure for 12 hours. For 3%Ca/MgO catalyst, the glycerol conversion decreased slightly from 89% to 79% and methanol yield decreased slightly 17% to 14% after 6 hours. Whereas, 3%Co/MgO catalyst showed glycerol conversion decreased with the increased time and methanol yield was lower around 7.26% as showed in Figure 28-29. In Figure 30, it was observed that the physical characteristics was changed as the black of 3%Co/MgO catalyst. The deactivation phenomenon can be explained by the formation of coke. Obviously, the deactivation rate of 3%Ca/MgO was slower than 3%Co/MgO. In addition, the characterization of fresh and used catalyst was performed using XRD as showed in

Figure 31. For used 3%Ca/MgO catalyst, the peaks that correspond to CaCO_3 was higher intensity while the intensity of CaO decreased. The results suggested that CaO easily absorbed CO_2 and formed CaCO_3 during the reaction[46]. For 3%Co/MgO catalyst, both the fresh and used represented similar due to appear MgO phase only.

According to consideration of the product distribution as showed in Figure 32, it was displayed that both gaseous and liquid products that occurred were slightly changed over time. In accordance with the glycerol conversion and methanol yield for 3%Ca/MgO, the 3%Co/MgO showed CO_2 distribution decreased significantly due to the reaction of the C–C bond cleavage of glycerol that occurred more easily. Whereas, the methanol distribution was relatively stable. For these reasons, the 3%Ca/MgO catalyst was considered in the central composite design.

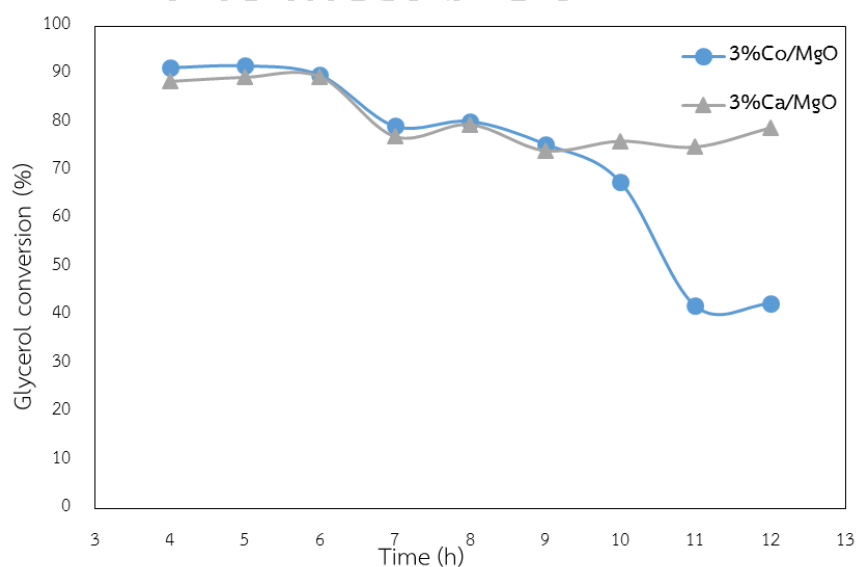


Figure 28 Glycerol conversion over 3%Ca/MgO and 3%Co/MgO catalyst.

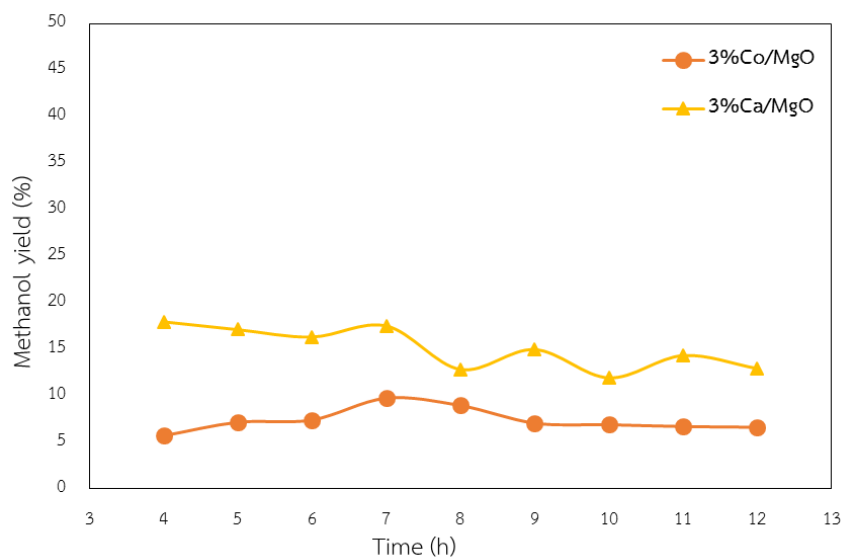


Figure 29 Methanol yield over 3%Ca/MgO and 3%Co/MgO catalyst.



Figure 30 Fresh and used catalyst of 3%Ca/MgO and 3%Co/MgO catalyst.

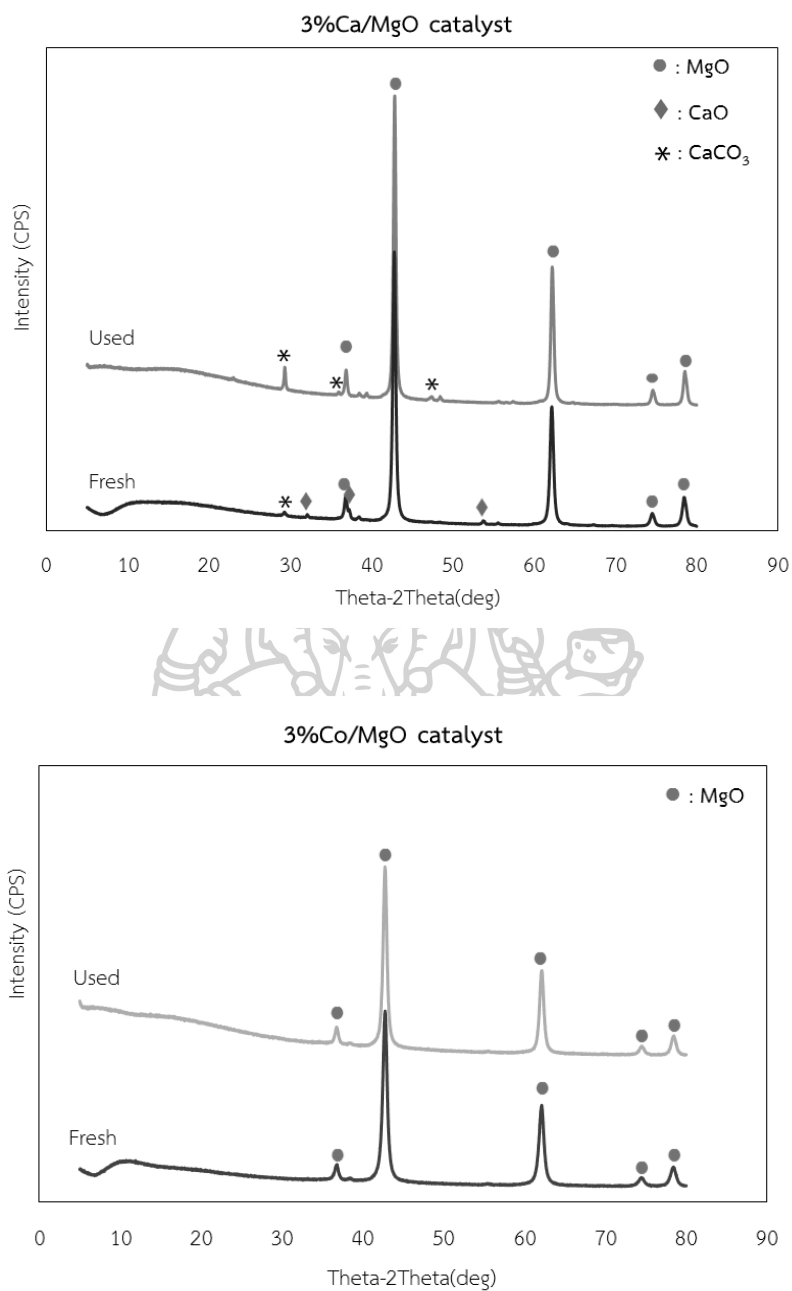


Figure 31 XRD pattern of fresh and used catalysts of 3%Ca/MgO and 3%Co/MgO catalyst.

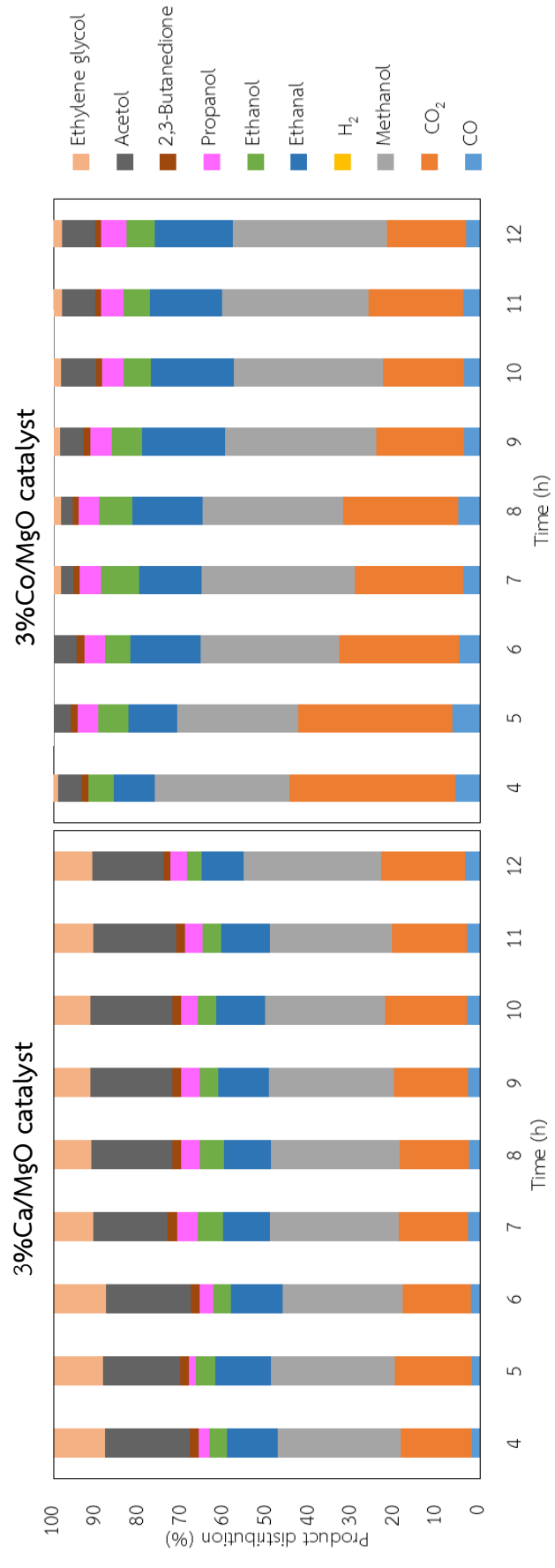


Figure 32 Product distribution over 3%Ca/MgO and 3%Co/MgO catalyst.

Central composite design (CCD) was studied for the process variables of direct methanol synthesis from glycerol by using 3%Ca/MgO. Each experiment represented a unique combination of independent variable levels for glycerol conversion and methanol yield. Then, glycerol conversion and methanol yield were determined by performing the experiments as listed in the appendix C. The R^2 is the most important factor to show the variability of independent variables, which greater than 75% was accepted. It was found that R^2 was 91.22% and 90.31% for glycerol conversion and methanol yield, respectively. The Adj- R^2 which is a measure of the amount of variation around the mean determined by experiments and fitted for various terms in the model[11], which greater than 70%, was accepted. The result showed that Adj- R^2 was 83.31% and 81.58% for glycerol conversion and methanol yield, respectively. They indicated that both responses were accepted.

Considering the P-value, if the P-value is less than 0.05, then the equation of the factor has a significant effect on the experimental response. Then consider the p-value of the quadratic term or the effect that causes the quadratic equation. If the p-value is less than 0.05, the equation of the factor has a significant effect on the experimental response. So, regression equation was used to explain the mathematical relationship between the independent variables and dependent responses which was represented in terms of concentration (C), temperature (T) and feed flow rate (F) by Minitab 17 program as following Eq. (5-1)-(5-2):

$$\text{Glycerol conversion} = -363 + 15.12 C + 1.857 T - 0.002254 T^2 \quad (5-1)$$

$$\text{Methanol yield} = -41.5 + 0.417 T - 107.0 F - 0.000832 T^2 - 246.7 F^2 + 0.577 TF \quad (5-2)$$

In order to gain a better understanding of the interaction effects of independent variables on the response, 3D surface plot and contour plot for the measured responses were formed based on the equation model (5-1)-(5-2).

5.2.1 The optimum condition of glycerol conversion by using 3%Ca/MgO catalyst

The presence of equation model confirmed that responses depended on both single and mixture variables. According to equation (5-1) glycerol conversion indicated that there was a synergistic effect between glycerol concentration and temperature.

$$\text{Glycerol conversion} = -363 + 15.12 C + 1.857 T - 0.002254 T^2 \quad (5-1)$$

The resulted surface response 3D plots of glycerol conversion were set as a function of two independent variables, (a) temperature and glycerol concentration; (b) feed flow rate and temperature; (c) feed flow rate and glycerol concentration as showed in Figure 33 (a)-(c), respectively. Figure 33 (a), it was found that glycerol conversion was increased when temperature and glycerol concentration increased. Figure 33 (b) showed that glycerol conversion was increased when temperature increased from 250°C to 400°C, and reached its maximum at high temperature and feed flow rate. Whereas, the feed flow rate and glycerol concentration had low effected on glycerol conversion as showed in Figure 33 (c). Therefore, temperature and glycerol concentration had a significant effected on glycerol conversion. It was explained that C–C bond cleavage of glycerol was easier and the primary product was completely consumed to provide the secondary products at high temperature[47]. The contour plot was showed in Figure 34, glycerol conversion was about 80-100% in temperature ranking of 250-400°C at >12 wt.% glycerol concentration. Glycerol conversion was about 60-80% at all temperatures and >8 wt.% glycerol concentration. At lower glycerol concentration, the glycerol conversion was lower than 60%.

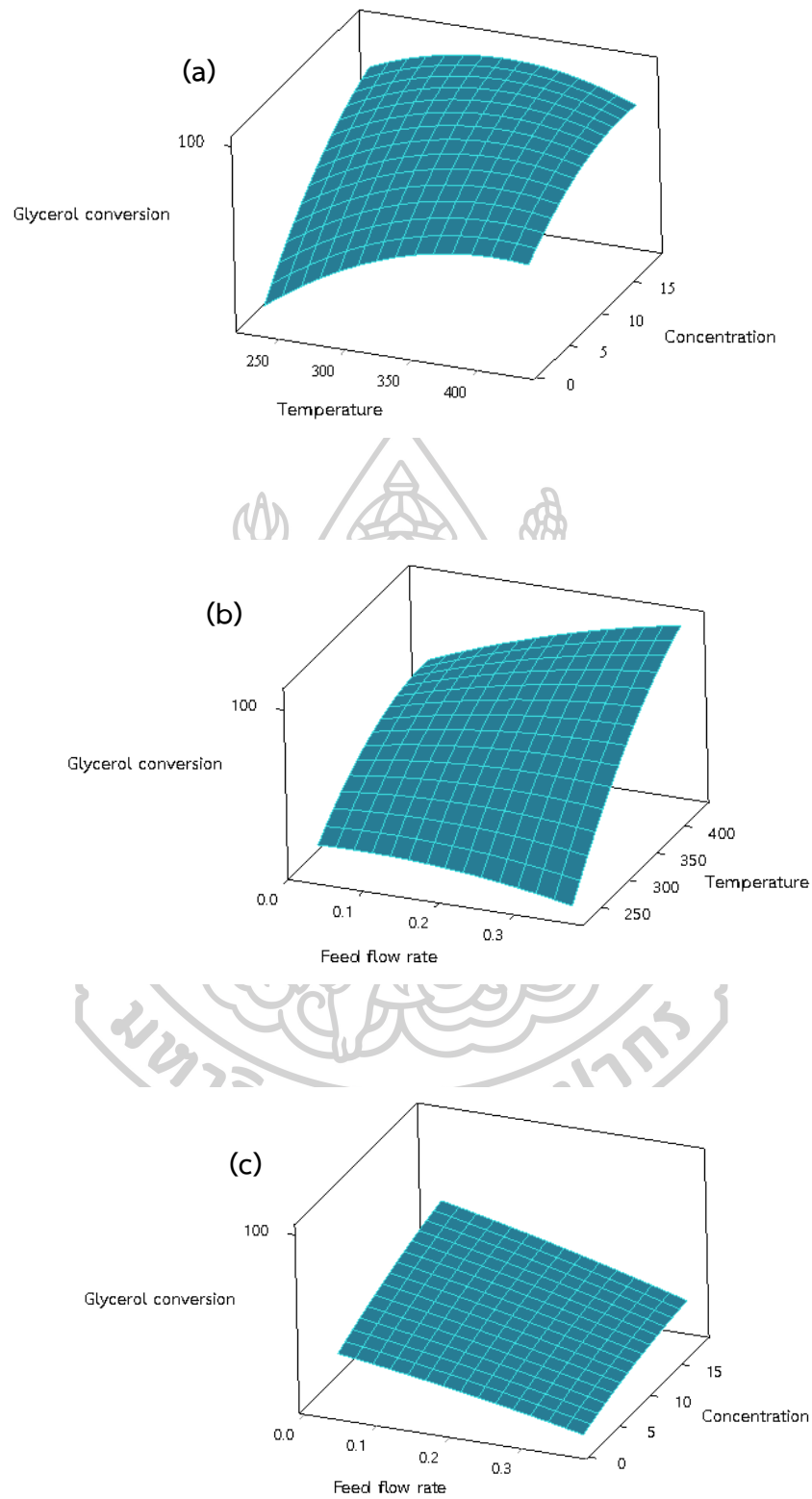


Figure 33 3D Surface plot: Glycerol conversion versus concentration, temperature and feed flow rate.

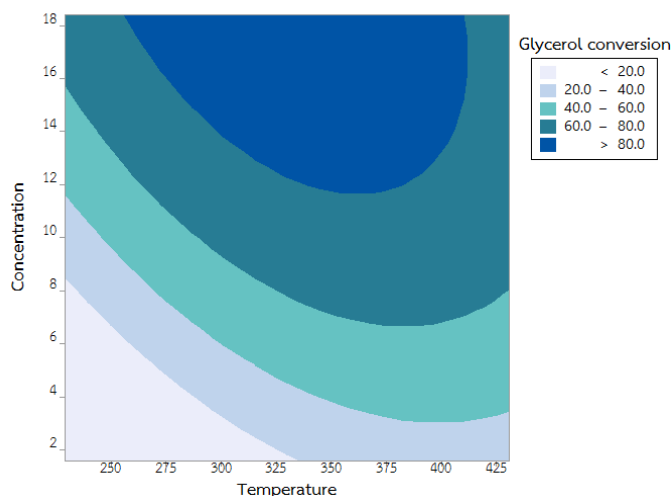


Figure 34 Contour plot: Glycerol conversion versus glycerol concentration and temperature.

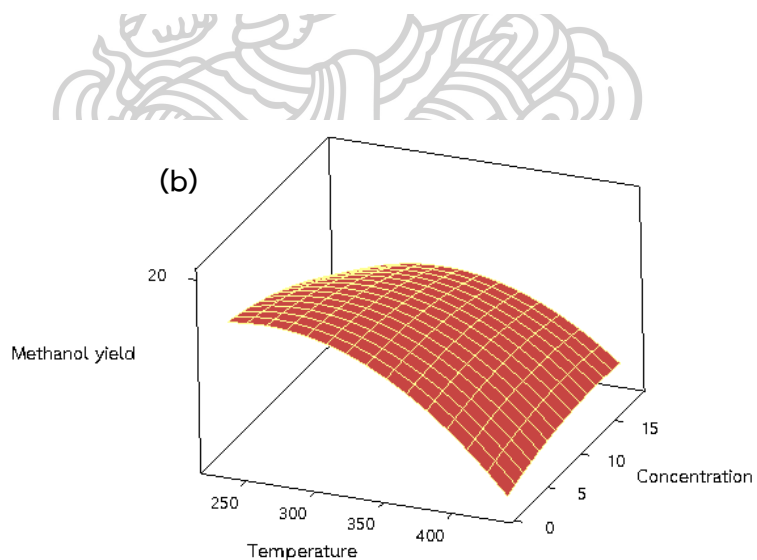
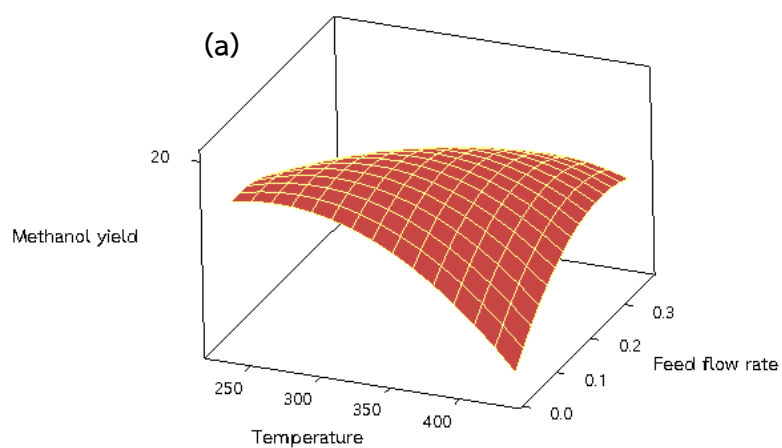
5.2.2 The optimum condition for methanol yield by using 3%Ca/MgO catalyst

According to equation (5-2) methanol yield indicated that there was a synergistic effect between feed flow rate and temperature.

$$\text{Methanol yield} = -41.5 + 0.417 T - 107.0 F - 0.000832 T^2 - 246.7 F^2 + 0.577 TF \quad (5-2)$$

The resulted surface response 3D plots of methanol yield were set as a function of two independent variables, (a) temperature and feed flow rate; (b) glycerol concentration and temperature; (c) feed flow rate and glycerol concentration as showed in Figure 35 (a)-(c), respectively. Figure 35 (a), the interaction between temperatures and feed flow rate, resulting in methanol yield was increased. Figure 35 (b) showed that methanol yield was increased when temperature decreased at low glycerol concentration. Alternatively, the methanol yield was increased when feed flow rate decreased at low glycerol concentration. Therefore, the temperature and feed flow rate had significant effected on methanol yield. The feed flow rate was decreased, resulting in increasing the residence time of the reactants in reactor. It was indicated that the reaction of substrate on the surface catalyst was increased, which affected the product distribution.

The contour plot was showed in Figure 36, methanol yield was about 15-20% in temperature $< 375^{\circ}\text{C}$ and feed flow rate < 0.25 ml/min. It was concluded that the optimal conditions of the direct methanol synthesis from pure glycerol was 10wt.% glycerol concentration, 0.1 ml/min feed flow rate and 330°C resulting to high methanol yield of 20.17% and glycerol conversion of 97.48%.



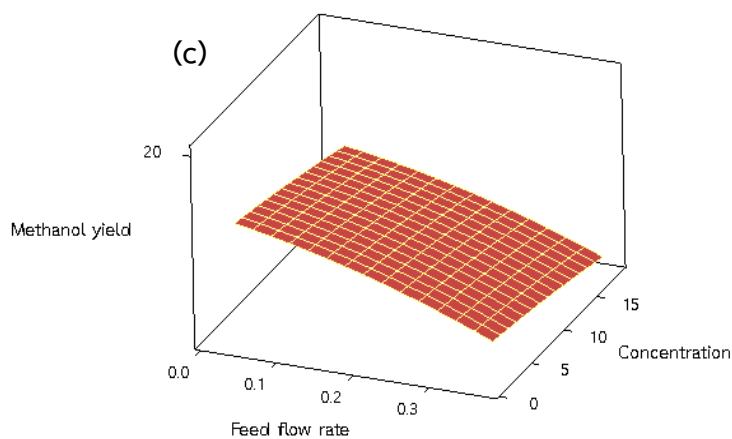


Figure 35 3D Surface plot: Methanol yield versus concentration, temperature and feed flow rate.

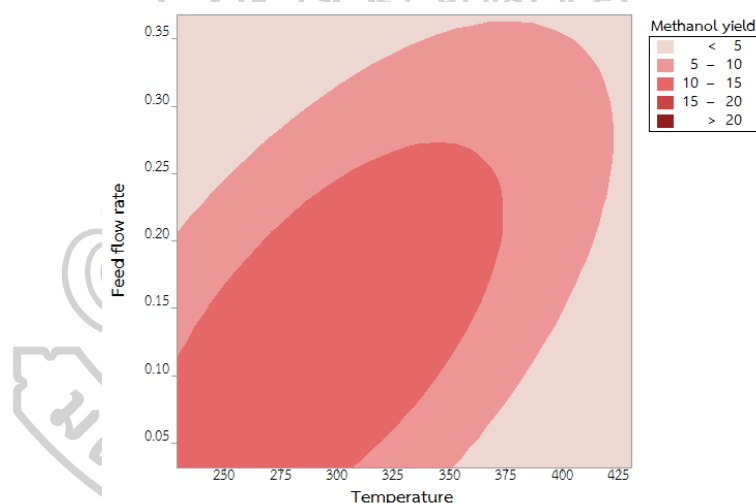


Figure 36 Contour plot: Methanol yield versus feed flow rate and temperature.

Ultimately the process was optimized and the optimum conditions for the direct methanol synthesis from pure glycerol were 10 wt.% glycerol concentration, 0.1 ml/min feed flow rate and temperature 330°C. At the optimized conditions, glycerol conversion and methanol yield were found to be 75.60% and 16.23%, respectively. It can be seen that 3%Ca/MgO catalyst exhibited catalytic activity more than 30 hours as showed in Figure 37.

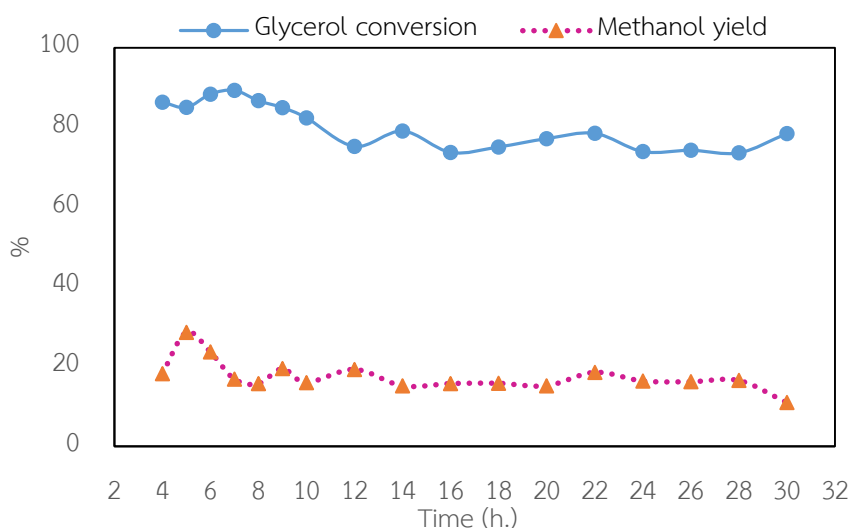


Figure 37 Glycerol conversion and methanol yield over 3%Ca/MgO catalyst at optimum condition.

5.3 The effect of CaO loading to direct methanol synthesis for pure glycerol

5.3.1 Catalyst characterization

Synthesis of Ca/MgO catalyst was prepared by wet impregnation methods that CaO loading was 3, 5 and 10wt.%. The synthesized samples were characterized by BET, which showed surface area, pore volume and mean pore diameter in Table 11. In case of increasing CaO loading, surface area of the catalyst decreased from 39.95 to 17.10 m²/g and pore volume decreased from 0.51 to 0.12 cm³/g. This was obviously attributed to the formation of CaO within pore of MgO, resulting in low surface and pore volume.

Table 11 CaO loading on MgO catalyst properties by using BET technique.

Catalyst	Surface area (m ² /g)	Pore volume (cm ³ /g)	Mean pore diameter (nm)
3%Ca/MgO	39.95	0.51	50.94
5%Ca/MgO	27.00	0.18	27.13
10%Ca/MgO	17.10	0.12	29.06

Table 12 The elemental composition of CaO loading on MgO catalyst by using XRF technique.

3%Ca/MgO			5%Ca/MgO			10%Ca/MgO		
Mg	Ca	unknown	Mg	Ca	unknown	Mg	Ca	unknown
60.0	3.3	36.7	60.0	5.1	34.9	60.0	9.0	31.0

The CaO loading into the MgO catalyst at 3, 5 and 10 wt.% were presented by XRF as showed in Table 12. It was confirmed that the CaO loading was found into modified MgO catalyst by impregnation method, which accorded to calculations.

XRD patterns of CaO loading on MgO catalysts were showed in Figure 38. All catalysts showed appeared diffraction peaks at 2θ of 37.0° , 43.0° , 62.5° , 74.6° and 78.4° corresponding to MgO phase (JCPDS: 78-0430). The presence of the cubic CaO phase showed intensity peaks at 2θ of 32.3° , 37.5° , 54.0° , 64.5° , and 67.7° (JCPDS:77-2376)[33]. It was confirmed that CaO loading was increased from 3 to 10 wt.% resulted in the intensity of CaO peaks increased.

CO₂-TPD profiles of 3%Ca/MgO, 5%Ca/MgO and 10%Ca/MgO catalyst as showed in Figure 39. The previously work mentioned that Ca/MgO catalyst exhibited three desorption peaks: these can be defined as weak (100-200°C), medium (200-400°C) and strong (500-700°C) basicities. When increasing CaO loading, the peak of CO₂ desorption decreased as desorption temperature of 100-400°C, which the desorption maximum peak was shifted towards higher temperatures[33]. The 5%Ca/MgO and 10%Ca/MgO catalyst had higher peak areas (CO₂ uptake) and maximum desorption temperatures of 628°C and 638°C, respectively. This was indicated that 5%Ca/MgO and 10%Ca/MgO catalyst had high basicity.

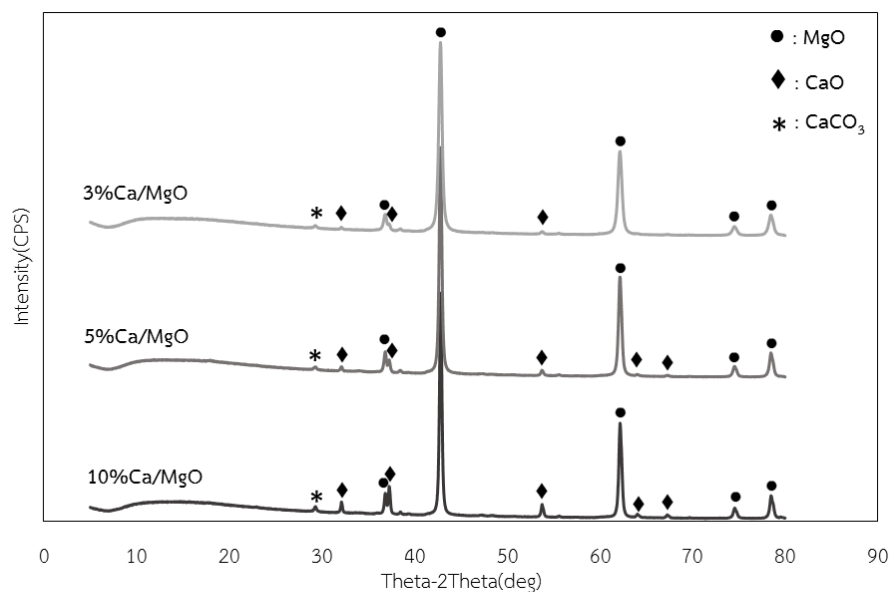


Figure 38 XRD pattern of 3%Ca/MgO, 5%Ca/MgO and 10%Ca/MgO catalyst.

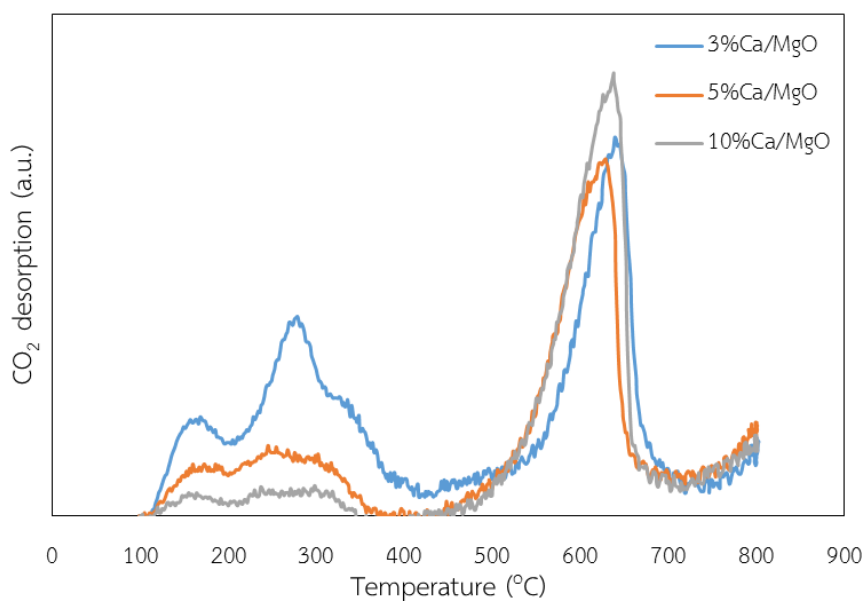


Figure 39 CO₂-TPD of 3%Ca/MgO, 5%Ca/MgO and 10%Ca/MgO catalyst.

5.3.2 Catalyst activity in direct methanol synthesis from pure glycerol

As the optimum condition, direct methanol synthesis from pure glycerol by using 3%Ca/MgO, 5%Ca/MgO and 10%Ca/MgO catalyst at 10wt.% glycerol concentration, 0.1 ml/min feed flow rate, 330°C under atmospheric pressure for

30 hours reaction time was showed in Figure 40. The increasing CaO loading effected to increasing in glycerol conversion but decreasing methanol yield. Consequently, 3%Ca/MgO catalyst improved methanol yield rather than 5%Ca/MgO and 10%Ca/MgO catalyst, respectively. According to the products that occurred as proposed in term of product distribution as showed in Figure 41, it was suggested that methanol distribution decreased, whereas acetol and ethylene glycol increased significantly for 5%Ca/MgO and 10%Ca/MgO. The result was in agreement with Sun et al. work, which it was explained that Lewis acid sites and basis sites favor the formation of another dehydration product of acetol[48], and corresponded to tha previous CO₂-TPD result as well. According to the catalyst characterization, glycerol conversion and methanol yield were significantly influenced by CaO loading and basicity of catalyst.

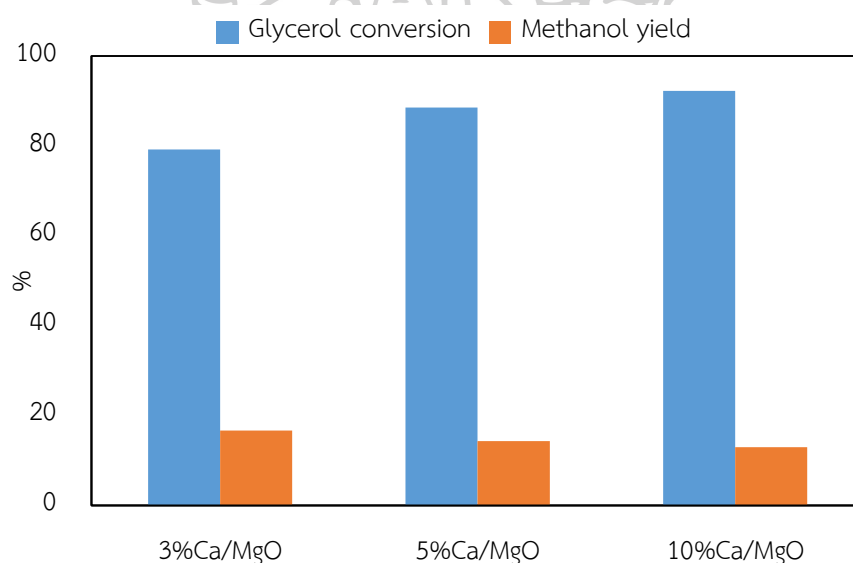


Figure 40 Glycerol conversion and methanol yield over 3%Ca/MgO, 5%Ca/MgO and 10%Ca/MgO catalyst.

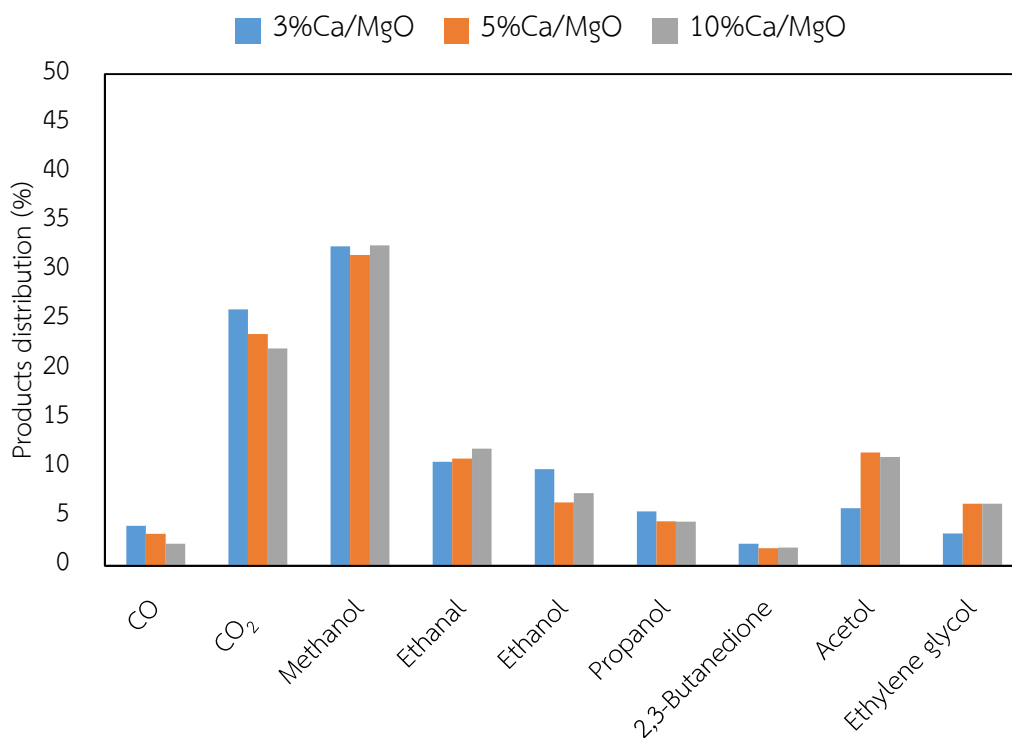


Figure 41 Products distribution over 3%Ca/MgO, 5%Ca/MgO and 10%Ca/MgO catalyst.

5.4 Comparison of pure and crude glycerol for direct methanol synthesis over 3%Ca/MgO catalyst

The crude glycerol composition based on data provided by the GI Green Power Company limited is: 65.69 wt.% glycerol, 1.65 wt.% ash, 0.05 wt.% water and 4.21 wt.% methanol. The optimum condition of direct methanol synthesis from pure glycerol was tested with crude glycerol, which consisted of 10wt.% glycerol concentration, 0.1 ml/min feed flow rate, 330°C atmospheric pressure, 30 hours reaction time, respectively. Figure 42-43 showed glycerol conversion and methanol yield as a function of reaction time during pure and crude glycerol. It was clearly seen that glycerol conversion of crude glycerol higher than pure glycerol. The glycerol conversion was observed for pure and crude glycerol levels of approximately 76.24% and 87.37%, respectively. Whereas methanol yield of pure and crude glycerol was similar in ranging of 15-20%. Analysis of all products by GC showed methanol as the

main liquid products of both pure and crude glycerol. As a result, the distribution products of pure and crude glycerol were also showed in Figure 44. The result indicated that the distribution of the gaseous and liquid products were not strongly affected by the addition of low concentration impurities agreed with the report of Seretis and Tsiakaras[49].

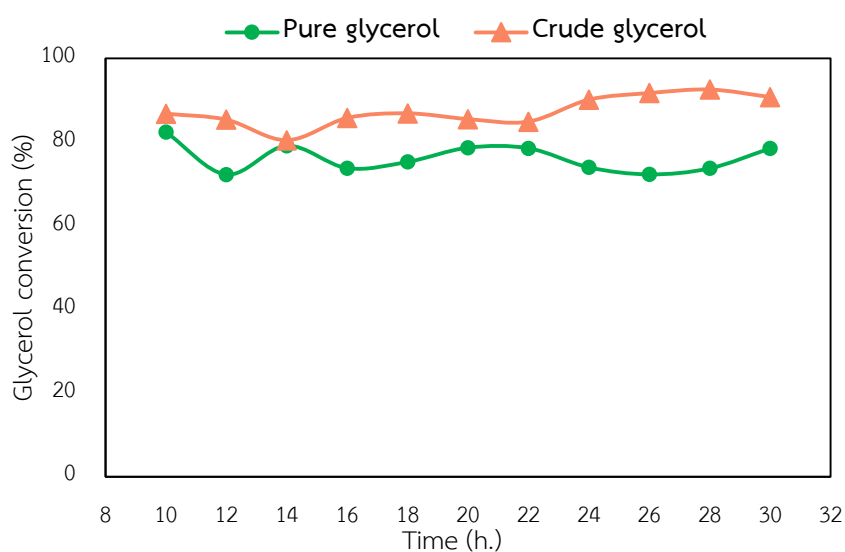


Figure 42 Glycerol conversion for pure and crude glycerol as function of reaction time.

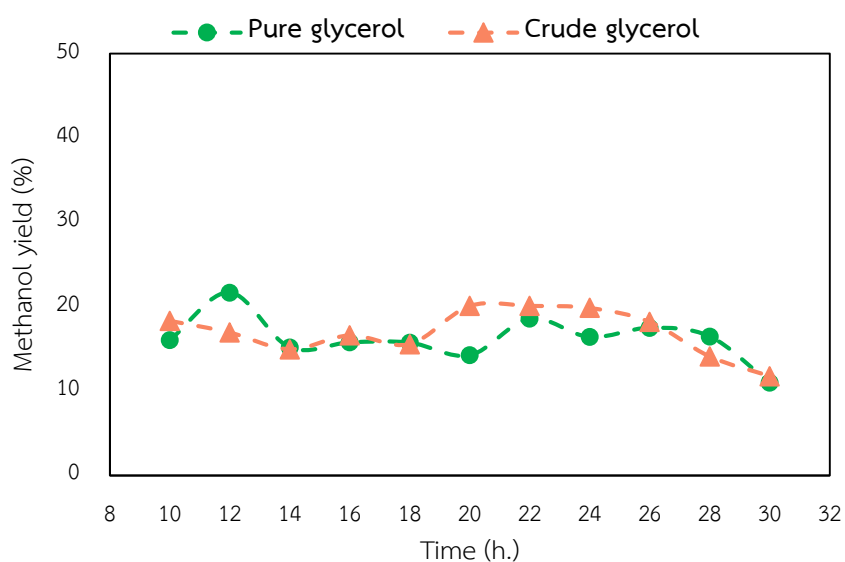


Figure 43 Methanol yield for pure and crude glycerol as function of reaction time.

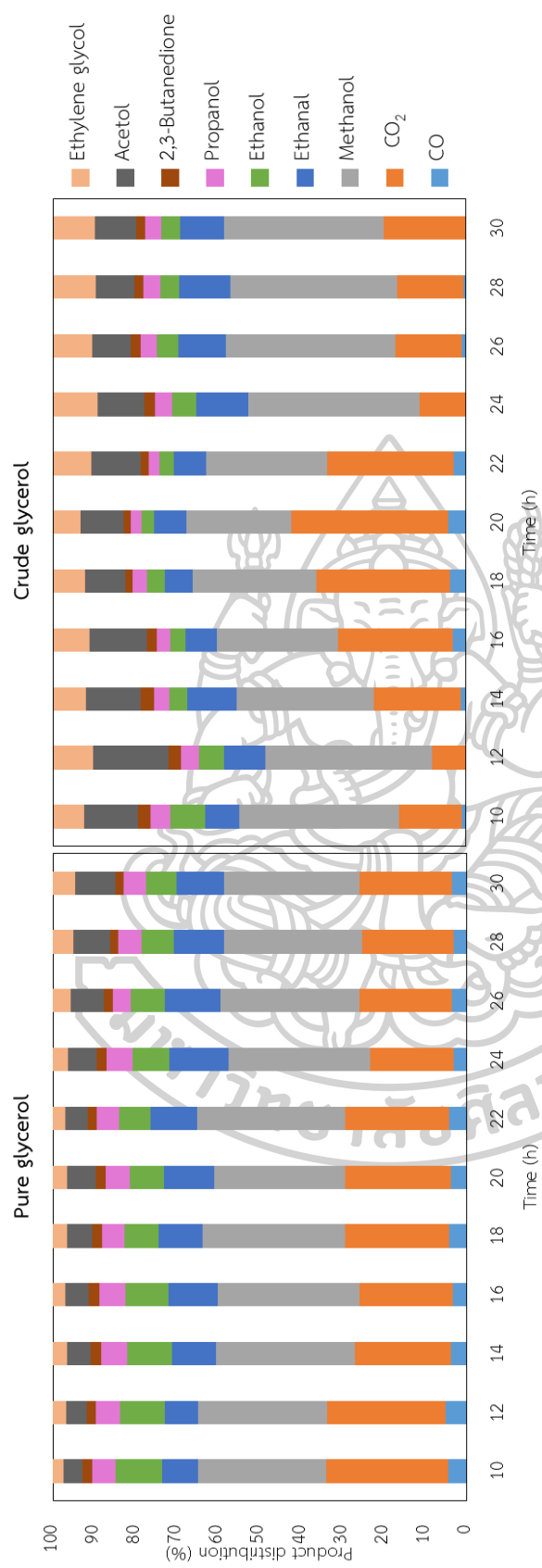


Figure 44 Products distribution for pure and crude glycerol as function of reaction time.

5.4.1 Optimization of direct methanol synthesis from crude glycerol over 3%Ca/MgO catalyst

Based on the results obtained from the experiment, it can be compared with the prediction of the response surface methodology (RSM) at optimum condition as showed in Figure 45. It was found that experimental results for glycerol conversion and methanol yield were 87.37% and 16.95%, respectively. The predicted by the response surface methodology (RSM) for glycerol conversion and methanol yield were 100% and 11.38%, respectively. The error percentage was calculated by equation in App. C. Although the error was high, the results of the experiment were in the range of the RSM predicted as showed in section 5.2. In addition, the rate law of glycerol was calculated as showed in App. D. The estimates of the kinetics parameters for 3%Ca/MgO catalyst showed that specific reaction rate (k) was 0.168 L/mol-h and reaction was first order. The rate law was

$$-r_{\text{glycerol}} = kC_{\text{glycerol}} = 0.168C_{\text{glycerol}} \quad (5-3)$$

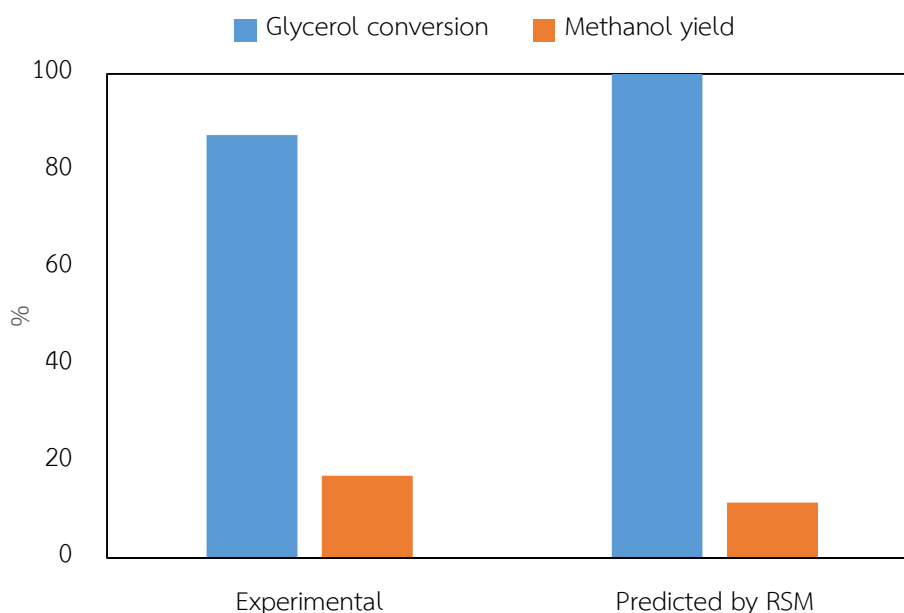


Figure 45 The experimental and RSM predicted responses for direct methanol synthesis from crude glycerol over 3%Ca/MgO catalyst.

5.5 Comparison the preparation of 3%Ca/MgO catalyst for direct methanol synthesis for crude glycerol.

5.5.1 Catalyst characterization

The XRD patterns of 3%Ca/MgO catalyst with different methods of wet impregnation and co-precipitation were showed in Figure 46. The catalysts showed appeared diffraction peaks at 2θ of 37.0° , 43.0° , 62.5° , 74.6° and 78.4° , corresponding to MgO phase (JCPDS: 78-0430). The presence of the cubic CaO phase showed intensity peaks at 2θ of 32.3° , 37.5° and 54.0° (JCPDS: 77-2376) [33]. The 3%Ca/MgO catalyst prepared by co-precipitation method, it was observed that the intensity peak of CaO and MgO decreased slightly compared with the catalyst prepared by impregnation method. However, Ca(OH)_2 was detected due to temperature calcined at 600°C [23]. The intensity peak at 29.4 reveals the presence of CaCO_3 as calcite in the samples containing Ca as normally observed[50].

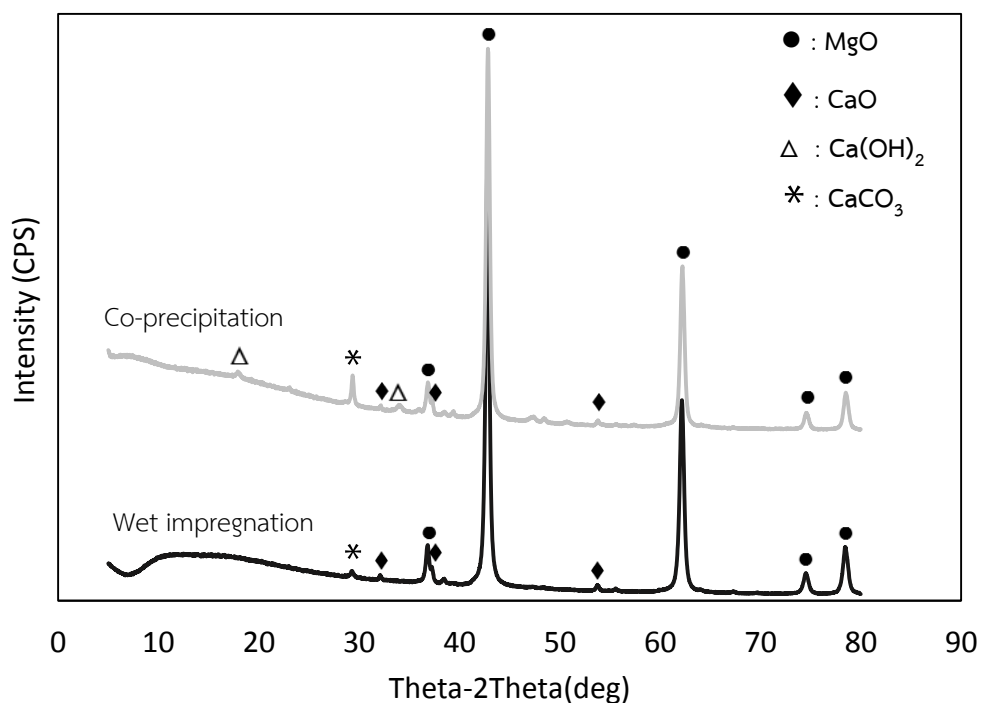


Figure 46 XRD pattern of 3%Ca/MgO with difference method.

Synthesis of 3%Ca/MgO catalyst was prepared by wet impregnation and co-precipitation method that the properties showed in Table 13. The synthesized samples were characterized by BET, which showed surface area, pore volume and mean pore diameter. The 3%Ca/MgO catalyst prepared by wet impregnation method, resulting in high pore volume and pore diameter of 0.509 cm³/g and 50.936 nm, respectively. On the other hand, 3%Ca/MgO prepared by co-precipitation method showed low pore volume and pore diameter of 0.136 cm³/g and 14.596 nm, respectively. The surface area was slightly decreased by co-precipitation method.

Table 13 The 3%Ca/MgO catalyst properties with difference method by using BET technique

Method	Surface area (m ² /g)	Pore volume (cm ³ /g)	Mean pore diameter (nm)
Wet impregnation	39.95	0.509	50.936
Co-precipitation	37.06	0.136	14.659

The N₂ adsorption/desorption isotherm of 3%Ca/MgO catalyst was prepared by wet impregnation and co-precipitation method as showed in Figure 47. The 3%Ca/MgO catalyst prepared by wet impregnation method, showed that a type II isotherm based on IUPAC's classification which exhibited multilayer adsorption and attributed to a macroporous material [36]. However, 3%Ca/MgO prepared by co-precipitation showed a type IV isotherm based on IUPAC's classification of adsorption isotherms which attributed to the filling/vacating of mesopores by capillary condensation[35]. A type IV isotherm with hysteresis loop according to the type H₃, suggesting that aggregates of plate-like particles giving rise to slit-shaped pores [34, 35].

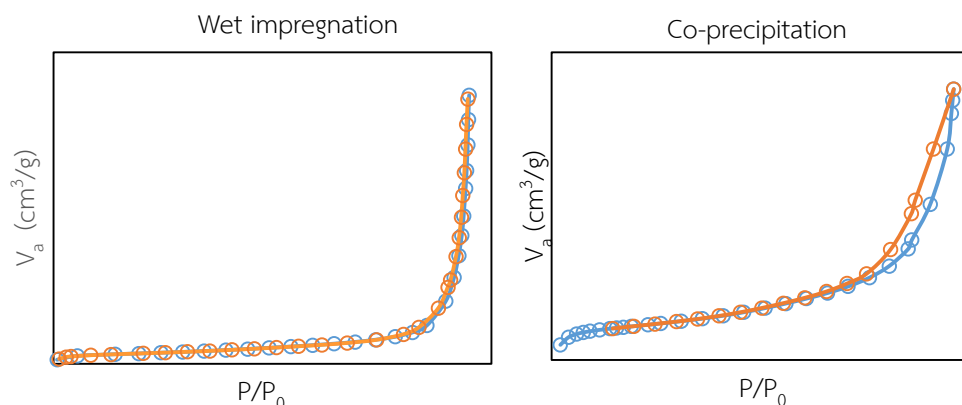


Figure 47 N_2 adsorption/desorption isotherm of 3%Ca/MgO catalyst properties with difference method.

The SEM images of the 3%Ca/MgO catalyst prepared with different methods of wet impregnation and co-precipitation were showed in Figure 48. The 3%Ca/MgO catalyst prepared by wet impregnation presented an irregular shape, large size of particles and exposing rough surface as showed in Figure 48(A). For the 3%Ca/MgO catalyst prepared by co-precipitation, the surface was comprised of a large number of agglomerates of catalyst particles and showed to have a platelet-like structure on its surface[38] as showed in Figure 48(B).

The observations of the BET results and SEM image of 3%Ca/MgO prepared by co-precipitation method, indicating that platelet-like particle catalyst resulted in lowest pore volume and pore diameter. This was according to the reports of Achouri, I., et al that the co-precipitation method caused metal oxide dispersed in the bulk of catalyst[51]. Therefore, CaO dispersed in the bulk of MgO. Whereas, the wet impregnation method caused CaO only deposited on the MgO surface.

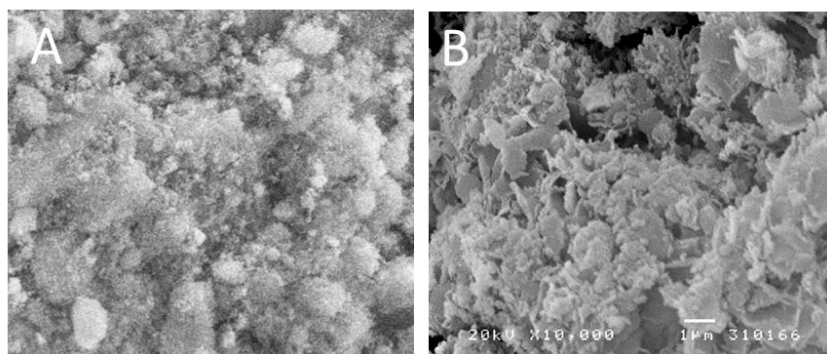


Figure 48 The SEM images of the 3%Ca/MgO prepared with different methods of (A) wet impregnation and (B) co-precipitation.

5.5.2 Catalyst activity

The 3%Ca/MgO catalyst prepared by the difference method of wet impregnation and co-precipitation defined as 3%Ca/MgO-impregnation and 3%Ca/MgO-co-precipitation catalyst, respectively. Direct methanol synthesis from crude glycerol was carried out at optimum condition, which consisted of 10wt.% glycerol concentration, 0.1 ml/min feed flow rate, 330°C, atmospheric pressure and 30 hours reaction time. Glycerol conversion was showed in Figure 49. It was clearly seen that the highest glycerol conversion was obtained over 3%Ca/MgO-co-precipitation catalyst, it was relatively stabled after 10 hours at around 95%. Alternatively, the glycerol conversion was slightly increased from 85% to 92% over 3%Ca/MgO-impregnation catalyst. It was seen that the glycerol conversion for co-precipitation method higher that wet impregnation method. On the other hand, it was found that 3%Ca/MgO-impregnation catalyst was more active than 3%Ca/MgO-co-precipitation catalyst as showed in Figure 50. The methanol yield of 3%Ca/MgO-impregnation and 3%Ca/MgO-co-precipitation catalyst was in range of 15-20% and 8-13%, respectively.

The comparison of the products produced by 3%Ca/MgO-co-precipitation catalyst with 3%Ca/MgO-impregnation catalyst resulted to methanol as a main

product. Other products with a similar product distribution; CO, CO₂, H₂, ethylene glycol, ethanal, ethanol, propanol, 2,3-butanedione and acetol were showed in Figure 51. For 3%Ca/MgO-co-precipitation catalyst, it was found that the products were relatively stable in the period, according to glycerol conversion. The ethanal and ethanol were increased while acetol and ethylene glycol were decrease. These indicated that 3%Ca/MgO-co-precipitation catalyst enhanced dehydration and two steps of hydrogenation on glycerol comparing with 3%Ca/MgO-impregnation catalyst as the reaction pathway of the previous studied[17, 47].

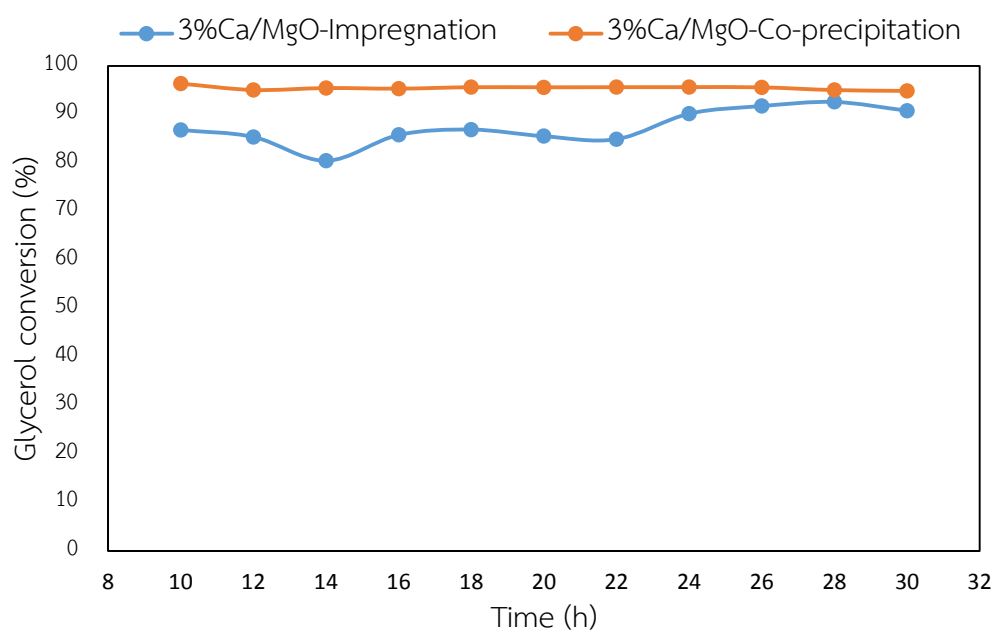


Figure 49 Glycerol conversion over 3%Ca/MgO catalyst with difference method.

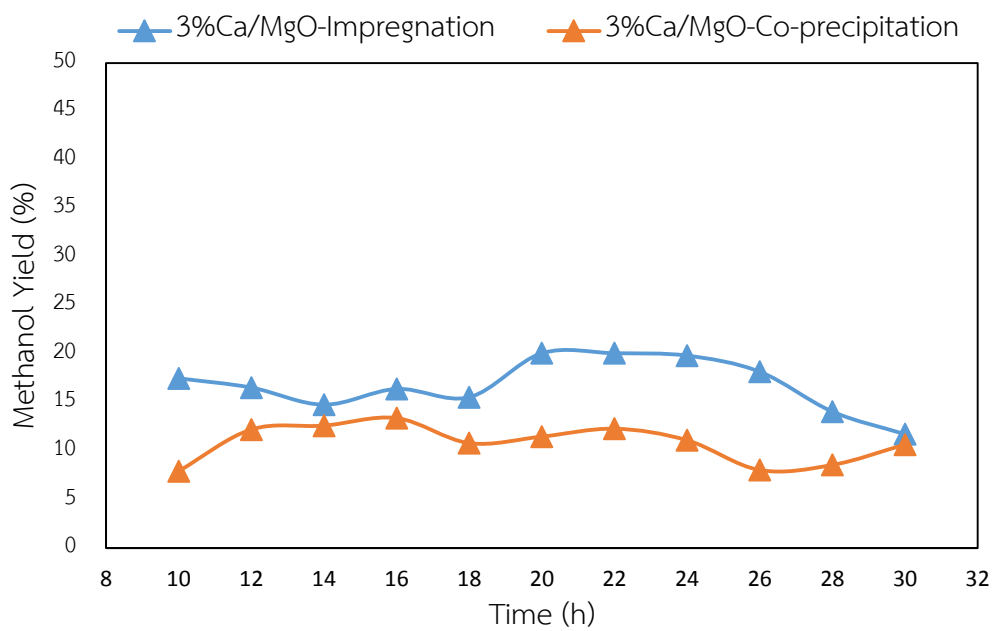


Figure 50 Methanol yield over 3%Ca/MgO catalyst with difference method.



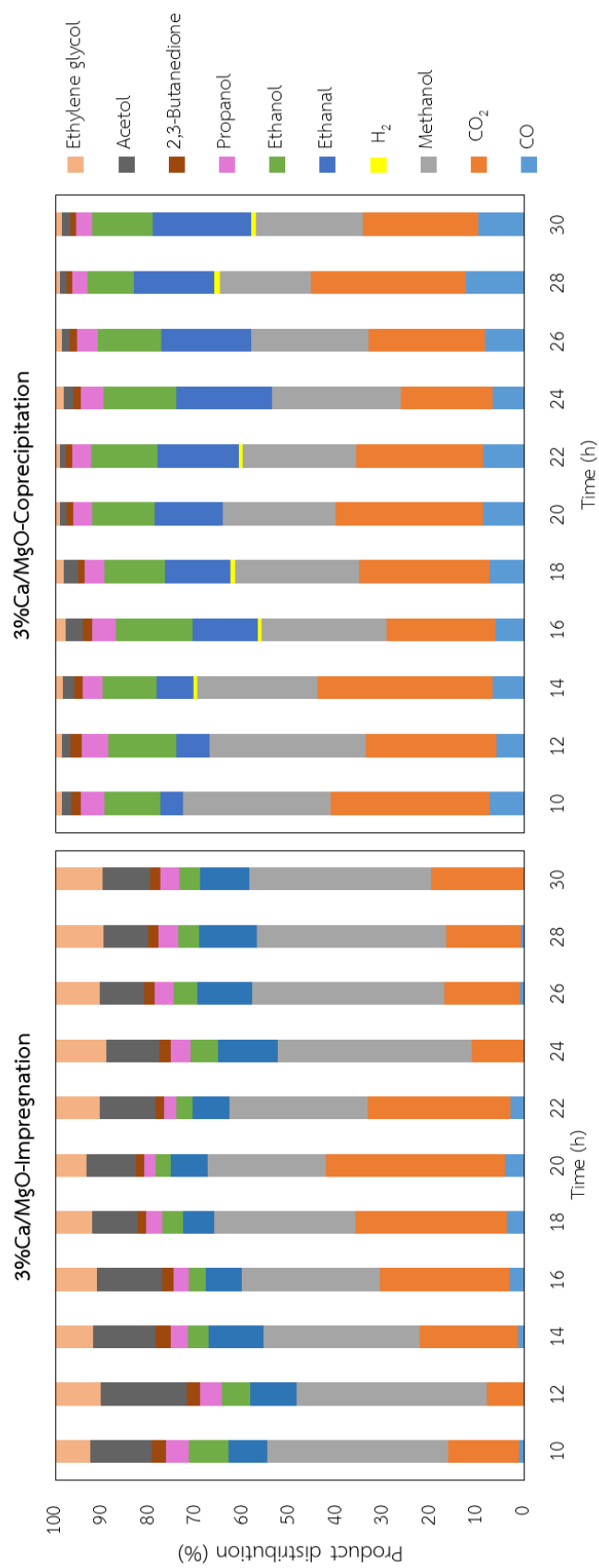


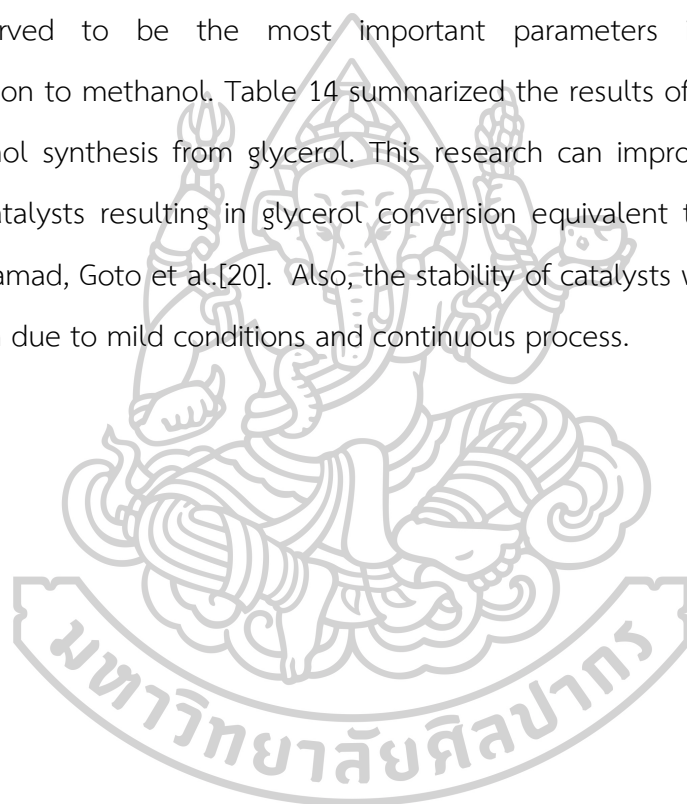
Figure 51 Products distribution over 3%Ca/MgO catalyst with difference method.

5.6 The comparison of catalyst performance in the synthesis of methanol from glycerol.

Table 14 Comparison studies of methanol synthesis from glycerol

Catalyst	Reaction conditions	Glycerol conversion	Methanol yield	Ref.
5%Cu/HZSM-5	1 ml/h, 10 wt.% pure glycerol/H ₂ O, T=500°C, P= 1 bar, 4 h.	100%	6.70%	[18]
MgO	1 ml/h, 10 wt.% pure glycerol/H ₂ O, T=320°C, P= 1 bar, 3 h.	31%	7.3 g _{methanol} /kg _{Scat} ⁻¹ h ⁻¹	[16]
CaO	1 ml/h, 10 wt.% pure glycerol/H ₂ O, T=320°C P= 1 bar, 3 h.	38%	14 g _{methanol} /kg _{Scat} ⁻¹ h ⁻¹	[16]
CeO ₂	1 ml/h, 10 wt.% pure glycerol/H ₂ O, T=340°C P= 1 bar, 3 h.	55%	19 g _{methanol} /kg _{Scat} ⁻¹ h ⁻¹	[16]
CeO ₂	1 ml/h, 15 wt.% crude glycerol/H ₂ O, T=340°C P= 1 bar, 3 h.	70%	16 g _{methanol} /kg _{Scat} ⁻¹ h ⁻¹	[16]
FTO	20 wt.% pure glycerol/H ₂ O, T= 300°C in sub-critical water, 30 min	77-80%	77-85%	[20]
3%Ca/MgO	6 ml/h, 10 wt.% pure glycerol/H ₂ O, T=330°C P= 1 bar, 30 h.	72-82%	15-19%	This work
3%Ca/MgO	6 ml/h, 10 wt.% crude glycerol/H ₂ O, T=330°C P= 1 bar, 30 h.	65-92%	15-20%	work

Studies on the methanol synthesis from glycerol have been conducted by several researchers in the presence as well as absence catalysts. It was found that glycerol can be converted to highest methanol at high condition. In addition, the most of the previous research studies reported high glycerol conversion, but rather low product yield. It has been proved that the glycerol can potentially convert to some value-added chemicals such as ethanol, propanol, acetaldehyde, formaldehyde, acetol and other unidentified products. Reaction temperature and various catalyst were observed to be the most important parameters influencing glycerol transformation to methanol. Table 14 summarized the results of previous studies on the methanol synthesis from glycerol. This research can improve the efficiency of modified catalysts resulting in glycerol conversion equivalent to the experimental results of Samad, Goto et al.[20]. Also, the stability of catalysts was much durable in the reaction due to mild conditions and continuous process.



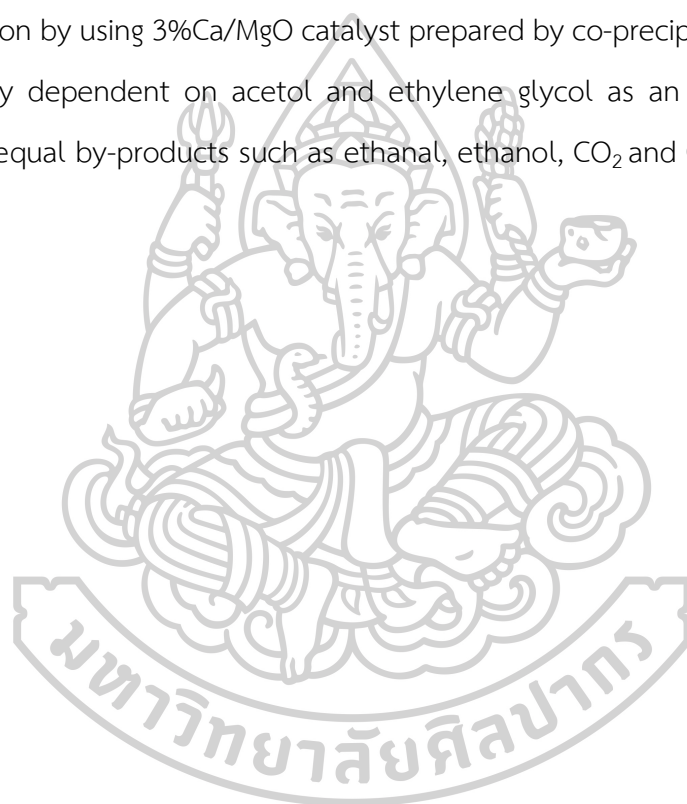
CHAPTER 6 CONCLUSIONS AND RECOMMENDATIONS

The modified MgO catalysts (3%Ca/MgO, 3%Co/MgO and 3%Cu/MgO catalyst) prepared by wet impregnation method. The catalysts showed that a different activity in the catalytic direct methanol synthesis from pure glycerol. The total basicity, the texture of the metal oxide loading strongly influenced both the glycerol conversion, methanol yield and the distribution of products. The 3%Ca/MgO catalyst with large pores exhibited more active than 3%Co/MgO and 3%Cu/MgO. It was clearly that 3%Ca/MgO and 3%Co/MgO catalyst showed higher glycerol conversion and methanol yield than MgO catalyst at 10wt.% glycerol concentration, 0.1 ml/min feed flow rate, 330°C under atmospheric pressure.

The design of experimental with response surface methodology was used to determine the optimum condition over 3%Ca/MgO and 3%Co/MgO catalyst. It was confirmed that 3%Ca/MgO catalyst resulted to high methanol yield of 20.17% and glycerol conversion of 97.48% at the optimal conditions of the direct methanol synthesis from pure glycerol at 10wt.% glycerol concentration, 0.1 ml/min feed flow rate and 330°C for 10 h. Then, the effect of CaO loading on MgO catalyst was investigated at 3, 5, 10 wt.%. The result displayed that increasing of CaO loading can improve the basicity of MgO catalyst, whereas the surface area and pore volume of modified MgO catalyst were decreased. Therefore, the highest glycerol conversion and the lowest methanol yield were obtained from 10%Ca/MgO.

The comparison of direct methanol synthesis of pure and crude glycerol over 3%Ca/MgO catalyst resulted that methanol yield was similar. It was clearly seen that glycerol conversion of crude glycerol was higher than pure glycerol after 16 h reaction time. Whereas, the glycerol conversion of pure glycerol was more stabled comparing with crude glycerol. It was anticipated that a result of impurities in crude glycerol affected to glycerol conversion but did not affect to methanol yield.

Finally, the preparation of 3%Ca/MgO catalyst was studied by impregnation and co-precipitation methods. The presence of CaO on MgO catalyst was confirmed by XRD technique. It was evident that the particle size of the catalyst obtained the co-precipitation method was observed uniform and a platelet-like structure. Therefore, the 3%Ca/MgO catalyst prepared by co-precipitation method exhibited a higher glycerol conversion and more stable over time than the 3%Ca/MgO catalyst prepared by wet impregnation method. The amount and distribution of final products observed in the reaction by using 3%Ca/MgO catalyst prepared by co-precipitation method were also strongly dependent on acetol and ethylene glycol as an intermediate, which resulted in equal by-products such as ethanal, ethanol, CO₂ and CO.



REFERENCES

1. Bennekom, J.G.v., R. H. Venderbosch and H. J. Heeres, *Biomethanol from Glycerol. Biodiesel - Feedstocks, Production and Applications*. Z. Fang. Rijeka, InTech, 2012: p. Ch. 12.
2. A.G. Quispe, C., C.J.R. Coronado, and J. Carvalho, *Glycerol: Production, consumption, prices, characterization and new trends in combustion*. Vol. 27. 2013. 475-493.
3. Xiao, Y., G. Xiao, and A. Varma, *A Universal Procedure for Crude Glycerol Purification from Different Feedstocks in Biodiesel Production: Experimental and Simulation Study*. Industrial & Engineering Chemistry Research, 2013. **52**(39): p. 14291-14296.
4. Luo, X., et al., *Value-added processing of crude glycerol into chemicals and polymers*. Bioresource Technology, 2016. **215**: p. 144-154.
5. Bagheri, S., N.M. Julkapli, and W.A. Yehye, *Catalytic conversion of biodiesel derived raw glycerol to value added products*. Renewable and Sustainable Energy Reviews, 2015. **41**: p. 113-127.
6. Cheng, C.K., S.Y. Foo, and A.A. Adesina, *Glycerol Steam Reforming over Bimetallic Co-Ni/Al₂O₃*. Industrial & Engineering Chemistry Research, 2010. **49**(21): p. 10804-10817.
7. Pompeo, F., G. Santori, and N.N. Nichio, *Hydrogen and/or syngas from steam reforming of glycerol. Study of platinum catalysts*. International Journal of Hydrogen Energy, 2010. **35**(17): p. 8912-8920.
8. Sanchez, E.A. and R.A. Comelli, *Hydrogen by glycerol steam reforming on a nickel-alumina catalyst: Deactivation processes and regeneration*. International Journal of Hydrogen Energy, 2012. **37**(19): p. 14740-14746.
9. Kousi, K., et al., *Glycerol steam reforming over modified Ni-based catalysts*. Applied Catalysis A: General, 2016. **518**: p. 129-141.

10. Papageridis, K.N., et al., *Comparative study of Ni, Co, Cu supported on γ -alumina catalysts for hydrogen production via the glycerol steam reforming reaction*. Fuel Processing Technology, 2016. **152**: p. 156-175.
11. Zarei Senseni, A., et al., *A comparative study of experimental investigation and response surface optimization of steam reforming of glycerol over nickel nano-catalysts*. International Journal of Hydrogen Energy, 2016. **41**(24): p. 10178-10192.
12. van Bennekom, J.G., et al., *Bench scale demonstration of the Supermethanol concept: The synthesis of methanol from glycerol derived syngas*. Chemical Engineering Journal, 2012. **207-208**: p. 245-253.
13. Gutiérrez Ortiz, F.J., et al., *Methanol synthesis from syngas obtained by supercritical water reforming of glycerol*. Fuel, 2013. **105**: p. 739-751.
14. Nor Shahirah, M.N., et al., *A study on the kinetics of syngas production from glycerol over alumina-supported samarium–nickel catalyst*. International Journal of Hydrogen Energy, 2016. **41**(25): p. 10568-10577.
15. Delgado, S.N., et al., *Influence of the nature of the support on the catalytic properties of Pt-based catalysts for hydrogenolysis of glycerol*. Journal of Molecular Catalysis A: Chemical, 2013. **367**: p. 89-98.
16. Haider, M.H., et al., *Efficient green methanol synthesis from glycerol*. Nature Chemistry, 2015. **7**: p. 1028.
17. Rajkhowa, T., G.B. Marin, and J.W. Thybaut, *A comprehensive kinetic model for Cu catalyzed liquid phase glycerol hydrogenolysis*. Applied Catalysis B: Environmental, 2017. **205**: p. 469-480.
18. Mohamed, M., et al. *Conversion of glycerol to methanol in the presence of zeolite based catalysts*. in *2011 IEEE Conference on Clean Energy and Technology (CET)*. 2011.
19. Carr, A.G., et al., *Methanol formation from the treatment of glycerol in supercritical water and with ethylsulfide*. The Journal of Supercritical Fluids, 2016. **117**: p. 80-88.

20. Samad, W.Z., et al., *Fluorine-doped tin oxide catalyst for glycerol conversion to methanol in sub-critical water*. *The Journal of Supercritical Fluids*, 2017. **120**: p. 366-378.
21. Di Cosimo, J.I., et al., *Chapter 1 Basic catalysis on MgO: generation, characterization and catalytic properties of active sites*, in *Catalysis: Volume 26*. 2014, The Royal Society of Chemistry. p. 1-28.
22. Banković-Ilić, I.B., et al., *Application of nano CaO-based catalysts in biodiesel synthesis*. *Renewable and Sustainable Energy Reviews*, 2017. **72**: p. 746-760.
23. Daud, F.D.M., et al., *Improved CO₂ adsorption capacity and cyclic stability of CaO sorbents incorporated with MgO*. *New Journal of Chemistry*, 2016. **40**(1): p. 231-237.
24. Mirzaei, F., et al., *Carbon dioxide reforming of methane for syngas production over Co-MgO mixed oxide nanocatalysts*. *Journal of Industrial and Engineering Chemistry*, 2015. **21**: p. 662-667.
25. El-Molla, S.A., *Dehydrogenation and condensation in catalytic conversion of isopropanol over CuO/MgO system doped with Li₂O and ZrO₂*. *Applied Catalysis A: General*, 2006. **298**: p. 103-108.
26. Yuan, Z., et al., *Biodiesel derived glycerol hydrogenolysis to 1,2-propanediol on Cu/MgO catalysts*. *Bioresource Technology*, 2010. **101**(18): p. 7088-7092.
27. Zhou, C.H., et al., *Cleaner hydrothermal hydrogenolysis of glycerol to 1,2-propanediol over Cu/oxide catalysts without addition of external hydrogen*. *Molecular Catalysis*, 2017. **432**: p. 274-284.
28. A. Dumesic, J., G. Huber, and M. Boudart, *Principles of Heterogeneous Catalysis*. 2008.
29. Gupta, P. and S. Paul, *Solid acids: Green alternatives for acid catalysis*. *Catalysis Today*, 2014. **236**: p. 153-170.
30. Hattori, H., *Solid base catalysts: fundamentals and their applications in organic reactions*. *Applied Catalysis A: General*, 2015. **504**: p. 103-109.
31. Sadhukhan, B., N.K. Mondal, and S. Chattoraj, *Optimisation using central composite design (CCD) and the desirability function for sorption of methylene*

- blue from aqueous solution onto Lemna major*. Karbala International Journal of Modern Science, 2016. **2**(3): p. 145-155.
32. Mahdavi, V. and A. Monajemi, *Optimization of operational conditions for biodiesel production from cottonseed oil on CaO-MgO/Al₂O₃ solid base catalysts*. Journal of the Taiwan Institute of Chemical Engineers, 2014. **45**(5): p. 2286-2292.
33. Mahdavi, V. and F. Abedini, *Preparation and Characterization of CaO/MgO Catalyst and Its Application for Transesterification of n-Butyl Acetate with Methanol*. Chemical Engineering Communications, 2016. **203**(1): p. 114-122.
34. Ruminski, A., K.-J. Jeon, and J. Urban, *Size-dependent CO₂ capture in chemically synthesized magnesium oxide nanocrystals*. Vol. 21. 2011. 11486.
35. Muttakin, M., et al., *Theoretical framework to evaluate minimum desorption temperature for IUPAC classified adsorption isotherms*. International Journal of Heat and Mass Transfer, 2018. **122**: p. 795-805.
36. Roschat, W., et al., *Synthesis of glycerol carbonate from transesterification of glycerol with dimethyl carbonate catalyzed by CaO from natural sources as green and economical catalyst*. Materials Today: Proceedings, 2018. **5**(6, Part 1): p. 13909-13915.
37. Pandhare, N.N., et al., *Selective Hydrogenolysis of Glycerol to 1,2-Propanediol over Highly Active and Stable Cu/MgO Catalyst in the Vapor Phase*. Organic Process Research & Development, 2016. **20**(6): p. 1059-1067.
38. Sudsakorn, K., et al., *Biodiesel production from Jatropha Curcas oil using strontium-doped CaO/MgO catalyst*. Journal of Environmental Chemical Engineering, 2017. **5**(3): p. 2845-2852.
39. Guo, X., et al., *Co/MgO catalysts for hydrogenolysis of glycerol to 1, 2-propanediol*. Applied Catalysis A: General, 2009. **371**(1): p. 108-113.
40. Yang, G.-Y., et al., *The conversion of glycerol to lactic acid catalyzed by ZrO₂-supported CuO catalysts*. Chemical Engineering Journal, 2016. **283**: p. 759-767.
41. Kulkarni, J., et al., *Structural, Optical and Photocatalytic Properties of MgO/CuO Nanocomposite Prepared by a Solution Combustion Method*. Materials Today: Proceedings, 2017. **4**(11, Part 3): p. 11756-11763.

42. Tushar Shamba Anvekar, K.K.K., Hari Kadam, *Synthesis, characterization and catalytic application of MgO supported metal catalysts in synthesis of dihydropyrimidinone*. Research Journal of Material Sciences, 2017. **5**(2): p. 1-6.
43. Gao, W., T. Zhou, and Q. Wang, *Controlled synthesis of MgO with diverse basic sites and its CO₂ capture mechanism under different adsorption conditions*. Chemical Engineering Journal, 2018. **336**: p. 710-720.
44. Zhu, S., et al., *One-step hydrogenolysis of glycerol to biopropanols over Pt-H₄SiW₁₂O₄₀/ZrO₂ catalysts*. Green Chemistry, 2012. **14**(9): p. 2607-2616.
45. Ren, S. and X.P. Ye, *Catalytic conversion of glycerol to value-added chemicals in alcohol*. Fuel Processing Technology, 2015. **140**: p. 148-155.
46. Ismail, K., et al., *The effect of particle size of CaO and MgO as catalysts for gasification of oil palm empty fruit bunch to produce hydrogen*. International Journal of Hydrogen Energy, 2012. **37**(4): p. 3639-3644.
47. Martinuzzi, I., et al., *Reaction mechanism for glycerol dehydration in the gas phase over a solid acid catalyst determined with on-line gas chromatography*. Chemical Engineering Science, 2014. **116**: p. 118-127.
48. Sun, D., et al., *Glycerol as a potential renewable raw material for acrylic acid production*. Green Chemistry, 2017. **19**(14): p. 3186-3213.
49. Seretis, A. and P. Tsiakaras, *Crude bio-glycerol aqueous phase reforming and hydrogenolysis over commercial SiO₂ Al₂O₃ nickel catalyst*. Renewable Energy, 2016. **97**: p. 373-379.
50. Albuquerque, M.C.G., et al., *Transesterification of ethyl butyrate with methanol using MgO/CaO catalysts*. Journal of Molecular Catalysis A: Chemical, 2009. **300**(1): p. 19-24.
51. Achouri, I., et al., *Diesel Steam Reforming: Comparison of Two Nickel Aluminate Catalysts Prepared by Wet-Impregnation and Co-Precipitation*. Vol. 207. 2013. 13-20.

APPENDICES



APPENDIX A

Raw data obtained from the experiment of direct methanol synthesis from glycerol

A-1 The results of the product analysis for direct methanol synthesis from pure glycerol.

Table A-1.1 Reaction condition: 10wt.% pure glycerol concentration, 0.1 ml/min feed flow rate, 330°C under atmospheric pressure for 10 hours over 3%Ca/MgO Catalyst.

Time (h)	Gas Products (%)				Liquid Products (wt.%)								
	CO	CO ₂	Methanol	H ₂	Ethanal	Methanol	Ethanol	Propanol	2,3-Butanedione	Acetol	Ethylene glycol	Glycerol	water
5	0.658	2.102	0.000	0.000	0.562	2.707	1.328	0.421	0.203	0.116	0.118	1.415	84.180
6	0.546	1.717	0.000	0.000	0.530	2.275	1.075	0.379	0.172	0.146	0.103	1.116	84.183
7	0.562	1.853	0.000	0.000	0.390	1.679	0.729	0.288	0.120	0.194	0.125	1.061	89.860
8	0.552	2.381	0.000	0.000	0.398	1.559	0.680	0.285	0.113	0.208	0.128	1.315	84.183
9	0.492	2.181	0.000	0.000	0.570	2.051	0.742	0.372	0.157	0.306	0.169	1.577	84.183
10	0.478	1.781	0.000	0.000	0.430	1.653	0.575	0.305	0.115	0.265	0.169	1.812	89.860

Table A-1.2 Reaction condition: 10wt.% pure glycerol concentration, 0.1 ml/min feed flow rate, 330°C under atmospheric pressure for 10 hours over 3%Co/MgO Catalyst.

Time (h)	Gas Products (%)				Liquid Products (wt.%)									
	CO	CO ₂	Methanol	H ₂	Ethanal	Methanol	Ethanol	Propanol	2,3-Butanedione	Acetol	Ethylene glycol	Glycerol	water	
5	0.189	1.000	0.009	0.000	0.302	1.332	0.541	0.157	0.053	0.000	0.074	0.476	95.600	
6	0.224	1.130	0.009	0.000	0.378	1.455	0.612	0.176	0.055	0.000	0.086	0.444	95.600	
7	0.233	1.135	0.009	0.000	0.394	1.266	0.517	0.170	0.049	0.000	0.074	0.436	95.600	
8	0.207	1.028	0.009	0.000	0.464	1.492	0.621	0.201	0.054	0.000	0.086	0.442	95.600	
9	0.267	1.161	0.009	0.000	0.673	1.991	0.653	0.259	0.070	0.000	0.117	0.460	95.600	
10	0.348	1.325	0.009	0.000	0.779	1.946	0.551	0.157	0.074	0.110	0.098	0.467	95.600	

Table A-1.3 Reaction condition: 10wt.% pure glycerol concentration, 0.1 ml/min feed flow rate, 330°C under atmospheric pressure for 10 hours over 3%Cu/MgO Catalyst.

Time (h)	Gas Products (%)				Liquid Products (wt.%)								
	CO	CO ₂	Methanol	H ₂	Ethanal	Methanol	Ethanol	Propanol	2,3-Butanedione	Acetol	Ethylene glycol	Glycerol	water
5	0.037	1.230	0.012	1.337	0.194	0.684	0.244	0.000	0.000	0.000	0.000	0.676	96.333
6	0.029	0.998	0.012	1.016	0.280	1.227	0.451	0.141	0.048	0.000	0.000	0.851	96.333
7	0.114	1.121	0.012	1.149	0.318	1.335	0.473	0.153	0.048	0.000	0.000	0.715	96.333
8	0.117	1.096	0.012	1.076	0.398	1.447	0.524	0.172	0.054	0.000	0.061	0.629	96.333
9	0.164	1.272	0.011	1.178	0.421	1.485	0.500	0.189	0.052	0.000	0.063	0.599	96.333
10	0.198	1.344	0.011	1.221	0.488	1.624	0.451	0.218	0.059	0.000	0.071	0.549	96.333

Table A-1.4 Reaction condition: 10wt.% pure glycerol concentration, 0.2 ml/min feed flow rate, 330°C under atmospheric pressure for 12 hours over 3%Ca/MgO Catalyst.

Time (h)	Gas Products (%)				Liquid Products (wt.%)									
	CO	CO ₂	Methanol	H ₂	Ethanal	Methanol	Ethanol	Propanol	2,3-Butanedione	Acetol	Ethylene glycol	Glycerol	water	
4	0.448	2.633	0	0	0.737	1.765	0.249	0.152	0.125	1.225	0.732	1.125	85.518	
5	0.448	2.640	0	0	0.799	1.755	0.263	0.103	0.127	1.092	0.690	1.087	85.518	
6	0.449	2.330	0	0	0.684	1.557	0.229	0.174	0.114	1.117	0.671	0.999	85.518	
7	0.594	2.232	0	0	0.495	1.375	0.278	0.218	0.104	0.791	0.417	1.796	85.518	
8	0.435	1.720	0	0	0.495	1.333	0.245	0.195	0.096	0.837	0.386	2.117	85.518	
9	0.525	2.007	0	0	0.501	1.239	0.182	0.181	0.088	0.813	0.359	2.381	85.518	
10	0.545	2.133	0	0	0.532	1.292	0.192	0.185	0.094	0.886	0.388	2.580	85.518	
11	0.554	2.090	0	0	0.556	1.357	0.202	0.197	0.095	0.934	0.435	2.369	85.518	
12	0.518	1.897	0	0	0.397	1.294	0.145	0.151	0.064	0.677	0.363	2.106	85.518	

Table A-1.5 Reaction condition: 10wt.% pure glycerol concentration, 0.2 ml/min feed flow rate, 330°C under atmospheric pressure for 12 hours over 3%Co/MgO Catalyst.

Time (h)	Gas Products (%)				Liquid Products (wt.%)									
	CO	CO ₂	Methanol	H ₂	Ethanal	Methanol	Ethanol	Propanol	2,3-Butanedione	Acetol	Ethylene glycol	Glycerol	water	
4	0.225	0.925	0	0	0.093	0.302	0.057	0.000	0.016	0.053	0.010	0.862	95.940	
5	0.398	1.400	0	0	0.226	0.562	0.137	0.097	0.032	0.080	0.000	0.896	95.940	
6	0.365	1.299	0	0	0.379	0.739	0.137	0.109	0.041	0.123	0.000	1.114	95.940	
7	0.363	1.400	0	0	0.344	0.836	0.206	0.117	0.035	0.071	0.040	0.959	95.940	
8	0.496	1.676	0	0	0.434	0.868	0.207	0.126	0.035	0.073	0.046	1.189	95.940	
9	0.439	1.469	0	0	0.507	0.931	0.184	0.135	0.038	0.148	0.038	1.977	95.940	
10	0.423	1.373	0	0	0.526	0.946	0.170	0.138	0.039	0.217	0.051	2.080	95.940	
11	0.330	1.131	0	0	0.395	0.806	0.144	0.125	0.032	0.182	0.047	2.782	95.940	
12	0.282	0.982	0	0	0.366	0.725	0.134	0.117	0.028	0.155	0.040	3.382	95.940	

Table A-1.6 Reaction condition: 10wt.% pure glycerol concentration, 0.1 ml/min feed flow rate, 330°C under atmospheric pressure for 30 hours over 3%Ca/MgO Catalyst.

Time (h)	Gas Products (%)				Liquid Products (wt.%)									
	CO	CO ₂	Methanol	H ₂	Ethanal	Methanol	Ethanol	Propanol	2,3-Butanedione	Acetol	Ethylene glycol	Glycerol	water	
4	0.756	2.446	0	0	0.422	2.277	1.083	0.321	0.196	0.072	0.068	1.700	84.180	
5	0.658	2.102	0	0	0.562	2.707	1.328	0.421	0.203	0.116	0.118	1.415	84.180	
6	0.546	1.717	0	0	0.530	2.275	1.075	0.379	0.172	0.146	0.103	1.116	84.183	
7	0.562	1.853	0	0	0.390	1.679	0.729	0.288	0.120	0.194	0.125	1.061	89.860	
8	0.552	2.381	0	0	0.398	1.559	0.680	0.285	0.113	0.208	0.128	1.315	84.183	
9	0.492	2.181	0	0	0.570	2.051	0.742	0.372	0.157	0.306	0.169	1.577	84.183	
10	0.478	1.781	0	0	0.430	1.653	0.575	0.305	0.115	0.265	0.169	1.812	89.860	
12	0.448	1.747	0	0	0.606	1.925	0.631	0.354	0.148	0.330	0.193	2.463	89.860	
14	0.321	1.383	0	0	0.662	1.902	0.581	0.345	0.144	0.313	0.168	2.616	89.860	
16	0.370	1.479	0	0	0.480	1.541	0.368	0.247	0.100	0.278	0.151	2.563	84.655	
18	0.343	1.559	0	0	0.620	1.629	0.433	0.297	0.117	0.358	0.180	2.557	89.860	
20	0.316	1.264	0	0	0.482	1.539	0.329	0.234	0.092	0.239	0.127	2.304	84.655	

Time (h)	Gas Products (%)				Liquid Products (wt.%)									
	CO	CO ₂	Methanol	H ₂	Ethanal	Methanol	Ethanol	Propanol	2,3-Butanedione	Acetol	Ethylene glycol	Glycerol	water	
22	0.331	1.372	0	0	0.760	1.835	0.481	0.332	0.127	0.367	0.198	2.117	90.415	
24	0.322	1.328	0	0	0.710	1.775	0.444	0.221	0.119	0.420	0.229	2.816	90.415	
26	0.311	1.427	0	0	0.602	1.630	0.383	0.269	0.099	0.436	0.243	2.581	89.860	
28	0.326	1.353	0	0	0.565	1.596	0.354	0.269	0.093	0.474	0.265	2.544	84.655	
30	0.248	1.123	0	0	0.411	1.206	0.245	0.207	0.073	0.398	0.231	2.362	89.860	

Table A-1.7 Reaction condition: 10wt.% pure glycerol concentration, 0.1 ml/min feed flow rate, 330°C under atmospheric pressure for 30 hours over 5%Ca/MgO Catalyst.

Time (h)	Gas Products (%)				Liquid Products (wt.%)									
	CO	CO ₂	Methanol	H ₂	Ethanal	Methanol	Ethanol	Propanol	2,3-Butanedione	Acetol	Ethylene glycol	Glycerol	water	
4	0.506	1.735	0	0	0.225	1.154	0.451	0.189	0.103	0.124	0.089	1.086	90.10	
5	0.405	1.495	0	0	0.426	2.120	0.804	0.313	0.135	0.433	0.294	0.894	90.10	
6	0.371	1.473	0	0	0.570	2.948	1.035	0.408	0.154	0.985	0.057	1.435	90.10	
7	0.299	1.268	0	0	0.458	2.051	0.722	0.312	0.112	0.607	0.368	0.962	90.10	
8	0.290	1.267	0	0	0.471	1.897	0.510	0.274	0.104	0.613	0.364	0.862	90.10	
9	0.294	1.340	0	0	0.348	1.326	0.325	0.210	0.070	0.476	0.296	1.147	90.10	
10	0.212	1.085	0	0	0.381	1.259	0.284	0.197	0.072	0.472	0.287	1.163	90.10	
12	0.264	1.208	0	0	0.455	1.387	0.283	0.208	0.087	0.520	0.296	1.223	90.10	
14	0.371	1.585	0	0	0.446	1.267	0.239	0.185	0.070	0.477	0.250	1.247	90.10	
16	0.311	1.306	0	0	0.526	1.406	0.238	0.194	0.079	0.544	0.286	1.433	90.10	
18	0.265	1.241	0	0	0.568	1.435	0.241	0.199	0.084	0.524	0.274	1.244	90.10	
20	0.321	1.414	0	0	0.571	1.366	0.223	0.192	0.083	0.482	0.255	1.143	90.10	

Time (h)	Gas Products (%)				Liquid Products (wt.%)									
	CO	CO ₂	Methanol	H ₂	Ethanal	Methanol	Ethanol	Propanol	2,3-Butanedione	Acetol	Ethylene glycol	Glycerol	water	
22	0.261	1.372	0	0	0.598	1.375	0.213	0.189	0.078	0.489	0.249	1.116	90.10	
24	0.219	1.104	0	0	0.581	1.364	0.197	0.180	0.080	0.516	0.261	1.110	90.10	
26	0.267	1.280	0	0	0.527	1.308	0.170	0.163	0.072	0.588	0.280	1.246	90.10	
28	0.234	1.417	0	0	0.653	1.632	0.216	0.200	0.093	0.737	0.328	1.185	90.10	
30	0.188	1.097	0	0	0.811	1.899	0.256	0.219	0.108	0.841	0.368	1.237	90.10	

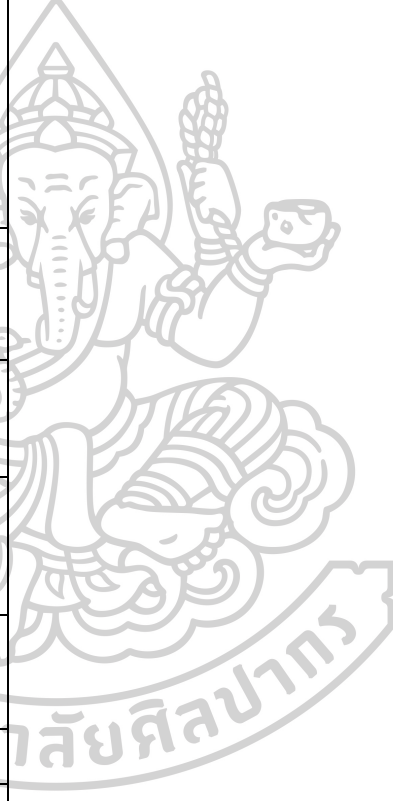
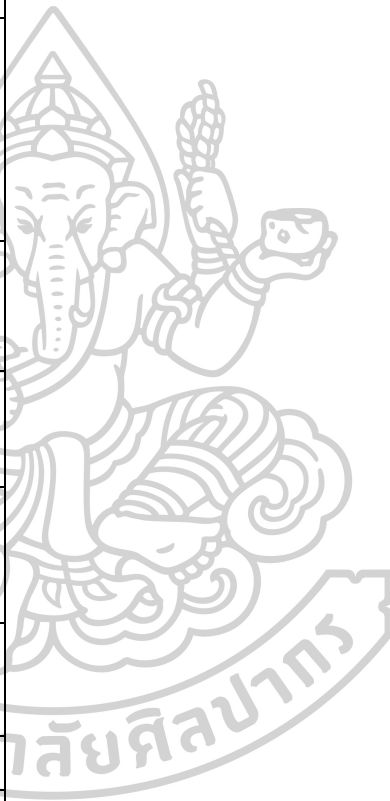


Table A-1.8 Reaction condition: 10wt.% pure glycerol concentration, 0.1 ml/min feed flow rate, 330°C under atmospheric pressure for 30 hours over 10%Ca/MgO Catalyst.

Time (h)	Gas Products (%)				Liquid Products (wt.%)									
	CO	CO ₂	Methanol	H ₂	Ethanal	Methanol	Ethanol	Propanol	2,3-Butanedione	Acetol	Ethylene glycol	Glycerol	water	
4	0.175	0.633	0	0	0.238	1.194	0.307	0.165	0.141	0.197	0.129	0.985	93.978	
5	0.195	1.098	0	0	0.277	1.368	0.429	0.184	0.107	0.299	0.205	0.893	93.978	
6	0.105	0.527	0	0	0.366	1.556	0.409	0.206	0.107	0.391	0.255	0.855	93.978	
7	0.184	0.865	0	0	0.360	1.351	0.355	0.189	0.092	0.396	0.228	0.837	93.978	
8	0.200	1.410	0	0	0.444	1.550	0.410	0.211	0.086	0.510	0.295	1.064	93.978	
9	0.199	1.077	0	0	0.454	1.419	0.376	0.202	0.080	0.380	0.225	0.744	93.978	
10	0.212	1.412	0	0	0.476	1.440	0.371	0.202	0.080	0.414	0.234	0.784	93.978	
12	0.185	1.128	0	0	0.575	1.617	0.405	0.220	0.091	0.493	0.298	0.894	93.978	
14	0.198	1.182	0	0	0.540	1.491	0.353	0.207	0.083	0.482	0.280	0.905	93.978	
16	0.168	1.051	0	0	0.558	1.441	0.321	0.201	0.083	0.479	0.257	0.757	93.978	
18	0.177	1.173	0	0	0.575	1.390	0.287	0.189	0.081	0.514	0.254	0.864	93.978	
20	0.181	1.137	0	0	0.425	1.049	0.197	0.153	0.059	0.419	0.270	0.722	93.978	

Time (h)	Gas Products (%)				Liquid Products (wt.%)									
	CO	CO ₂	Methanol	H ₂	Ethanal	Methanol	Ethanol	Propanol	2,3-Butanedione	Acetol	Ethylene glycol	Glycerol	water	
22	0.182	1.156	0	0	0.537	1.254	0.242	0.176	0.071	0.463	0.249	0.729	93.978	
24	0.158	1.133	0	0	0.621	1.431	0.267	0.184	0.082	0.572	0.302	0.856	93.978	
26	0.150	1.120	0	0	0.594	1.419	0.254	0.190	0.078	0.598	0.366	0.808	93.978	
28	0.136	1.125	0	0	0.426	1.001	0.172	0.147	0.056	0.394	0.254	0.842	93.978	
30	0.124	0.966	0	0	0.437	1.035	0.164	0.150	0.057	0.469	0.286	0.910	93.978	



A-2 The results of the product analysis for direct methanol synthesis from crude glycerol.

Table A-2.1 Reaction condition: 10wt.% crude glycerol concentration, 0.1 mL/min feed flow rate, 330°C under atmospheric pressure for 30 hours over 3%Ca/MgO Catalyst prepared by wet impregnation.

Time (h)	Gas Products (%)				Liquid Products (wt.%)								
	CO	CO ₂	Methanol	H ₂	Ethanal	Methanol	Ethanol	Propanol	2,3-Butanedione	Acetol	Ethylene glycol	Glycerol	water
6	0.000	0.094	0	0	0.000	0.376	0.031	0.000	0.000	0.035	0.000	1.895	90.053
7	0.140	0.775	0	0	0.163	0.896	0.235	0.124	0.071	0.090	0.000	4.424	90.053
8	0.534	1.901	0	0	0.334	1.362	0.448	0.183	0.119	0.181	0.098	5.915	90.053
9	0.061	0.742	0	0	0.694	2.831	0.695	0.327	0.222	0.587	0.360	7.773	90.085
10	0.097	0.829	0	0	0.345	1.618	0.351	0.205	0.123	0.549	0.309	5.164	81.525
12	0.000	0.431	0	0	0.403	1.635	0.248	0.182	0.119	0.740	0.387	3.412	81.525
14	0.119	1.150	0	0	0.525	1.478	0.197	0.165	0.143	0.592	0.348	2.931	91.540
16	0.348	1.924	0	0	0.452	1.755	0.224	0.196	0.139	0.827	0.524	2.503	84.990
18	0.403	2.116	0	0	0.391	1.752	0.259	0.200	0.102	0.565	0.448	1.476	84.990
20	0.644	3.615	0	0	0.585	1.878	0.237	0.184	0.135	0.777	0.485	1.353	84.990
22	0.400	2.625	0	0	0.550	2.072	0.245	0.185	0.132	0.838	0.651	1.556	87.820
24	0.000	0.679	0	0	0.614	2.018	0.282	0.204	0.120	0.556	0.517	1.000	87.820

Time (h)	Gas Products (%)				Liquid Products (wt.%)								
	CO	CO ₂	Methanol	H ₂	Ethanol	Methanol	Ethanol	Propanol	2,3-Butanedione	Acetol	Ethylene glycol	Glycerol	water
26	0.081	0.821	0	0	0.490	1.725	0.212	0.171	0.095	0.399	0.394	0.783	84.990
28	0.047	0.674	0	0	0.483	1.572	0.179	0.162	0.089	0.365	0.398	0.827	91.540
30	0.000	0.728	0	0	0.413	1.505	0.173	0.157	0.083	0.390	0.388	1.179	91.540

Table A-2.2 Reaction condition: 10wt.% crude glycerol concentration, 0.1 ml/min feed flow rate, 330°C under atmospheric pressure for 30 hours over 3%Ca/MgO Catalyst prepared by co-precipitation.

Time (h)	Gas Products (%)				Liquid Products (wt.%)								
	CO	CO ₂	Methanol	H ₂	Ethanol	Methanol	Ethanol	Propanol	2,3-Butanedione	Acetol	Ethylene glycol	Glycerol	water
5	0.295	0.912	0		0.114	0.994	0.420	0.156	0.082			0.536	95.723
6	0.200	0.742	0		0.744	0.728	0.291	0.127	0.058			0.466	95.723
7	0.361	1.006	0		0.123	0.822	0.324	0.137	0.064			0.455	95.723
8	0.561	1.513	0	1.096	0.209	0.988	0.394	0.156	0.071			0.544	95.723
9	0.379	1.008	0		0.177	1.067	0.403	0.167	0.069	0.077	0.047	0.474	95.723
10	0.355	1.037	0		0.164	1.066	0.398	0.169	0.071	0.066	0.045	0.487	89.415
12	0.400	1.199	0		0.252	1.203	0.525	0.201	0.087	0.070	0.044	0.486	89.415

Time (h)	Gas Products (%)				Liquid Products (wt.%)									
	CO	CO ₂	Methanol	H ₂	Ethanal	Methanol	Ethanol	Propanol	2,3-Butanedione	Acetol	Ethylene glycol	Glycerol	water	
14	0.645	2.249	0	1.06	0.396	1.303	0.579	0.214	0.091	0.127	0.074	0.469	89.415	
16	0.607	1.484	0	1.054	0.708	1.356	0.835	0.257	0.101	0.180	0.108	0.472	89.415	
18	0.610	1.483	0	1.055	0.612	1.157	0.565	0.180	0.068	0.133	0.070	0.467	89.415	
20	0.764	1.738	0		0.723	1.208	0.670	0.200	0.078	0.066	0.047	0.461	89.415	
22	0.908	1.768	0	1.198	0.923	1.285	0.751	0.217	0.074	0.063	0.051	0.456	89.415	
24	0.522	0.981	0		0.863	1.166	0.662	0.205	0.072	0.083	0.072	0.456	89.415	
26	0.518	0.982	0		0.659	0.862	0.462	0.153	0.055	0.055	0.047	0.471	89.415	
28	0.989	1.692	0	1.441	0.703	0.795	0.414	0.131	0.049	0.053	0.039	0.460	89.415	
30	0.947	1.529	0	1.438	0.948	1.031	0.578	0.157	0.053	0.086	0.054	0.496	89.660	

APPENDIX B

Calculation and preparation of chemicals

B-1 Calculation

Glycerol conversion, methanol yield and product distribution were calculated as following equation:

$$\text{Glycerol conversion (\%)} = \frac{W_{\text{glycerol, in}} - W_{\text{glycerol, out}}}{W_{\text{glycerol, in}}} \times 100$$

$$\text{Methanol yield (\%)} = \frac{W_{\text{methanol, out}}}{W_{\text{Glycerol, in}}} \times 100$$

$$\text{Product distribution (\%)} = \frac{W_{\text{product, } i}}{W_{\text{product, total}}} \times 100$$

Where

W is the weight, kg/h, of glycerol and a specific product formed,

i is a specific product formed.

B-2 The preparation of chemicals solution

B-2.1 The preparation of 5 wt.% glycerol solution 500 g from pure glycerol

25 g of pure glycerol and dissolves it in enough deionized (DI) water 475 g.

The concentration of glycerol solution is:

$$\frac{25 \text{ g of pure glycerol}}{25 \text{ g of pure glycerol} + 475 \text{ g of DI water}} \times 100 = 5 \text{ wt.}\%$$

B-2.2 The preparation of 10 wt.% glycerol solution 500 g from pure glycerol

50 g of pure glycerol and dissolves it in enough deionized (DI) water 450 g.

The concentration of glycerol solution is:

$$\frac{50 \text{ g of pure glycerol}}{50 \text{ g of pure glycerol} \times 450 \text{ g of DI water}} \times 100 = 10 \text{ wt.}\%$$

B-2.3 The preparation of 15 wt.% glycerol solution 500 g from pure glycerol

75 g of pure glycerol and dissolves it in enough deionized (DI) water 425 g.

The concentration of glycerol solution is:

$$\frac{75 \text{ g of pure glycerol}}{75 \text{ g of pure glycerol} \times 425 \text{ g of DI water}} \times 100 = 15 \text{ wt.}\%$$

B-2.4 The preparation of 10 wt.% glycerol solution 500 g from crude glycerol

Crude glycerol component from GI Green Power Company limited consisted of 65.69 wt.% glycerol, 1.65 wt.% ash, 0.05 wt.% water, 4.21 wt.% methanol and 28.4 wt.% other. The preparation of glycerol solution as follows:

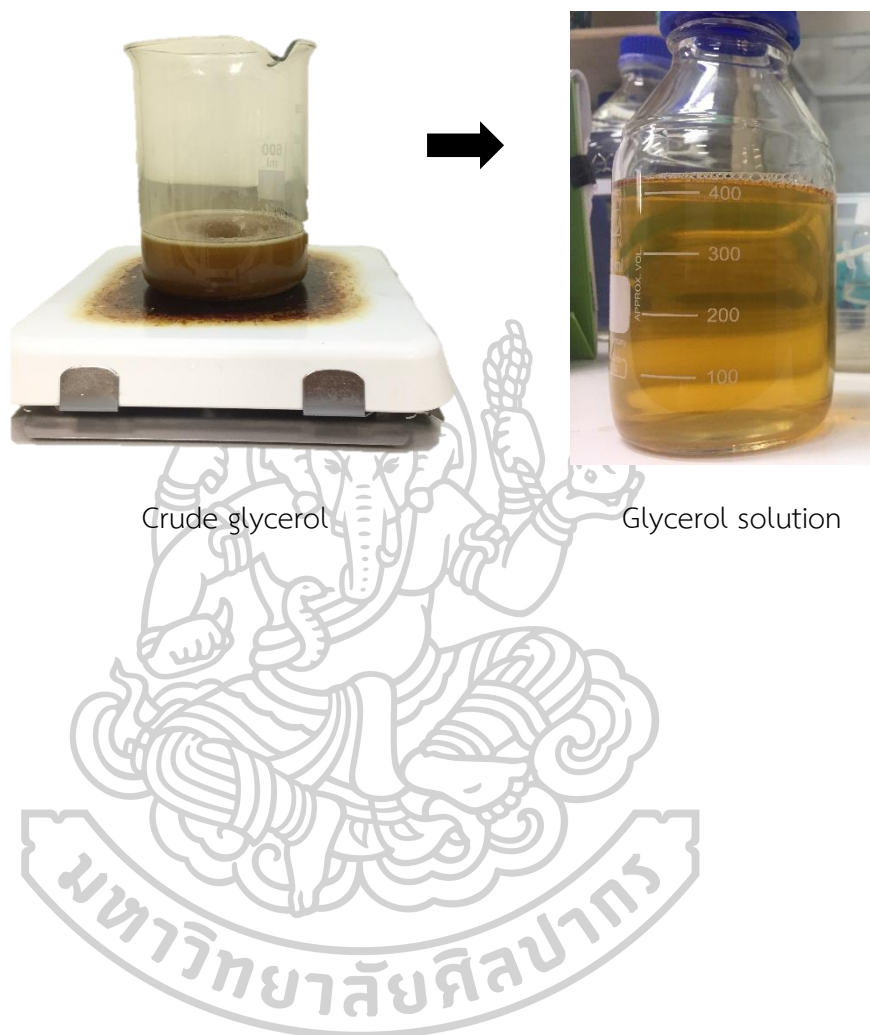
1. The evaporation of methanol, 100 g of crude glycerol was kept under vigorous stirring at 80 C for 30 min. The new concentration of glycerol in the crude glycerol is:

$$\frac{65.69}{65.69+1.65+0.05+28.4} \times 100 = 68.58 \text{ wt.}\%$$

2. 50 g of glycerol in crude glycerol were calculated according to the following equations:

$$\frac{50 \text{ g of glycerol} \times 100 \text{ g of crude glycerol}}{68.58 \text{ g of glycerol}} = 72.91 \text{ g of crude glycerol}$$

- 72.91 g of crude glycerol and dissolves it in enough deionized (DI) water to make 500 g of solution.



APPENDIX C

The data for Response surface methodology

Table C-1 The result of glycerol concentration (G), feed flow rate (F) and temperature (T) response glycerol conversion and methanol yield by using 3%Ca/MgO catalyst.

Independent variables				Response (%)	
Run	G (wt.%)	T (°C)	F (ml/min)	Glycerol conversion	Methanol yield
1	5	270	0.1	27.77	15.77
2	15	270	0.1	75.76	9.21
3	5	390	0.1	92.59	6.66
4	15	390	0.1	94.39	9.27
5	5	270	0.3	14.45	3.75
6	15	270	0.3	15.53	2.75
7	5	390	0.3	93.92	11.88
8	15	390	0.3	94.87	13.29
9	1.591	330	0.2	28.25	11.14
10	18.409	330	0.2	82.42	12.01
11	10	229.093	0.2	0.00	0.00
12	10	430.908	0.2	94.95	9.65
13	10	330	0.0318	54.09	5.29
14	10	330	0.368	70.23	7.36
15	10	330	0.2	77.11	14.52
16	10	330	0.2	74.19	14.99
17	10	330	0.2	74.94	14.35
18	10	330	0.2	76.29	14.24
19	10	330	0.2	78.29	14.49
20	10	330	0.2	77.40	14.05

Table C-2 Response Surface Regression: Glycerol conversion versus concentration, temperature and feed flow rate

Analysis of Variance					
Source	DF	Adj SS	Adj MS	F-Value	P-Value
Model	9	16025	1780.56	11.54	0
Linear	3	2492.4	830.81	5.38	0.018
Conc	1	1045.6	1045.62	6.77	0.026
Temp	1	1310.9	1310.91	8.49	0.015
Feed	1	180.8	180.77	1.17	<u>0.305</u>
Square	3	1290.3	430.09	2.79	0.096
Conc*Conc	1	410.2	410.17	2.66	<u>0.134</u>
Temp*Temp	1	948.6	948.59	6.15	0.033
Feed*Feed	1	123.3	123.32	0.8	<u>0.392</u>
2-Way Interaction	3	1263.3	421.1	2.73	0.1
Conc*Temp	1	268.2	268.23	1.74	<u>0.217</u>
Conc*Feed	1	285.1	285.1	1.85	<u>0.204</u>
Temp*Feed	1	710	709.98	4.6	<u>0.058</u>
Error	10	1543.4	154.34		
Lack-of-Fit	5	1531.3	306.26	126.7	0
Pure Error	5	12.1	2.42		
Total	19	17568.4			
Model Summary					
	S	R-sq	R-sq(adj)	R-sq(pred)	
	12.4232	91.22%	83.31%	31.38%	

Regression Equation in Uncoded Units

$$\text{Glycerol conversion} = -363 + 15.12 C + 1.857 T - 314 F - 0.213 C^2 - 0.002254 T^2 - 293 F^2 - 0.0193 CT - 11.94 CF + 1.570 TF$$

Table C-3 Response Surface Regression: Methanol yield versus concentration, temperature and feed flow rate.

Analysis of Variance					
Source	DF	Adj SS	Adj MS	F-Value	P-Value
Model	9	364.746	40.527	10.35	0.001
Linear	3	130.907	43.636	11.15	0.002
Conc	1	8.414	8.414	2.15	<u>0.173</u>
Temp	1	66.018	66.018	16.86	0.002
Feed	1	20.952	20.952	5.35	0.043
Square	3	197.87	65.957	16.85	0
Conc*Conc	1	5.347	5.347	1.37	<u>0.27</u>
Temp*Temp	1	129.234	129.234	33.01	0
Feed*Feed	1	87.581	87.581	22.37	0.001
2-Way Interaction	3	115.235	38.412	9.81	0.003
Conc*Temp	1	16.822	16.822	4.3	<u>0.065</u>
Conc*Feed	1	2.376	2.376	0.61	<u>0.454</u>
Temp*Feed	1	96.037	96.037	24.53	0.001
Error	10	39.147	3.915		
Lack-of-Fit	5	38.632	7.726	75.03	0
Pure Error	5	0.515	0.103		
Total	19	403.892			
Model Summary					
	S	R-sq	R-sq(adj)	R-sq(pred)	
	1.97855	90.31%	81.58%	25.04%	

Regression Equation in Uncoded Units

$$\text{Methanol yield} = -41.5 - 1.356 C + 0.417 T - 107.0 F - 0.0244 C^2 - 0.000832 T^2 - 246.7 F^2 + 0.00483 CT + 1.09 CF + 0.577 TF$$

Consider the P-value of each factor, if the P-value is less than 0.05, then the equation of the factor has a significant effect on the experimental response. Then consider the p-value of the quadratic term or the effect that causes the quadratic equation. If the p-value is less than 0.05, the equation of the factor has a significant effect on the experimental response. So, regression equation was used to explain the mathematical relationship between the independent variables and dependent responses which is represented by terms of concentration (C), temperature (T) and feed flow rate (F) as following Eq. (1)-(2):

$$\begin{aligned} \text{Glycerol conversion} = & -363 + 15.12 C + 1.857 T - 314 F - 0.213 C^2 - 0.002254 T^2 \\ & - 293 F^2 - 0.0193 CT - 11.94 CF + 1.570 TF \end{aligned}$$

$$\text{Glycerol conversion} = -363 + 15.12 C + 1.857 T - 0.002254 T^2 \quad (\text{C-1})$$

$$\begin{aligned} \text{Methanol yield} = & -41.5 - 1.356 C + 0.417 T - 107.0 F - 0.0244 C^2 - 0.000832 T^2 \\ & - 246.7 F^2 + 0.00483 CT + 1.09 CF + 0.577 TF \end{aligned}$$

$$\text{Methanol yield} = -41.5 + 0.417 T - 107.0 F - 0.000832 T^2 - 246.7 F^2 + 0.577 TF \quad (\text{C-2})$$

The error (%) was calculated by equation[11]

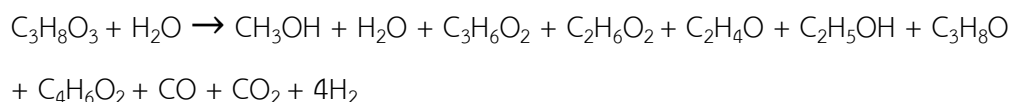
$$\text{Error percentage} = \left| \frac{Y_{\text{exp}} - Y_{\text{pred}}}{Y_{\text{exp}}} \right| \quad (\text{C-3})$$

Where Y_{exp} is experimental value and Y_{pred} is predicted value.

APPENDIX D

Kinetics rate modeling

1. The reaction of glycerol (A) and water (B)



2. Postulate a rate law $-r_A = kC_A^\alpha C_B^\beta$ (D-1)

whereby

$-r_A$ = rate of glycerol (mol/L·h)

k = specific reaction rate

α, β = reaction order

Table D-1 The data for rate law of direct methanol synthesis from glycerol over 3%Ca/MgO catalyst.

Experiment	Initial concentration (mol/L)		Final concentration (mol/L)		Rate of glycerol and water (mol/L·h)	
	Glycerol (A)	Water (B)	Glycerol (A)	Water (B)	$-dC_A/dt$	$-dC_B/dt$
1	1.959	45.495	0.091	53.370	0.374	-1.575
2	1.086	49.958	0.156	52.082	0.186	-0.425
3	0.543	52.734	0.084	54.426	0.076	-0.282

3. The reaction could first be run in an excess of water (B) so that C_B remains essentially unchanged during the course of reaction and

$$C_B = C_{B0} \quad (\text{D-2})$$

Substituting for C_B in equation (C-1)

$$-r_A = k C_{B0}^\beta C_A^\alpha \quad (D-3)$$

$$k' = k C_{B0}^\beta \quad (D-4)$$

$$-r_A = k' C_A^\alpha \quad (D-5)$$

4. Differential method

$$-\frac{dC_A}{dt} = k' C_A^\alpha \quad (D-6)$$

Taking the natural log of both sides of equation (C-6),

$$\ln\left(-\frac{dC_A}{dt}\right) = \ln k' + \alpha \ln C_A \quad (D-7)$$

observe that the slope of $\ln(-dC_A/dt)$ as a function of $\ln C_A$ is reaction order, α

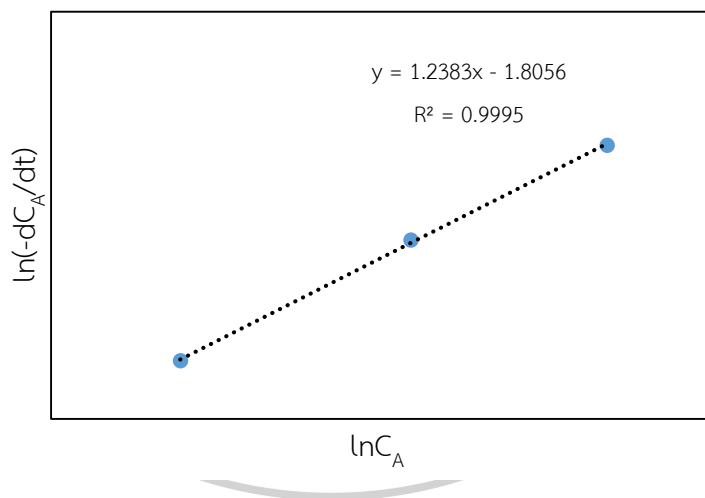


Figure 52 Differential method to determine reaction order.

The graph showed that reaction order, $\alpha = 1.24$ and $k' = 0.164$ L/mol·h. We could set $\alpha = 1, 2, 3$ and regress again to find k' .

5. Finding order reaction of C_A and k' .

$$\alpha=1, -r_A = k'C_A$$

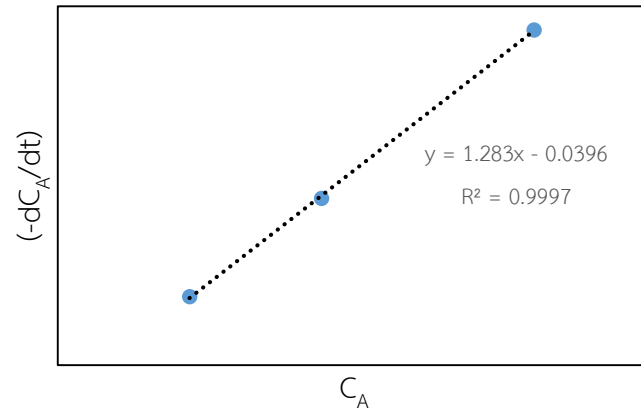


Figure 53 First-order reaction

$$\alpha = 2, -r_A = k'C_A^2$$

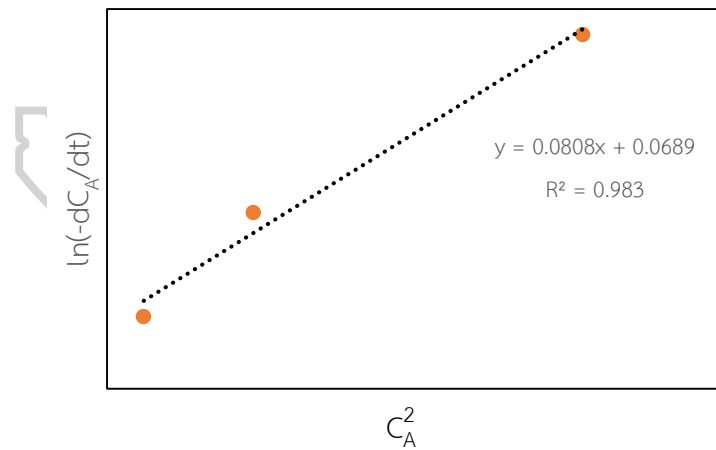


Figure 54 Second-order reaction

$$\alpha = 3, -r_A = k'C_A^3$$

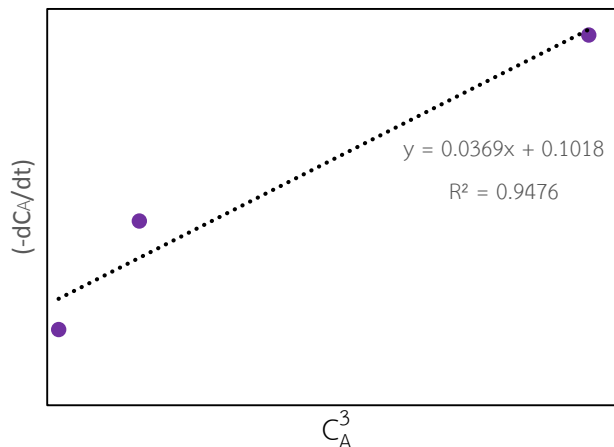


Figure 55 Third-order reaction

A plot of $(-dC_A/dt)$ as a function of C_A will be linear. It was found that reaction order was first-order and regress again to find $k' = 0.168 \text{ L/mol}\cdot\text{h}$ at $R^2 = 0.9997$ in Figure 53.

6. Finding kC_B^β

Because the concentration of water is not less than the initial concentration for all experiments

$$k' = kC_{B0}^\beta = kC_B^\beta \quad (\text{D-8})$$

$$\beta = 0; \quad k' = k = 0.168 \text{ L/mol}\cdot\text{h}$$

$$\text{The rate law is} \quad -r_A = kC_A = 0.168C_A$$

VITA

NAME Mukrawee Maneewuthiworasakul

DATE OF BIRTH 06 October 1991

PLACE OF BIRTH Ratchaburi

INSTITUTIONS ATTENDED Bachelor of Engineering (Chemical Engineering), Silpakorn University

HOME ADDRESS 4 M.9 Malaiman Rd., Thap Luang sub-district, Muang district, Nakhon Pathom, 73000, Thailand

PUBLICATION Proceedings of 8th IUPAC International Conference on Green Chemistry

